

# Cell Biology Research

**Whioce Publishing Pte. Ltd.**  
**10 Anson Road #10-13a International Plaza**  
**Singapore (079903)**





# Cell Biology Research

## Focus and Scope

Cell Biology Research (CBR) is a peer-reviewed scholarly journal dedicated to the dissemination of cutting-edge research in the field of cell biology. With a commitment to advancing our understanding of cellular processes, the journal provides a platform for scientists, researchers, and scholars to share their latest findings and insights.

## About Publisher

Whioce Publishing was established in Singapore in 2014 with a global orientation. The core business of the company focuses on publication of academic journals and organization of international academic conferences, at the same time providing educational trainings, consultations on scientific and technological information, translation services and publications of e-books.

Albeit being a young company, Whioce Publishing has placed huge focus on initiating and publishing top quality international academic journals. The eventual aim is to be indexed by top-notch databases such as EI, SCI, SSCI and AHCI, at the same time growing to become a recognized international academic publishing company that provides a knowledge sharing and communication platform to top researchers all over the world.

**EXPANSION STRATEGY:** Constantly expanding and strengthening collaborations with publishing companies and relevant industry associations all over the world, building a group of knowledgeable academic personnel and a quality management team. Disseminate scientific and technical information of high quality, gradually growing to a publishing enterprise with worldwide influence.

## Publisher Headquarter

**WHIOCE PUBLISHING PTE. LTD.**

Publishing Office: 10 Anson Road #10-13A International Plaza Singapore 079903

Website: [whioce.com](http://whioce.com)

TEL: +65-91818774

Email: [info@whioce.com](mailto:info@whioce.com)



# C

# ONTENTS

---

- 1 Molecular Mechanisms of Osteoclast Precursor Fusion: From DC-STAMP to Novel Regulatory Proteins**  
*Xin Cai, Tingting Long, Zhaoyang Huang*
- 13 Research on Restoration Strategies for Human Body Functions Due to Gut Microbiota Dysbiosis in High-Altitude Hypoxia**  
*Yanyan Wang, Pan Geng, Rui Xia, Yuan Xing, Yanxia Han*
- 19 Discussion on the Value of Six-item Detection of Sex Hormones by Chemiluminescence Immunoassay in the Diagnosis and Treatment of Gynecological Endocrine Diseases**  
*Yuan Xiu*
- 25 Analysis of the Application Effect of Preoperative Prehabilitation Based on the ERAS Concept in the Rapid Postoperative Recovery of Elderly Patients with Lung Cancer**  
*Xiaoping Huang, Qiaoming Gao*
- 31 Evaluation of the Application Value of Routine Blood Tests in the Diagnosis of Iron Deficiency Anemia**  
*Xilin Kuai*
- 37 Research on Vaccine Distribution and Reserve Based on Service Level during Major Infectious Disease Epidemics**  
*Hong Zhang*
- 43 Remodeling the Ischemic Stroke Immuno-Microenvironment via Microglial Phenotypic Switching**  
*Xiaowen Wang, Bingcang Huang*
- 53 Application of Integrated Animal and Cell Experiment Teaching Model in Demonstrating Ferroptosis in Cerebral Ischemia-Reperfusion Injury**  
*Guangjie Sun, Bingcang Huang*
- 62 Plant-derived Extracellular Vesicles in the Central Nervous System: Emerging Mechanisms and Therapeutic Opportunities**  
*Zelun Zheng, Fanfan Cao*

# C

## ONTENTS

---

- 72 The Effect of Health Education Using Clinical Nursing Pathways  
in Patients with Schizophrenia and Diabetes**

*Jingwen Hu*

- 78 Exploration and Analysis of the Efficacy of Tubeless Percutaneous  
Nephroscopy in Treating Upper Urinary Tract Stones**

*Liang Zhu, Wenchao Zhao*

# Molecular Mechanisms of Osteoclast Precursor Fusion: From DC-STAMP to Novel Regulatory Proteins

Xin Cai, Tingting Long, Zhaoyang Huang\*

Department of Clinical Laboratory, Institute of Translational Medicine, Renmin Hospital of Wuhan University, Wuhan 430060, Hubei, China

\*Corresponding author: Zhaoyang Huang, [huangzhy85@mail2.sysu.edu.cn](mailto:huangzhy85@mail2.sysu.edu.cn)

**Copyright:** © 2025 Author(s). This is an open-access article distributed under the terms of the Creative Commons Attribution License (CC BY 4.0), permitting distribution and reproduction in any medium, provided the original work is cited.

**Abstract:** Osteoclasts are multinucleated giant cells responsible for bone resorption in the skeletal system. Osteoclast precursors originate from monocytes and macrophages, as well as dendritic cells. Their multinucleation process is crucial for maintaining bone homeostasis. Studies indicate that efficient fusion of mononuclear precursor cells is a prerequisite for forming fully functional multinucleated osteoclasts. This unique cell fusion capability allows osteoclasts to form large, multinucleated cells with enhanced bone resorptive capacity. Under physiological conditions, a precisely regulated fusion process generates multinucleated osteoclasts of predictable size, with the number of nuclei positively correlating with bone resorption activity. Notably, each fusion event significantly increases the bone resorptive activity of osteoclasts, a characteristic vital for lifelong bone remodeling processes.

**Keywords:** Osteoclasts; DC-STAMP; Osteoclast precursor; Cell fusion

**Online publication:** December 26, 2025

## 1. Introduction

### 1.1. Cell fusion as a rate-limiting step in osteoclast maturation

The fusion of osteoclast precursors is a rate-limiting step in osteoclast maturation, subject to multi-layered, precise regulation. Fusion of osteoclast precursors (OCPs) is a complex process regulated by multiple factors. The fusion process can be divided into four steps: (1) cell attraction/migration; (2) cell recognition; (3) cell adhesion; and (4) cell fusion <sup>[1]</sup>. Various fusion-related genes are upregulated during osteoclast maturing, including CD9, MFR/SIRP $\alpha$ , ATP6V0d2, and DA-STAMP etc. Those proteins involved in the fusion procedure can be categorized into RANKL-independent or dependent proteins (**Figure 1**). RANKL-dependent proteins include CD47, CD9/CD81, ATP6V0d2, MFR/SIRP $\alpha$ , OC-STAMP, A2A, and DC-STAMP <sup>[2]</sup>, whereas CD44 and TREM2 are classified as RANKL-independent proteins <sup>[3]</sup>. DC-STAMP and ATP6V0d2 are directly regulated by the transcription factor NFATc1; other fusion proteins, including MFR/SIRP $\alpha$ , CD9, CD44, E-cadherin, and meltrin- $\alpha$ , are not regulated by NFATc1 <sup>[4]</sup>. Otherwise, the number of nuclei in mature osteoclasts positively correlates with their bone resorption capacity; larger volume osteoclasts exhibit high resorption ability. Breaking the fusion or multinucleation process in osteoclasts can lead to decreased bone resorption, resulting in high bone mineral density (BMD) <sup>[5]</sup>. Research shows that RANKL-mediated caspase-8 activation is an early key event in osteoclast fusion <sup>[6,7]</sup>, accompanied by the activation of

certain molecules related to apoptotic mechanisms<sup>[6]</sup>. This fusion process requires specific molecules, such as Dendritic Cell-Specific Transmembrane Protein (DC-STAMP)<sup>[8]</sup>, and the expression of key transcription factors like c-Fos and NFATc1 etc.<sup>[9]</sup> Importantly, differentiating osteoclast precursors undergo mechanical changes, including reduced plasma membrane tension, which serves as a mechanical prerequisite for cell fusion<sup>[10]</sup>. Furthermore, the nuclear RNA chaperone La protein has been identified to possess a novel function in regulating osteoclast fusion<sup>[11]</sup>, indicating that the regulatory network of fusion is far more complex than previously understood.

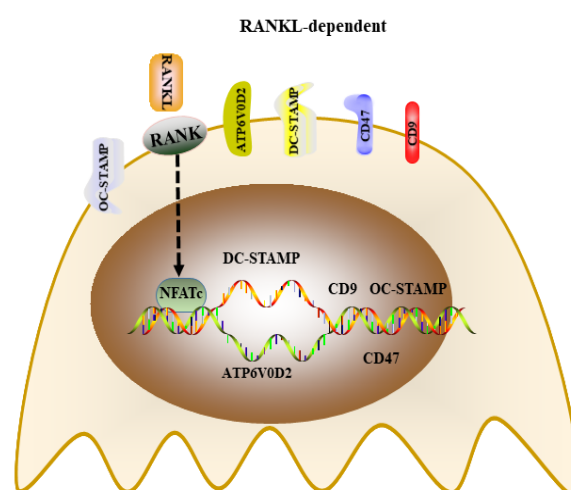


**Figure1.** RANKL-dependent proteins and the role they plays in the osteoclast differentiation stage.

Note: In response to RANKL stimulation, the expression of CD47, CD9/CD81, ATP6V0d2, MFR/SIRP $\alpha$ , OC-STAMP, A2A and DC-STAMP increases, ATP6V0d2 and DC-STAMP directly regulated by transcription factor NFATc1.

## 1.2. Clinical translational value of molecular mechanism research

Investigating the molecular mechanisms of osteoclast fusion holds significant clinical translational value. DC-STAMP-deficient mice exhibit an osteopetrotic phenotype<sup>[12]</sup>, suggesting that targeting fusion regulation could be a novel strategy for treating bone metabolic diseases. Current clinical drugs often completely inhibit osteoclast function, disrupting normal bone turnover<sup>[13]</sup>, whereas specifically regulating precursor cell fusion might be more suitable for maintaining bone homeostasis<sup>[13]</sup>. Studies have attempted to use engineered bacteria for the targeted delivery of the osteoclast precursor fusion protein DC-STAMP<sup>[14]</sup>, demonstrating good bone-targeting capability. Furthermore, regulating fusion-related molecules like NFATc1 and DC-STAMP can effectively inhibit pathological bone resorption<sup>[15,16]</sup>, providing new therapeutic targets for osteolytic diseases such as osteoporosis. These findings highlight the importance of studying osteoclast fusion mechanisms for developing precise bone metabolism intervention strategies.

## 2. Research progress on the core osteoclast fusion molecule DC-STAMP

### 2.1. Molecular structure and functional characteristics of DC-STAMP

Dendritic Cell-Specific Transmembrane Protein (DC-STAMP) is a key molecule for forming functional multinucleated osteoclasts<sup>[17]</sup>. DC-STAMP-deficient mice exhibit an osteopetrotic phenotype under physiological conditions and develop systemic autoimmune symptoms with age<sup>[12]</sup>. This protein is highly expressed on the membrane of osteoclast precursors and mediates their phagocytosis of apoptotic bodies<sup>[16]</sup>. Structurally, DC-STAMP belongs to the seven-transmembrane protein family, with its extracellular domain involved in intercellular recognition and its intracellular domain participating in downstream signal transduction<sup>[18]</sup>. Functional studies show that DC-STAMP is not only a master regulator of osteoclast fusion<sup>[15]</sup> but also involved in regulating bone resorption function; its expression level increases synchronously with osteoclast markers (Nfatc1, Acp5, Ctsk, etc.) on stiffer matrix surfaces<sup>[15]</sup>.

## 2.2. Molecular mechanism of DC-STAMP-mediated cell membrane fusion

DC-STAMP regulates the cell membrane fusion process through a unique molecular mechanism. During the fusion initiation stage, DC-STAMP promotes the formation of phagocytic cup-like structures between osteoclast precursors<sup>[19]</sup>. Experiments confirm that precursors with knocked-down DC-STAMP lose their ability to be phagocytosed<sup>[16]</sup>. In the membrane fusion stage, DC-STAMP activates the expression of cytoskeleton-related adhesion molecules (including fibronectin and integrin  $\alpha\text{v}\beta 3$ ), subsequently triggering biochemical signaling cascades involving paxillin, FAK, PKC, and RhoA<sup>[15]</sup>. Notably, SNX10 protein-deficient osteoclasts show persistent peripheral aggregation of DC-STAMP, which might be a key reason for their uncontrolled fusion<sup>[20]</sup>. Besides, immunoreceptor Tyrosine-based Inhibitory Motif (ITIM) in the cytoplasmic tail of DC-STAMP is a critical regulator of osteoclast differentiation through the  $\text{Ca}^{2+}$ /NFATc1 signaling axis<sup>[21]</sup>. Using optogenetic and mutational approaches shows that deletion of the ITIM disrupts intracellular  $\text{Ca}^{2+}$  flux, impairs NFATc1 nuclear translocation, and reduces osteoclast fusion, bone resorption, and cell motility<sup>[21]</sup>.

## 2.3. Transcriptional network regulating DC-STAMP expression

DC-STAMP expression is subject to multi-level transcriptional regulation. The RANKL-NFATc1 signaling pathway upregulates DC-STAMP expression by inducing key transcription factors like c-Fos and NFATc1<sup>[22,23]</sup>. Research indicates that RANKL-activated JNK, p38, and ERK MAPK signaling pathways, as well as the I $\kappa$ B $\alpha$  degradation pathway, are upstream events regulating DC-STAMP expression<sup>[22]</sup>. At the epigenetic level, the histone modification enzyme Ctsk might affect the chromatin accessibility of the NFATc1 promoter by regulating H3K27me3 cleavage status, indirectly modulating DC-STAMP expression<sup>[24]</sup>. Additionally, Chi311 significantly promotes RANKL-induced upregulation of DC-STAMP expression by activating the MAPK (ERK/P38/JNK) and AKT pathways<sup>[25]</sup>.

## 2.4. Synergistic effects of DC-STAMP with other fusion-related proteins

DC-STAMP forms a functional synergistic network with various fusion-related proteins. Studies found correlations between the expression levels of DC-STAMP and the co-receptor CCR5, as well as tetraspanins CD9 and CD81<sup>[26]</sup>. At the signaling level, DC-STAMP, together with transcription factors like NFATc1 and c-Fos, constitutes the core regulatory module for osteoclast fusion<sup>[27]</sup>. Experimental evidence shows that inhibiting DC-STAMP simultaneously downregulates the expression of osteoclast-specific marker genes such as ATP6V0D2 and CtsK<sup>[22,28]</sup>. In inflammatory arthritis models, DC-STAMP interacts with the TNF- $\alpha$  signaling pathway, jointly regulating synovitis and bone erosion progression<sup>[12,29]</sup>. Furthermore, recent studies reveal that SARS-CoV-2 variants can upregulate osteoclastogenesis-related genes like DC-STAMP, promoting RANKL-independent osteoclast formation<sup>[30]</sup>.

# 3. Discovery and functional validation of novel regulatory proteins

## 3.1. Role of La protein in precursor recognition

La is generally recognised as an abundant and ubiquitous RNA-binding protein, also known as LARP3 and La autoantigen<sup>[31]</sup>. The most extensively studied function of nuclear La is its role in protecting precursor tRNAs from exonuclease digestion. This is achieved through specific interactions between La's highly conserved N-terminal La domain and the 3' ends of tRNA. La protein exhibits unique regulatory functions during osteoclast precursor fusion. In the initial stage of monocyte differentiation into osteoclasts, La protein levels decrease significantly<sup>[8,15,19]</sup>. As the fusion process initiates, a low molecular weight form of La protein reappears on the osteoclast surface<sup>[11]</sup>. This non-classical form of La protein anchors to transiently exposed phosphatidylserine on the fusing cell surface by directly interacting with membrane-anchored Annexin A5<sup>[8,11]</sup>. Notably, the function of La protein in promoting osteoclast fusion is independent of its classical RNA-binding activity<sup>[8,11]</sup>. Reactive Oxygen Species (ROS) signaling regulates the subcellular localization and functional switch of La protein by oxidizing cysteine residues at its C-terminus, leading to the formation of this fusion-promoting atypical La protein form<sup>[8,11]</sup>.



La was present in primary human monocytes but virtually absent in m-CSF-derived osteoclast precursor cells. However, following rankl-induced osteoclastogenesis, La protein reappeared on the surface of fused osteoclasts. As osteoclast fusion entered the stable phase, LMW La was observed to gradually disappear, and higher molecular weight phosphorylated full-length La protein (FL-La) was observed in the nuclei of mature multinucleated osteoclasts. Inhibition of La expression, cleavage, or surface function impedes osteoclast fusion, whereas the addition of exogenous La facilitates osteoclast fusion. In fact, the carboxy-terminal portion of La promotes human osteoclast fusion, unlike the classical function of La<sup>[11]</sup>. Osteoclasts secrete factors that regulate osteoblast activity<sup>[32]</sup>. The targeted blockade of the RANKL pathway may impede osteoclast-osteoblast signalling, whereas the targeting of La to inhibit the fusion phase of osteoclast formation may simultaneously preserve osteoclast differentiation capacity and maintain this osteoclast-osteoblast crosstalk within bone remodelling lesions.

### 3.2. Spatial regulatory role of the CD47-SIRP $\alpha$ signaling axis

The CD47-SIRP $\alpha$  signaling axis plays an important spatial regulatory role in osteoclast fusion. CD47, a transmembrane protein, interacts with the SIRP $\alpha$  receptor expressed on osteoclast precursor surfaces<sup>[33,34]</sup>, transmitting intercellular recognition signals<sup>[35]</sup>.

In the immune system, CD47-SIRP $\alpha$  interaction generates a “don’t eat me” signal<sup>[36,37]</sup>; this mechanism might participate in regulating the recognition and contact of precursor cells during osteoclast fusion. The SIRP $\alpha$  receptor belongs to the immunoreceptor tyrosine-based inhibitory motif (ITIM)-bearing receptor family; its N-terminal Ig-like domain triggers downstream signaling upon binding to CD47<sup>[38,39]</sup>. Studies indicate that CD47-SIRP $\alpha$  interaction can influence cell metabolism by regulating JAK/STAT and ERK/MAPK signaling pathways<sup>[40]</sup>. Additionally, this signaling axis can activate the Hedgehog/SMAD pathway and regulate NF- $\kappa$ B activity<sup>[41]</sup>, potentially forming a multi-layered regulatory network in osteoclast fusion. CD47 could facilitate leukocyte chemotaxis and migration by binding receptor MFR. Furthermore, blocking CD47/SIRP $\alpha$  recognition with monoclonal antibodies significantly inhibits osteoclast maturation<sup>[42]</sup>. In RANKL-treated BMMs, CD47<sup>-/-</sup> cells generate significantly fewer TRAP<sup>+</sup> osteoclasts than wild-type controls<sup>[43,44]</sup>. Similarly, CD47<sup>-/-</sup> mice exhibit a clear reduction in TRAP<sup>+</sup> osteoclasts in vivo<sup>[45]</sup>. CD47 inhibition decreases fusion events between mononuclear OCPs and between binuclear osteoclasts, without affecting fusion involving osteoclasts with three or more nuclei<sup>[46,47]</sup>.

### 3.3. Other identified new regulatory factors

Besides the aforementioned proteins, various other novel regulatory factors are involved in osteoclast fusion. ROS signaling has been confirmed to promote osteoclast fusion and bone resorption activity<sup>[8,11]</sup>. During differentiation, ROS signaling regulates the subcellular localization and functional switch of La protein via redox-sensitive cysteine residues<sup>[8]</sup>. Furthermore, Annexin A5, as an anchoring protein for La protein, forms functional complexes on transiently exposed phosphatidylserine on the fusing cell surface<sup>[11]</sup>. Recent studies also found that caspase-8 activation is an early key event in osteoclast fusion<sup>[6]</sup>, suggesting that proteins associated with programmed cell death might also regulate the fusion process. These newly discovered regulatory factors collectively constitute a complex regulatory network for osteoclast precursor fusion.

## 4. Cascade signaling network in osteoclast fusion

### 4.1. Central role of the RANKL-NFATc1 signaling pathway

The RANKL/RANK signaling pathway is the core cascade regulating osteoclast differentiation, with NFATc1 acting as a pivotal transcription factor<sup>[48]</sup>. Studies show that NFATc1 activation is regulated through three aspects: direct activation by the upstream RANKL/RANK signaling pathway, amplification by Ca<sup>2+</sup>-related co-stimulatory signals, and positive feedback regulation at the NFATc1 transcriptional level itself<sup>[48]</sup>. Mechanistically, RANKL stimulation promotes the non-apoptotic cleavage of downstream effector molecules via caspase-8 activation, an early event critical for osteoclast fusion<sup>[49,50]</sup>. Single-cell RNA sequencing analysis confirms that NFATc1-associated super-enhancers (SEs) and their resulting enhancer RNAs



(eRNAs) play key regulatory roles in osteoclast differentiation; interfering with these elements significantly reduces NFATc1 expression and osteoclast differentiation capacity <sup>[40]</sup>. Moreover, various inhibitors like PLM and musaendoside O block osteoclast formation by inhibiting the RANKL-induced p38/JNK-cFos/NFATc1 signaling cascade <sup>[51,52]</sup>.

## 4.2. Enhanced fusion via extracellular signals by collagenase inhibition

Extracellular matrix remodeling plays a significant role in osteoclast fusion. Research suggested that the collagenase inhibitor CA significantly inhibits RANKL-induced actin ring formation, osteoclastogenesis, and bone resorption function <sup>[37]</sup>. Its mechanism involves two aspects: On the one hand, it suppresses RANKL-induced ROS production by elevating antioxidant enzyme levels like catalase and NQO1; on the other hand, it interferes with the fusion process by modulating the expression of key proteins such as integrin  $\alpha\beta3$ , NFATc1, and Cathepsin K (CTSK) <sup>[37]</sup>. Notably, CA has no significant effect on cortical bone, suggesting its potential as a candidate drug for targeted therapy of bone metabolic diseases due to this selective action <sup>[37]</sup>.

## 4.3. Molecular basis of stage-specific regulation by IFN $\gamma$ R

Interferon- $\gamma$  receptor (IFN $\gamma$ R) regulation of osteoclast fusion exhibits a unique stage dependency <sup>[53]</sup>. In early osteoclast precursor stages, IFN $\gamma$ R activation completely inhibits multinucleated osteoclast formation; whereas, in immature osteoclast stages, the same activation further enhances cell fusion <sup>[53]</sup>. The molecular basis for this biphasic regulation lies in the differential downstream activation of MAPK pathways: IFN $\gamma$ R activation in early precursor cells induces Fc $\gamma$ R expression, a co-regulatory phenomenon dependent on MAPK signaling. Phosphokinase array analyses reveal significant differences in IFN $\gamma$ R signal transduction between precursor cells and immature osteoclasts, providing new insights into the dynamic regulation of bone resorption under inflammatory conditions <sup>[53]</sup>.

## 4.4. Association between Metabolic Reprogramming (PKM2) and fusion capacity

Pyruvate Kinase M2 (PKM2), a key molecule in metabolic reprogramming, has been identified as a novel switch regulating osteoclast differentiation <sup>[54]</sup>. Immunoglobulin superfamily member 11 (IgSF11) regulates osteoclast differentiation in a PKM2-dependent manner by interacting with the postsynaptic scaffolding protein PSD-95. Experiments confirm that inhibiting PKM2 activity with the specific inhibitor Shikonin rescues the osteoclast differentiation defect in IgSF11-deficient cells, while the activator TEPP46 inhibits osteoclast differentiation in wild-type cells <sup>[54]</sup>. More importantly, PKM2 activation inhibits osteoclast-mediated bone loss without affecting bone formation, making it a potential target for treating pathological bone loss due to this selective regulation <sup>[38]</sup>. The link between metabolic reprogramming and cell fusion capacity is also reflected in PKM2's influence on the expression of fusion-related proteins like DC-STAMP via regulating NFATc1 activity <sup>[52,54]</sup>.

# 5. Dynamic regulatory mechanisms of the fusion process

## 5.1. Molecular events in precursor chemotaxis and initial contact

The chemotaxis and initial contact of osteoclast precursors are critical initiating steps of the fusion process. Studies indicate that RANKL-mediated caspase-8 activation is a core molecular event at this stage <sup>[6]</sup>. Single-cell RNA sequencing analysis shows that partial activation of apoptotic mechanisms accompanies the differentiation of osteoclast precursors into mature multinucleated osteoclasts <sup>[53]</sup>. Caspase-8 activation promotes the non-apoptotic cleavage of downstream effector molecules, which subsequently translocate to the plasma membrane, triggering the activation of phospholipid scramblase Xkr8 <sup>[6]</sup>. Xkr8-mediated phosphatidylserine exposure provides the molecular basis for mutual recognition and initial contact between precursor cells <sup>[6]</sup>. Additionally, the binding of Siglec15 to TLR2 has been confirmed as an indispensable cell recognition mechanism in RANKL-mediated osteoclast formation <sup>[55]</sup>.

## 5.2. Molecular switches in the membrane fusion execution stage

The membrane fusion execution stage is precisely regulated by various molecular switches. Research finds that decreased plasma membrane (PM) tension is a mechanical prerequisite for osteoclast fusion<sup>[10]</sup>. During RANKL-induced differentiation, reduced ezrin expression in fusion-committed progenitors leads to Membrane-Cortex Attachment (MCA)-dependent PM tension reduction<sup>[10,11]</sup>. Artificially increasing PM tension inhibits cell fusion. Furthermore, La protein plays a key role at this stage, reappearing on the osteoclast surface in a low molecular weight form and anchoring to transiently exposed phosphatidylserine on fusing cell surfaces via direct interaction with Annexin A5, thereby promoting fusion<sup>[11,56]</sup>. Notably, La protein's fusion-promoting role is independent of its classical RNA-binding function.

## 5.3. Regulation of multinucleation maintenance and functional polarization

The maintenance of the multinucleated state and functional polarization involves complex regulatory networks. Research finds that dynamic changes in O-GlcNAcylation are crucial for osteoclast maturation: increased O-GlcNAcylation in early stages promotes differentiation, while its downregulation later favors maturation<sup>[57]</sup>. In inflammatory arthritis, TNF $\alpha$  promotes osteoclastogenesis by regulating the dynamic changes of O-GlcNAcylation<sup>[57]</sup>. Additionally, ROS signaling and the atypical low molecular weight form of La protein jointly promote osteoclast fusion and bone resorption function<sup>[11]</sup>. Abnormal expression of SELENOW protein also affects cell fusion; its overexpression stimulates cell fusion, crucial for osteoclast maturation, while its deficiency inhibits osteoclast formation<sup>[58]</sup>. These findings collectively reveal a multi-layered regulatory mechanism for maintaining multinucleation and functional polarization.

# 6. Research models and technological methodological breakthroughs

## 6.1. Optimization and standardization of in vitro fusion models

Significant progress has been made in recent years in optimizing in vitro osteoclast fusion models. Researchers have established standardized culture systems based on bone marrow-derived macrophages (BMMs) and RAW264.7 monocytic cells by optimizing culture conditions<sup>[15]</sup>. Particularly noteworthy is the finding that modulating the stiffness of polydimethylsiloxane (PDMS) substrates significantly influences osteoclast differentiation progression; stiffer substrates accelerate differentiation, manifested by morphological changes and enhanced fusion/division activity<sup>[15]</sup>. Regarding model standardization, studies confirm that RANKL-mediated caspase-8 activation is an early key event in osteoclast fusion<sup>[59]</sup>, providing an important basis for selecting molecular markers in vitro. Furthermore, interference experiments confirm that reduced plasma membrane (PM) tension is a mechanical prerequisite for osteoclast fusion<sup>[10]</sup>, a discovery offering new standards for setting mechanical parameters in vitro models.

## 6.2. Application advances in high-resolution imaging technologies

High-resolution imaging technologies have played a pivotal role in osteoclast fusion research. Scanning electron microscopy has successfully revealed the fine morphological characteristics of tunneling nanotubes (TNTs) during osteoclastogenic fusion<sup>[60]</sup>. These actin-based membrane structures are confirmed to participate in the cell-cell fusion process between osteoclast precursors and multinucleated osteoclast-like cells, allowing observation of membrane vesicle and nuclear movement<sup>[61]</sup>. Two-photon microscopy live imaging enables real-time visualization of immune cell dynamics within the synovial microenvironment<sup>[62]</sup>, providing a powerful tool for studying osteoclast fusion behavior in physiological contexts. Notably, these imaging techniques have also revealed the spatial localization characteristics of La protein reappearing on the osteoclast surface as a low molecular weight species promoting fusion<sup>[26]</sup>.

## 6.3. Application of single-cell omics in mechanism studies

Single-cell RNA sequencing (scRNA-seq) technology has greatly advanced the understanding of osteoclast fusion mechanisms. This technology successfully identified specific macrophage subpopulations in joints that differentiate into

pathological mature osteoclasts <sup>[62]</sup>. In a rheumatoid arthritis (RA) mouse model, scRNA-seq library analysis revealed a novel RANK+TLR2+ monocyte population <sup>[63]</sup>. Integrated multi-omics analysis combined with single-cell technology has uncovered the transcriptional and epigenetic mechanisms guiding the continuous fusion process of osteoclasts from monocytes in adulthood <sup>[64]</sup>. These technologies also confirmed that partial activation of apoptotic mechanisms accompanies the differentiation of osteoclast precursors into mature multinucleated osteoclasts <sup>[8]</sup>, providing new perspectives for understanding the molecular basis of fusion.

#### **6.4. Value of gene editing technologies in mechanism elucidation**

Gene editing technologies have become essential tools for studying osteoclast fusion mechanisms. Specific knockout of the chromatin remodeler *Arid1a* in bone marrow-derived macrophages (BMDMs) inhibits cell-cell fusion and maturation of osteoclast precursors <sup>[65]</sup>. RNA interference confirmed that reducing plasma membrane tension promotes osteoclast fusion, whereas forcibly increasing PM tension by enhancing membrane-cortex attachment (MCA) inhibits cell-cell fusion <sup>[10]</sup>. Genetic manipulation also revealed the critical regulatory role of Selenoprotein W (SELENOW) in cell-cell fusion during osteoclast maturation <sup>[58]</sup>. Furthermore, DLEU1 silencing was found to hinder the fusion process, leading to the disappearance of the phagocytic cup fusion pattern and reduced fusion events between mononuclear precursors and multinucleated osteoclasts <sup>[55]</sup>. These findings highlight the unique value of gene editing technologies in mechanism elucidation.

### **7. Current controversies and challenges in research**

#### **7.1. Controversy regarding the hierarchy of different regulatory factors**

There is significant controversy regarding the hierarchical relationship among different regulatory factors in osteoclast fusion. Although DC-STAMP is widely considered a core molecule <sup>[55]</sup>, recent studies identify RANKL-mediated caspase-8 activation as a key upstream event <sup>[57]</sup>, suggesting a more complex regulatory hierarchy. Furthermore, multiple studies show NFATc1's regulatory effect on DC-STAMP expression <sup>[63,66]</sup>, while HIV infection experiments indicate the virus simultaneously affects the transcription levels of multiple key factors like RANK, NFATc1, and DC-STAMP <sup>[26]</sup>, complicating the determination of causal relationships. Particularly noteworthy is that SARS-CoV-2 variants can even promote RANKL-independent osteoclast formation <sup>[30]</sup>, further challenging the completeness of the existing regulatory network.

#### **7.2. Limitations of species differences on mechanism studies**

Species differences pose significant limitations to osteoclast fusion mechanism research. Mouse DC-STAMP deficiency models exhibit clear osteopetrotic phenotypes <sup>[55]</sup>, but the spectrum of manifestations associated with DC-STAMP mutations in human diseases remains incompletely elucidated. In HIV infection studies, the extent of the virus's impact on osteoclast precursors was found to be closely related to the viral inoculum size <sup>[26]</sup>, and this dose-dependent response may vary between species. Additionally, studies on TNF-transgenic mouse arthritis models found that the impact of DC-STAMP deletion on the arthritic phenotype requires accurate evaluation through bone marrow chimera experiments <sup>[29]</sup>, indicating complex species-specificity in the immune-bone axis regulation.

#### **7.3. Issues with consistency validation between in vivo and in vitro models**

Current research exposes significant issues in consistency validation between in vivo and in vitro models. In vitro experiments show that the IGF-PI3K-AKT pathway influences osteoclast differentiation by regulating marker genes like DC-STAMP <sup>[67]</sup>, but the spatiotemporal specificity of this pathway's regulation in vivo remains unclear. While scRNA-seq can reveal the heterogeneity of osteoclast precursor differentiation <sup>[9,57]</sup>, in vitro culture systems struggle to fully simulate the cell interactions within the bone marrow microenvironment. Notably, experiments using engineered *E. coli* to deliver DC-STAMP protein show that targeting strategies validated in vitro may produce unexpected bone-targeting effects in vivo, highlighting the complexity of translational research between models <sup>[14]</sup>. Furthermore, the role of membrane

mechanical properties in fusion revealed by new technologies like optical tweezers requires further validation of their physiological relevance across different model systems <sup>[10,15]</sup>.

## 8. Future research directions and technological pathways

### 8.1. Single-cell resolution strategies for spatiotemporal dynamic regulation

Single-cell RNA sequencing has revealed the activation characteristics of apoptosis-related genes during osteoclast precursor differentiation <sup>[6]</sup>, but the spatiotemporal dynamics of the fusion process require deeper analysis. Future research needs to integrate single-cell transcriptomics with live-cell imaging to precisely capture molecular events at key fusion nodes (e.g., initial contact, membrane fusion execution) <sup>[9]</sup>. Particular attention should be paid to how RANKL-induced caspase-8 activation spatiotemporally regulates membrane fusion <sup>[6]</sup>, and the changes in La protein's subcellular localization at different fusion stages <sup>[68]</sup>. Developing novel time-resolved single-cell multi-omics technologies holds promise for constructing a continuous differentiation map from mononuclear precursors to mature multinucleated osteoclasts <sup>[69]</sup>.

### 8.2. AI-assisted construction of molecular interaction networks

Existing research indicates that DC-STAMP forms dynamic interaction networks with proteins like Annexin A5 <sup>[11]</sup>, but the hierarchical relationships among various regulatory factors (e.g., Dyrk2 kinase, CD47-SIRP $\alpha$  axis) remain controversial. Artificial intelligence (AI) can integrate vast omics data to predict the weight of key molecular switches (e.g., Cited2) in the fusion cascade <sup>[69]</sup>. Deep learning models can help analyze the synergistic regulation patterns between mechanical signals (matrix stiffness) and biochemical signals (RANKL pathway) <sup>[15]</sup> and predict the regulatory role of membrane trafficking proteins like Rab11A in later fusion stages <sup>[70]</sup>. Furthermore, based on the hypothesis that ROS signaling regulates La protein trafficking <sup>[10]</sup>, machine learning can be used to build redox-sensitive molecular interaction prediction models.

### 8.3. Translational medical research pathways targeting fusion regulation

Engineered bacterial vectors (BEV-DCS) have proven capable of targeted delivery of DC-STAMP fusion protein to precursor cells <sup>[67]</sup>, providing proof-of-concept for developing therapies based on membrane fusion inhibitors. Future translational research should focus on three directions: (1) Developing specific antibodies targeting the low molecular weight form of La protein <sup>[50]</sup> to block its binding to phosphatidylserine <sup>[11]</sup>; (2) Utilizing gene editing to construct DC-STAMP conditional knockout models <sup>[16]</sup> to evaluate the therapeutic differences of intervention at various differentiation stages; (3) Optimizing biomaterials based on matrix stiffness regulation <sup>[15]</sup> to physically intervene in the fusion tendency of precursor cells. These strategies have clear application prospects for osteoporosis and other osteolytic diseases <sup>[71]</sup>.

## 9. Summary and core biological insights

Current research has established a molecular regulatory framework for osteoclast fusion centered on DC-STAMP. This framework comprises three key layers: the upstream signal input layer (RANKL-NFATc1 pathway), the core execution layer (DC-STAMP-mediated membrane fusion), and the auxiliary regulatory layer (including novel regulators like La protein and Dyrk2 kinase) <sup>[12,16]</sup>. It is particularly noteworthy that RANKL signaling promotes the fusion readiness of precursor cells in a non-apoptotic manner by activating caspase-8 and other apoptosis-related molecules <sup>[15,72]</sup>. Simultaneously, NF- $\kappa$ B and MAPK signaling pathways influence the transcription levels of fusion marker genes like DC-STAMP by regulating the expression of c-Fos and NFATc1 <sup>[70,73]</sup>. These findings collectively depict a multi-layered, dynamically regulated molecular network, providing a systematic theoretical framework for understanding osteoclast multinucleation.

Based on fusion mechanism research, DC-STAMP has emerged as the most promising therapeutic target for translation. Animal experiments show that DC-STAMP deficiency significantly alleviates arthritis symptoms and bone



erosion in TNF-transgenic mice <sup>[12]</sup>. In osteoporosis models, engineered bacterial vectors (BEV-DCS) targeting DC-STAMP demonstrate excellent bone-targeting capability and therapeutic potential <sup>[14]</sup>. Furthermore, small molecule compounds targeting fusion-related signaling pathways (e.g., NF- $\kappa$ B, JNK/p38/ERK MAPKs) can effectively block pathological bone resorption by inhibiting the NFATc1-DC-STAMP axis <sup>[22,55]</sup>. These discoveries provide a molecular basis for developing therapeutic strategies that specifically intervene in osteoclast fusion, holding significant application promise, particularly in inflammatory bone diseases and postmenopausal osteoporosis <sup>[9,12]</sup>.

The mechanisms revealed by osteoclast fusion research have broad biological implications. First, the caspase-8-mediated non-apoptotic cell fusion mechanism might be widely present in multinucleated giant cell formation processes. Second, the membrane reorganization mechanisms mediated by transmembrane proteins like DC-STAMP provide important references for understanding other cell fusion phenomena, such as myotube formation and placental syncytiotrophoblast development. Particularly noteworthy are the metabolic reprogramming features and mechanical signal sensing capabilities (via the integrin  $\alpha\beta 3$ -FAK-RhoA pathway) exhibited during osteoclast fusion, revealing a deep-level connection between cell fusion and microenvironmental adaptation. These findings expand the understanding of cell multinucleation phenomena.

## Funding

National Natural Science Foundation of China (Project No.: 82302026)

## Disclosure statement

The authors declare no conflict of interest.

## References

- [1] S e K, Delaisse JM, Borggaard XG, 2021, Osteoclast Formation at the Bone Marrow/Bone Surface Interface: Importance of Structural Elements, Matrix, and Intercellular Communication. *Seminars in Cell & Developmental Biology*, 112: 8–15.
- [2] Chen EH, Grote E, Mohler W, et al., 2007, Cell-Cell Fusion. *FEBS Letters*, 581: 2181–2193.
- [3] Xing L, Xiu Y, Boyce BF, 2012, Osteoclast Fusion and Regulation by RANKL-Dependent and Independent Factors. *World Journal of Orthopedics*, 3: 212–222.
- [4] Kim K, Lee SH, Ha KJ, et al., 2008, NFATc1 Induces Osteoclast Fusion via Up-Regulation of Atp6v0d2 and the Dendritic Cell-Specific Transmembrane Protein (DC-STAMP). *Molecular Endocrinology* (Baltimore, Md.), 22: 176–185.
- [5] Ishii M, Saeki Y, 2008, Osteoclast Cell Fusion: Mechanisms and Molecules. *Modern Rheumatology*, 18: 220–227.
- [6] Krishnacoumar B, Stenzel M, Garibagaoglu H, et al., 2024, Caspase-8 Promotes Scramblase-Mediated Phosphatidylserine Exposure and Fusion of Osteoclast Precursors. *Bone Research*, 12: 40.
- [7] Barnea-Zohar M, Stein M, Reuven N, et al., 2024, SNX10 Regulates Osteoclastogenic Cell Fusion and Osteoclast Size in Mice. *J Bone Miner Res*, 39: 1503–1517.
- [8] Leikina E, Whitlock JM, Melikov K, et al., 2024, Formation of Multinucleated Osteoclasts Depends on an Oxidized Species of Cell Surface-Associated La Protein. *eLife*, 13.
- [9] Gu R, Liu H, Hu M, et al., 2023, D-Mannose Prevents Bone Loss under Weightlessness. *Journal of Translational Medicine*, 21: 8.
- [10] Wan Y, Nemoto YL, Oikawa T, et al., 2025, Mechanical Control of Osteoclast Fusion by Membrane-Cortex Attachment and BAR Proteins. *The Journal of Cell Biology*, 224.
- [11] Whitlock JM, Leikina E, Melikov K, et al., 2023, Cell Surface-Bound La Protein Regulates the Cell Fusion Stage of Osteoclastogenesis. *Nature Communications*, 14: 616.

- [12] Garcia-Hernandez ML, Rangel-Moreno J, Garcia-Castaneda M, et al., 2022, Dendritic Cell-Specific Transmembrane Protein Is Required for Synovitis and Bone Resorption in Inflammatory Arthritis. *Front Immunol*, 13: 1026574.
- [13] Wang Q, Wang H, Yan H, et al., 2022, Suppression of Osteoclast Multinucleation via a Posttranscriptional Regulation-Based Spatiotemporally Selective Delivery System. *Science Advances*, 8: eabn3333.
- [14] Kong X, Liu H, Chen S, et al., 2025, Bioengineered Bacterial Extracellular Vesicles for Targeted Delivery of an Osteoclastogenesis-Inhibitory Peptide to Alleviate Osteoporosis. *Journal of Controlled Release: Official Journal of the Controlled Release Society*, 382: 113751.
- [15] Wang Q, Xie J, Zhou C, et al., 2022, Substrate Stiffness Regulates the Differentiation Profile and Functions of Osteoclasts via Cytoskeletal Arrangement. *Cell Proliferation*, 55: e13172.
- [16] Li X, Jiang Y, Liu X, et al., 2023, Mesenchymal Stem Cell-Derived Apoptotic Bodies Alleviate Alveolar Bone Destruction by Regulating Osteoclast Differentiation and Function. *International Journal of Oral Science*, 15: 51.
- [17] Yagi M, Miyamoto T, Sawatani Y, et al., 2005, DC-STAMP Is Essential for Cell-Cell Fusion in Osteoclasts and Foreign Body Giant Cells. *The Journal of Experimental Medicine*, 202: 345–351.
- [18] Jansen BJ, Eleveld-Trancikova D, Sanecka A, et al., 2009, OS9 Interacts with DC-STAMP and Modulates Its Intracellular Localization in Response to TLR Ligation. *Molecular Immunology*, 46: 505–515.
- [19] Moura SR, Sousa AB, Olesen JB, et al., 2024, Stage-Specific Modulation of Multinucleation, Fusion, and Resorption by the Long Non-Coding RNA DLEU1 and miR-16 in Human Primary Osteoclasts. *Cell Death & Disease*, 15: 741.
- [20] van Duijn A, Van der Burg SH, Scheeren FA, 2022, CD47/SIRP $\alpha$  Axis: Bridging Innate and Adaptive Immunity. *Journal for Immunotherapy of Cancer*, 10.
- [21] Chiu YH, Schwarz E, Li D, et al., 2017, Dendritic Cell-Specific Transmembrane Protein (DC-STAMP) Regulates Osteoclast Differentiation via the Ca(2+)/NFATc1 Axis. *Journal of Cellular Physiology*, 232: 2538–2549.
- [22] Kim SC, Gu DR, Yang H, et al., 2025, Polysaccharides from *Psoralea Corylifolia* Seeds Suppress Osteoclastogenesis and Alleviate Osteoporosis. *International Journal of Biological Macromolecules*, 315: 144423.
- [23] Liu T, Jiang L, Xiang Z, et al., 2022, Tereticornate A Suppresses RANKL-Induced Osteoclastogenesis via the Downregulation of c-Src and TRAF6 and the Inhibition of RANK Signaling Pathways. *Biomedicine & Pharmacotherapy*, 151: 113140.
- [24] Zhu G, Chen W, Tang CY, et al., 2022, Knockout and Double Knockout of Cathepsin K and Mmp9 Reveals a Novel Function of Cathepsin K as a Regulator of Osteoclast Gene Expression and Bone Homeostasis. *International Journal of Biological Sciences*, 18: 5522–5538.
- [25] Xu W, Chao R, Xie X, et al., 2024, IL13R $\alpha$ 2 as a Crucial Receptor for Ch1311 in Osteoclast Differentiation and Bone Resorption through the MAPK/AKT Pathway. *Cell Communication and Signaling: CCS*, 22: 81.
- [26] Sviercz FA, Jarmoluk P, Cevallos CG, et al., 2023, Massively HIV-1-Infected Macrophages Exhibit a Severely Hampered Ability to Differentiate into Osteoclasts. *Front Immunol*, 14: 1206099.
- [27] Li Y, Yang JY, Lin ML, et al., 2025, ACT001 Improves OVX-Induced Osteoporosis by Suppressing the NF-kappaB/NLRP3 Signaling Pathway. *Molecular Medicine (Cambridge, Mass.)*, 31: 131.
- [28] Qu T, Li B, Wang Y, 2022, Targeting CD47/SIRP $\alpha$  as a Therapeutic Strategy, Where We Are and Where We Are Headed. *Biomarker Research*, 10: 20.
- [29] Chen F, Tian L, Pu X, et al., 2022, Enhanced Ectopic Bone Formation by Strontium-Substituted Calcium Phosphate Ceramics through Regulation of Osteoclastogenesis and Osteoblastogenesis. *Biomaterials Science*, 10: 5925–5937.
- [30] Sviercz F, Jarmoluk P, Godoy Coto J, et al., 2024, The Abortive SARS-CoV-2 Infection of Osteoclast Precursors Promotes Their Differentiation into Osteoclasts. *Journal of Medical Virology*, 96: e29597.
- [31] Wolin SL, Cedervall T, 2002, The La Protein. *Annual Review of Biochemistry*, 71: 375–403.
- [32] Sims NA, Walsh NC, 2012, Intercellular Cross-Talk among Bone Cells: New Factors and Pathways. *Current Osteoporosis Reports*, 10: 109–117.
- [33] van Duijn A, Van der Burg SH, Scheeren FA, 2022, CD47/SIRP $\alpha$  Axis: Bridging Innate and Adaptive Immunity. *Journal for Immunotherapy of Cancer*, 10.

- 
- [34] Zheng J, He W, Chen Y, et al., 2025, Erianin Serves as an NFATc1 Inhibitor to Prevent Breast Cancer-Induced Osteoclastogenesis and Bone Destruction. *Journal of Advanced Research*, 69: 399–411.
  - [35] Logtenberg MEW, Scheeren FA, Schumacher TN, 2020, The CD47-SIRP $\alpha$  Immune Checkpoint. *Immunity*, 52: 742–752.
  - [36] Zhu D, Hadjivassiliou H, Jennings C, et al., 2024, CC-96673 (BMS-986358), an Affinity-Tuned Anti-CD47 and CD20 Bispecific Antibody with Fully Functional Fc, Selectively Targets and Depletes Non-Hodgkin's Lymphoma. *mAbs*, 16: 2310248.
  - [37] Xu Y, Song D, Lin X, et al., 2023, Corylifol A Protects against Ovariectomized-Induced Bone Loss and Attenuates RANKL-Induced Osteoclastogenesis via ROS Reduction, ERK Inhibition, and NFATc1 Activation. *Free Radical Biology & Medicine*, 196: 121–132.
  - [38] van Helden MJ, Zwarthoff SA, Arends RJ, et al., 2023, BYON4228 Is a Pan-Allelic Antagonistic SIRP $\alpha$  Antibody That Potentiates Destruction of Antibody-Opsonized Tumor Cells and Lacks Binding to SIRP $\gamma$  on T Cells. *Journal for Immunotherapy of Cancer*, 11: 1–12.
  - [39] Cendrowicz E, Jacob L, Greenwald S, et al., 2022, DSP107 Combines Inhibition of CD47/SIRP $\alpha$  Axis With Activation of 4-1BB to Trigger Anticancer Immunity. *Journal of Experimental & Clinical Cancer Research: CR*, 41: 97.
  - [40] Bae S, Kim K, Kang K, et al., 2023, RANKL-Responsive Epigenetic Mechanism Reprograms Macrophages Into Bone-Resorbing Osteoclasts. *Cellular & Molecular Immunology*, 20: 94–109.
  - [41] Sheng M, Lin Y, Xu D, et al., 2021, CD47-Mediated Hedgehog/SMO/GLI1 Signaling Promotes Mesenchymal Stem Cell Immunomodulation in Mouse Liver Inflammation. *Hepatology (Baltimore, Md.)*, 74: 1560–1577.
  - [42] Han X, Sterling H, Chen Y, et al., 2000, CD47, a Ligand for the Macrophage Fusion Receptor, Participates in Macrophage Multinucleation. *The Journal of Biological Chemistry*, 275: 37984–37992.
  - [43] Maile LA, DeMambro VE, Wai C, et al., 2011, An Essential Role for the Association of CD47 to SHPS-1 in Skeletal Remodeling. *Journal of Bone and Mineral Research: The Official Journal of the American Society for Bone and Mineral Research*, 26: 2068–2081.
  - [44] Uluçkan O, Becker SN, Deng H, et al., 2009, CD47 Regulates Bone Mass and Tumor Metastasis to Bone. *Cancer Research*, 69: 3196–3204.
  - [45] Lundberg P, Koskinen C, Baldock PA, et al., 2007, Osteoclast Formation Is Strongly Reduced Both in Vivo and in Vitro in the Absence of CD47/SIRP $\alpha$ -Interaction. *Biochemical and Biophysical Research Communications*, 352: 444–448.
  - [46] Møller AM, Delaissé JM, Søe K, 2017, Osteoclast Fusion: Time-Lapse Reveals Involvement of CD47 and Syncytin-1 at Different Stages of Nuclearity. *Journal of Cellular Physiology*, 232: 1396–1403.
  - [47] Hobolt-Pedersen AS, Delaissé JM, Søe K, 2014, Osteoclast Fusion Is Based on Heterogeneity Between Fusion Partners. *Calcif Tissue Int*, 95: 73–82.
  - [48] Zheng H, Liu Y, Deng Y, et al., 2024, Recent Advances of NFATc1 in Rheumatoid Arthritis-Related Bone Destruction: Mechanisms and Potential Therapeutic Targets. *Molecular Medicine (Cambridge, Mass.)*, 30: 20.
  - [49] Che Z, Wang W, Zhang L, et al., 2025, Therapeutic Strategies Targeting CD47-SIRP $\alpha$  Signaling Pathway in Gastrointestinal Cancers Treatment. *Journal of Pharmaceutical Analysis*, 15: 101099.
  - [50] Biedermann A, Patra-Kneuer M, Mougiakakos D, et al., 2024, Blockade of the CD47/SIRP $\alpha$  Checkpoint Axis Potentiates the Macrophage-Mediated Antitumor Efficacy of Tafasitamab. *Haematologica*, 109: 3928–3940.
  - [51] Luo N, Zhang L, Xiu C, et al., 2024, Piperlongumine, a Piper Longum-Derived Amide Alkaloid, Protects Mice From Ovariectomy-Induced Osteoporosis by Inhibiting Osteoclastogenesis via Suppression of p38 and JNK Signaling. *Food & Function*, 15: 2154–2169.
  - [52] Gal M, Kim O, Tran PT, et al., 2022, Mussaendoside O, a N-Triterpene Cycloartane Saponin, Attenuates RANKL-Induced Osteoclastogenesis and Inhibits Lipopolysaccharide-Induced Bone Loss. *Phytomedicine: International Journal of Phytotherapy and Phytopharmacology*, 105: 154378.
  - [53] Groetsch B, Schachtschabel E, Tripal P, et al., 2022, Inflammatory Activation of the Fc $\gamma$ R and IFN $\gamma$ R Pathways Co-Influences the Differentiation and Activity of Osteoclasts. *Front Immunol*, 13: 958974.
-

- [54] Kim H, Takegahara N, Choi Y, 2023, IgSF11-Mediated Phosphorylation of Pyruvate Kinase M2 Regulates Osteoclast Differentiation and Prevents Pathological Bone Loss. *Bone Research*, 11: 17.
- [55] Dou C, Zhen G, Dan Y, et al., 2022, Sialylation of TLR2 Initiates Osteoclast Fusion. *Bone Research*, 10: 24.
- [56] Leikina E, Tsaturyan AK, Melikov K, et al., 2025, Phosphatidylserine Exposure and Extracellular Annexin A5 Weaken the Actin Cortex in Osteoclast Fusion. *bioRxiv: The Preprint Server for Biology*, 1–12.
- [57] Li YN, Chen CW, Trinh-Minh T, et al., 2022, Dynamic Changes in O-GlcNAcylation Regulate Osteoclast Differentiation and Bone Loss via Nucleoporin 153. *Bone Research*, 10: 51.
- [58] Kim H, Lee K, Kim JM, et al., 2021, Selenoprotein W Ensures Physiological Bone Remodeling by Preventing Hyperactivity of Osteoclasts. *Nature Communications*, 12: 2258.
- [59] Zhang JQ, Takahashi A, Gu JY, et al., 2021, In Vitro and In Vivo Detection of Tunneling Nanotubes in Normal and Pathological Osteoclastogenesis Involving Osteoclast Fusion. *Laboratory Investigation: A Journal of Technical Methods and Pathology*, 101: 1571–1584.
- [60] Ma Y, Shi X, Zhao H, et al., 2022, Potential Mechanisms of Osteoprotegerin-Induced Damage to Osteoclast Adhesion Structures via P2X7R-Mediated MAPK Signaling. *International Journal of Molecular Medicine*, 49: 1–12.
- [61] Kukita T, Hiura H, Gu JY, et al., 2021, Modulation of Osteoclastogenesis through Adrenomedullin Receptors on Osteoclast Precursors: Initiation of Differentiation by Asymmetric Cell Division. *Laboratory Investigation*, 101: 1449–1457.
- [62] Hasegawa T, Ishii M, 2022, Pathological Osteoclasts and Precursor Macrophages in Inflammatory Arthritis. *Frontiers in Immunology*, 13: 867368.
- [63] Zhang W, Noller K, Crane J, et al., 2023, RANK(+)TLR2(+) Myeloid Subpopulation Converts Autoimmune to Joint Destruction in Rheumatoid Arthritis. *eLife*, 12: e85553.
- [64] Das A, Saeki K, Dell’Orso S, et al., 2025, Integrative Single-Cell RNA-Seq and ATAC-Seq Identifies Transcriptional and Epigenetic Blueprint Guiding Osteoclastogenic Trajectory. *Journal of Bone and Mineral Research*, 40: 1127–1143.
- [65] Zhang Y, Sun H, Huang F, et al., 2024, The Chromatin Remodeling Factor Arid1a Cooperates with Jun/Fos to Promote Osteoclastogenesis by Epigenetically Upregulating Siglec15 Expression. *Journal of Bone and Mineral Research*, 39: 775–790.
- [66] Liao R, Dewey MJ, Rong J, et al., 2024, Matrix-Bound Nanovesicles Alleviate Particulate-Induced Periprosthetic Osteolysis. *Science Advances*, 10: eadn1852.
- [67] Ma J, Zhu L, Zhou Z, et al., 2021, The Calcium Channel TRPV6 Is a Novel Regulator of RANKL-Induced Osteoclastic Differentiation and Bone Absorption Activity through the IGF-PI3K-AKT Pathway. *Cell Proliferation*, 54: e12955.
- [68] Wu J, Zhang B, Du W, et al., 2025, OC-STAMP Is a Potential Biomarker and Therapeutic Target for Silicosis: An Exploratory Investigation. *Journal of Translational Medicine*, 23: 214.
- [69] Tsukasaki M, Huynh NC, Okamoto K, et al., 2020, Stepwise Cell Fate Decision Pathways during Osteoclastogenesis at Single-Cell Resolution. *Nature Metabolism*, 2: 1382–1390.
- [70] Okusha Y, Tran MT, Itagaki M, et al., 2020, Rab11A Functions as a Negative Regulator of Osteoclastogenesis through Dictating Lysosome-Induced Proteolysis of c-Fms and RANK Surface Receptors. *Cells*, 9: –.
- [71] Jagannatha P, Tankka AT, Lorenz DA, et al., 2024, Long-Read Ribo-STAMP Simultaneously Measures Transcription and Translation with Isoform Resolution. *Genome Research*, 34: 2012–2024.
- [72] Zhu L, Tang Y, Li XY, et al., 2023, A Zeb1/MtCK1 Metabolic Axis Controls Osteoclast Activation and Skeletal Remodeling. *The EMBO Journal*, 42: e111148.
- [73] Ha MT, Tran PT, Tran HNK, et al., 2021, Anti-Osteoclastogenic Effects of Indole Alkaloids Isolated from Barley (*Hordeum Vulgare* Var. *Hexastichon*) Grass. *Journal of Agricultural and Food Chemistry*, 69: 12994–13005.

**Publisher’s note**

*Whioce Publishing remains neutral with regard to jurisdictional claims in published maps and institutional affiliations.*



# Research on Restoration Strategies for Human Body Functions Due to Gut Microbiota Dysbiosis in High-Altitude Hypoxia

Yanyan Wang<sup>1</sup>, Pan Geng<sup>1</sup>, Rui Xia<sup>1</sup>, Yuan Xing<sup>2\*</sup>, Yanxia Han<sup>2\*</sup>

<sup>1</sup>School of Public Health, Gansu University of Chinese Medicine, Lanzhou 730000, Gansu, China

<sup>2</sup>Department of Clinical Laboratory, the 940th Hospital of Joint Logistic Support Force, People's Liberation Army, Lanzhou 730000, Gansu, China

*\*Author to whom correspondence should be addressed.*

**Copyright:** © 2025 Author(s). This is an open-access article distributed under the terms of the Creative Commons Attribution License (CC BY 4.0), permitting distribution and reproduction in any medium, provided the original work is cited.

**Abstract:** High-altitude hypoxia can cause dysbiosis of the gut microbiota and disrupt its functional equilibrium. Subsequently, the gut microbiota causes multi-organ dysfunction due to “gut-organ axis” disruption. This review discusses the mechanisms underlying high-altitude hypoxia-induced gut microbiota and body dysfunction. The study systematically discusses the possible effects and applications of microbiota-focused therapeutic approaches, such as nutrition, probiotics/prebiotics, traditional Chinese medicine, and scientific exercise training, for maintaining gut microbiota homeostasis and bodily function. Finally, the study discusses future research directions focused on personalized intervention technologies to protect health at high altitude.

**Keywords:** High-altitude hypoxia; Gut microbiota; Functional repair; Microecological modulation

**Online publication:** December 26, 2025

## 1. Introduction

The hypoxic environment of high altitude is a major challenge for human physiology. Among all the body systems involved, the gut microbiota is an essential modulator of host physiology, and its dysbiosis is increasingly reported to be a pivotal factor involved in high altitude responses<sup>[1]</sup>. Dysregulated composition and function of microbiota not only aggravate gastrointestinal symptoms, but also induce further functional damage in remote organs through the “gut-brain axis” and “gut-lung axis”. Therefore, it is of great importance to elucidate the mechanisms underlying high altitude hypoxia-induced dysregulation of gut microbiota and host functional impairment. In addition, the study of microbiota modulation-based intervention is of great theoretical and applied significance for high altitude adaptation, as well as for the prevention and treatment of altitude illnesses, acute and chronic.

## 2. The Impact of high-altitude hypoxia on gut microbiota and human physiology

### 2.1. Characteristics of high-altitude hypoxia and its effects on human physiology

The most prominent high-altitude condition is the gradual decrease in atmospheric pressure and partial oxygen pressure with altitude, which causes low oxygen intake. This is the main problem of high-altitude hypoxia. This physical condition of hypoxia activates a series of complex physiological stress responses in the body (**Figure 1**).

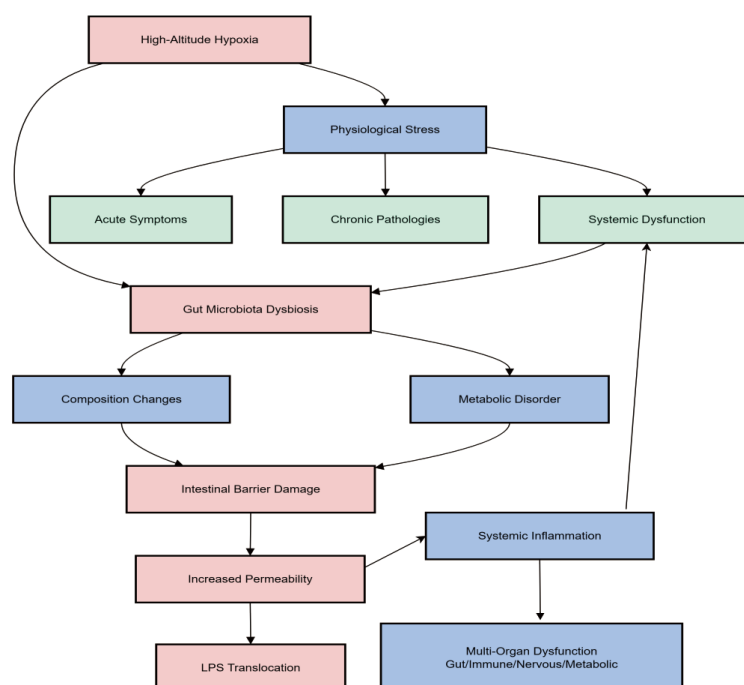


**Figure 1.** Mechanism of high-altitude hypoxia impact on human physiology via gut microbiota dysbiosis.

In order to get more oxygen to the vital organs such as the heart and brain, the body compensates for hypoxia by increasing respiration and heart rate and constricting peripheral blood vessels to redirect blood flow. Meanwhile, the kidneys release erythropoietin (EPO) to promote hematopoiesis in the bone marrow, increase the number of red blood cells and the concentration of hemoglobin and improve oxygen intake and transportation <sup>[2]</sup>. This compensation may also bring the potential risk of blood viscosity. In the acute process, the individuals will present typical acute high-altitude symptoms, such as headache, weakness, sleeplessness and indigestion. In the later period, high altitude can induce chronic pathological changes, such as high-altitude pulmonary hypertension and polycythemia. Moreover, hypoxia can directly or indirectly affect the energy metabolism, oxidative stress and immune function, which cause multiple organ dysfunction, providing a basis for subsequent dysbiosis of gut microbiota.

### 2.2. Changes in the structure and function of gut microbiota under high-altitude hypoxia

High-altitude hypoxia exerts a substantial and complicated effect on the composition and function of gut microbiota. At the phylum level, high-altitude hypoxia presents an imbalance in the F/B ratio, in which the relative abundance of Firmicutes increases while the relative abundance of Bacteroidetes decreases <sup>[3]</sup>. This change is closely related to energy absorption disturbance. At the genus level, high-altitude hypoxia causes a substantial decrease in the relative abundance of probiotics, such as *Lactobacillus* and *Bifidobacterium*, which have anti-inflammatory effects and can maintain the intestinal barrier, while the relative abundance of probiotics may decrease or the relative abundance of pathogenic microorganisms, such as *Desulfovibrio* and *Escherichia-Shigella*, may increase. In addition, high-altitude hypoxia can also affect the metabolic activity of the microbiota. One aspect is that the relative abundance of metabolites with protective effects on the intestinal barrier, such as butyrate and propionate, decreases, while the anti-inflammatory action of these metabolites is weakened <sup>[3]</sup>.

The other aspect is that the metabolism of amino acids and bile acids is disturbed, and the microbiota may produce more pro-inflammatory metabolites that participate in systemic inflammatory responses.

### **2.3. Mechanisms linking gut microbiota dysbiosis to abnormal human physiology**

Gut microbiota dysbiosis induces functional dysregulation in the human body via “gut-axis” pathways and cross-talk with multiple systems. The essence of gut microbiota dysbiosis may be focused on the intestinal barrier damage and the activation of the inflammatory response<sup>[4]</sup>. When gut microbiota dysbiosis is induced by hypoxia damage, the amount of SCFA decreases, which may lead to energy deficit in colon epithelial cells, down-regulation of expression of tight junction proteins, increased intestinal permeability, and “leaky gut.” Endotoxin (such as lipopolysaccharide, LPS) and other microbiota metabolites translocate into the blood and cause a low-grade whole-body inflammatory state. Inflammatory mediators not only directly damage the function of target tissues, but also affect the central nervous system through the “gut-brain axis” and aggravate cognitive dysfunction and mood disorders<sup>[5]</sup>. In addition, microbiota dysbiosis may increase metabolic burden in the liver and disturb immune homeostasis in the whole body. At the same time, the disturbance of microbiota metabolites, such as bile acid and tryptophan metabolites, may also interfere with energy metabolism, neuroendocrine regulation, and immune regulation of the host. These vicious cycles finally lead to dysfunction of the gut and digestive system, immune system, nervous system, and metabolic system.

## **3. Microbiota regulation-based strategies for functional repair under high-altitude hypoxia**

### **3.1. Nutritional intervention and dietary adjustment strategies**

Nutritional intervention and dietary regulation are two repair strategies that focus on enhancing gut microbiota homeostasis and recovery of human physiological functions in hypoxic environments at high altitudes. The essential principle of these strategies is to provide adequate dietary support to supply nutrients for beneficial bacteria and to simultaneously reduce the gastrointestinal burden. One fundamental strategy is to increase the intake of complex carbohydrates and dietary fibers, such as whole grain, vegetables, and fruits<sup>[6]</sup>. These foods act as prebiotics that are preferentially fermented by beneficial gut bacteria (mainly *Bifidobacterium* and *Lactobacillus*) to produce short-chain fatty acids (SCFAs), which can further repair the intestinal barrier, suppress inflammation, and regulate energy metabolism. In addition, an adequate amount of high-quality protein should be consumed to maintain tissue repair and immune function; meanwhile, the intake of red meat, which may stimulate the growth of harmful bacteria, should be reduced. Moreover, the intake of foods or supplements rich in polyunsaturated fatty acids (e.g., Omega-3) should be increased to reduce inflammatory responses<sup>[7]</sup>. Adequate intake of vitamins (e.g., Vitamin D, C, and E) and trace elements (e.g., zinc and iron) is essential to reduce oxidative stress and maintain the normal function of both the microbiota and host cells. Only with a well-balanced dietary structure can the study improve our gut microenvironment and lay the foundation for implementing other repair strategies.

### **3.2. Application of probiotics and prebiotics**

The use of probiotics and prebiotics is a precise approach to directly regulate the composition of gut microbiota and stimulate the proliferation of beneficial microbiota through exogenous supplementation (**Figure 2**). Probiotics are viable microorganisms that can provide a health benefit to the host at a defined dose, usually *Bifidobacterium* and *Lactobacillus*<sup>[8]</sup>. At high altitude, taking specific probiotics can directly supplement beneficial microbiota, compete with pathogenic microbiota for colonization sites, and keep the microbiota in a balanced state through their metabolic products, such as bacteriocins. More importantly, probiotics can improve the intestinal epithelial barrier, reduce endotoxin translocation, and regulate the host's immune response, thereby eliminating systemic inflammation. Prebiotics are non-digested dietary substances (such as inulin and oligosaccharides) that can serve as “fuel” and selectively stimulate the proliferation and

activity of beneficial microbiota<sup>[9]</sup>. When probiotics and prebiotics are used in combination, they often exhibit synergistic effects, and the overall effect of altering the microbiota structure and producing short-chain fatty acids is more pronounced, which can systematically regulate digestive, immune and metabolic abnormalities caused by high-altitude hypoxia. This is an effective and safe approach to microbiota manipulation.

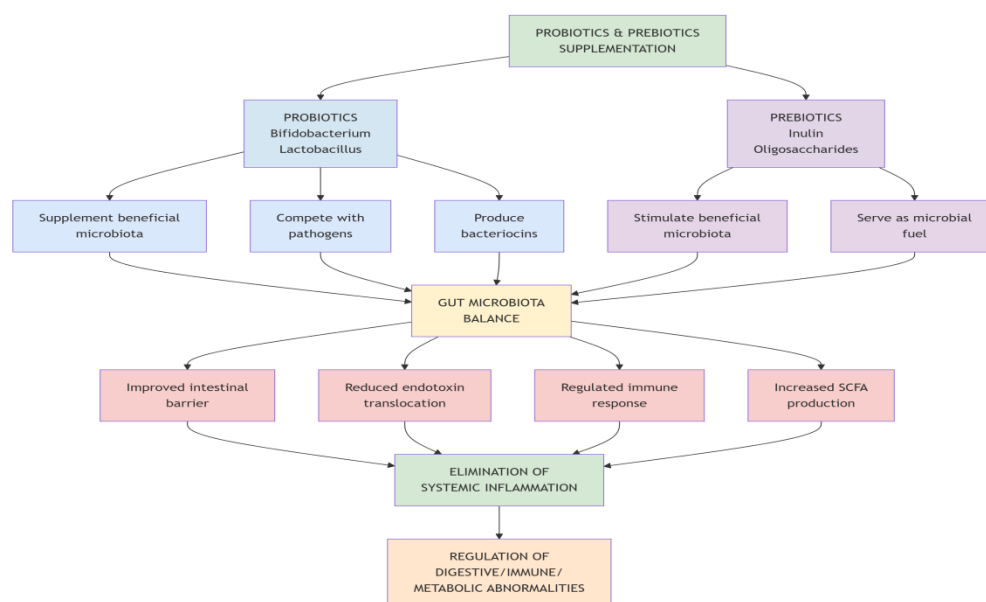


**Figure 2.** Mechanism of probiotics and prebiotics in regulating gut microbiota dysbiosis under high-altitude hypoxia.

### 3.3. Traditional Chinese Medicine (TCM) regulation strategy

The strategy of TCM regulation is based on the holistic view and differential treatment principle, and uses multiple components and multi-target actions to regulate microbiota dysbiosis induced by high-altitude hypoxia through the spleen and stomach dysfunction, qi and blood imbalance. According to the TCM theory, “high-altitude insufficient clear qi” would impair the spleen and stomach qi and cause “spleen dysfunction in transportation” and “poor gastric intake”, and then regulate the transformation of “food essence” and nourish the whole body, which is the TCM pathophysiology of microbiota dysbiosis<sup>[10]</sup>. Therefore, the therapeutic strategy usually focuses on “tonifying qi, strengthening the spleen, harmonizing the stomach, expelling dampness, and promoting blood circulation”. TCM herbs like Astragalus and Codonopsis can enhance the anti-hypoxia capacity and metabolic ability of the body. Poria and Atractylodes can regulate the spleen and stomach dysfunction and restore the function of transportation and absorption, and then improve the internal environment. Rhodiola and other herbs that tonify qi and promote blood circulation can enhance the body’s oxygen transport and microcirculation. These compound herbal medicines and their active ingredients (polysaccharides, flavonoids, and saponins) can directly regulate the composition of gut microbiota and promote the growth of beneficial bacteria and inhibit the growth of harmful microbes. Meanwhile, they can also improve the anti-inflammatory, antioxidant, and gut barrier repair functions, and then adjust the “gut-lung” and “gut-brain” axis by these multiple ways and improve the functional interactions of the axis by TCM strategy, so as to regulate microbiota and enhance the ability of the body to adapt to high-altitude hypoxia.

### 3.4. Combined application of exercise and adaptation training

Strategically combining exercise and adaptation training comprehensively improves the body’s repair capacity and overall hypoxic tolerance through physiological reconstruction of higher hypoxic tolerance, and directly adjusts gut microbiota by proactive intervention through regulating the gut microbiota–host interaction. This strategy is based on a

scientific and gradual approach. Pre-adaptation training (intermittent hypoxic training) before ascent to a high-altitude environment activates the HIF signaling pathway, improves cardiopulmonary function, enhances the ability of red blood cells to carry oxygen and improves the body's own resistance to oxidative damage, and thus creates a physiological basis for adapting to real high-altitude environment. After arriving at high altitude, individualized, moderate-intensity regular exercise (brisk walking, jogging, yoga) can improve intestinal peristalsis, promote the circulation of abdominal blood and protect intestinal barrier function and microbiota transport, creating a better mechanical and chemical environment for the proliferation of beneficial bacteria. Regular exercise can increase the amount of short chain fatty acid-producing bacteria and decrease the amount of inflammatory factors. Meanwhile, exhaustive exercise of high intensity may further damage the intestinal mucosa and induce ischemia, increase oxidative stress and aggravate microbiota homeostasis imbalance. Therefore, combining scientific exercise and stepwise adaptation training can improve the physiological function, maintain the internal environment and provide a better guarantee for microbiota reconstruction.

#### **4. Application and prospects of high-altitude gut microbiota regulation strategies**

Although the results of various intervention strategies for regulating gut microbiota at high altitude show some potential, their effects are significantly limited, and further comprehensive assessment is warranted. Nutritional dietary regulation is the most basic support method and is highly safe with easy implementation; however, its effects are low and gradually manifested based on the dependence of individuals' long-term compliance. The effects of probiotic/prebiotic intervention on regulating gut microbiota are evident in terms of enhancing the proportion of certain microbiota (such as *Lactobacillus* and *Bifidobacterium*) and ameliorating gastrointestinal hypoxia symptoms; however, the effects of this intervention are strain-specific and highly individualized. The long-term safety of this intervention and its effect on native microbiota remain unclear. The advantage of TCM formulations lies in their multi-target regulation, and they have a long history of application in ameliorating hypoxia symptoms and gastrointestinal function<sup>[11]</sup>. However, the advantages of TCM intervention are obscured by its composition complexity and unclear action mechanism, and the effect of TCM on microbiota is unclear. Furthermore, large samples and RCTs are lacking, making it difficult for TCM to be accepted by evidence-based medicine. The standardization and dose determination are also challenging issues for its widespread application. Exercise and adaptation training offer the most basic benefits; however, their application is limited by individuals' fitness levels and training conditions, and inappropriate exercise may increase the body's burden. In summary, existing strategies are single interventions without microbiota-based combinatory treatment based on individual differences, and their long-term effect and cost-effectiveness should be further assessed by comprehensive clinical studies.

#### **5. Conclusion**

In summary, high-altitude hypoxia causes obvious dysbiosis of gut microbiota and further leads to multisystem dysfunction via the "gut-organ axis." Nutritional regulation, probiotic/prebiotic intake, TCM regulation, and scientific exercise mode exhibit great potential in regulating dysbiotic gut microbiota and physiological function. In the future, researchers should focus on the "personalized medicine" principles to explore the underlying mechanisms in more detail and advance the development and translation of precise and effective microbiome intervention strategies. This will offer more theoretical basis and practical guidance for high altitude residents to maintain their health.

#### **Funding**

Key Program of Gansu Joint Research Fund (Project No.: 25JRRA1183)



## Disclosure statement

The authors declare no conflict of interest.

## References

- [1] Qiu F, Sun Y, Li W, et al., 2025, A Review on Drug-Metabolizing Enzymes, Transporters, and Gut Microbiota on Pharmacokinetics in High-Altitude Environment. *Current Drug Metabolism*, 25(10): 719–733.
- [2] Li W, Wang Y, Shi Y, et al., 2024, The Gut Microbiota Mediates Memory Impairment under High-Altitude Hypoxia via the Gut–Brain Axis in Mice. *The FEBS Journal*, 292(4): 809–826.
- [3] Wang J, Wang H, Li C, et al., 2025, Comprehensive Study of Tilapia Skin Collagen Peptide on Ileal Injury and Intestinal Flora in Rats Induced by High-Altitude Hypoxia. *Journal of Functional Foods*, 124: 106634–106634.
- [4] Ma Q, Ma J, Cui J, et al., 2023, Oxygen Enrichment Protects against Intestinal Damage and Gut Microbiota Disturbance in Rats Exposed to Acute High-Altitude Hypoxia. *Frontiers in Microbiology*, 14: 1268701–1268701.
- [5] Zhang J, Sun Y, He J, et al., 2023, Comprehensive Investigation of the Influence of High-Altitude Hypoxia on Clopidogrel Metabolism and Gut Microbiota. *Current Drug Metabolism*, 24(10): 723–733.
- [6] Liao Y, Chen Z, Yang Y, et al., 2023, Antibiotic Intervention Exacerbated Oxidative Stress and Inflammatory Responses in SD Rats under Hypobaric Hypoxia Exposure. *Free Radical Biology & Medicine*, 209(P1): 70–83.
- [7] Li B, Xu Y, Wang D, et al., 2025, High-Altitude Acute Hypoxia Endurance and Comprehensive Lung Function in Pilots. *Aerospace Medicine and Human Performance*, 96(3): 191–97.
- [8] Coronel-Oliveros C, Medel V, Whitaker G A, et al., 2024, Elevating Understanding: Linking High-Altitude Hypoxia to Brain Aging through EEG Functional Connectivity and Spectral Analyses. *Network Neuroscience*, 8(1): 18.
- [9] Liu G, Bai X, Yang J, 2023, Relationship between Blood–Brain Barrier Changes and Drug Metabolism under High-Altitude Hypoxia: Obstacle or Opportunity for Drug Transport? *Drug Metabolism Reviews*, 55(1–4): 107–125.
- [10] Storz J, Scott G, 2019, Life Ascending: Mechanism and Process in Physiological Adaptation to High-Altitude Hypoxia. *Annual Review of Ecology, Evolution, and Systematics*, 50(1): 503–526.
- [11] Chicco A, Le C, Gnaiger E, et al., 2018, Adaptive Remodeling of Skeletal Muscle Energy Metabolism in High-Altitude Hypoxia: Lessons from AltitudeOmics. *Journal of Biological Chemistry*, 293(18): RA117.000470.
- [12] Cao W, Zeng Y, Su Y, et al., 2024, The Involvement of Oxidative Stress and the TLR4/NF- $\kappa$ B/NLRP3 Pathway in Acute Lung Injury Induced by High-Altitude Hypoxia. *Immunobiology*, 229(3): 152809.

### Publisher's note

*Whoice Publishing remains neutral with regard to jurisdictional claims in published maps and institutional affiliations.*

# Discussion on the Value of Six-item Detection of Sex Hormones by Chemiluminescence Immunoassay in the Diagnosis and Treatment of Gynecological Endocrine Diseases

Yuan Xiu\*

Yancheng Dexin Hospital Yancheng 224000, Jiangsu, China

*\*Author to whom correspondence should be addressed.*

**Copyright:** © 2025 Author(s). This is an open-access article distributed under the terms of the Creative Commons Attribution License (CC BY 4.0), permitting distribution and reproduction in any medium, provided the original work is cited.

**Abstract:** *Objective:* To explore the value of using chemiluminescence immunoassay to detect six sex hormones in the diagnosis and treatment of gynecological endocrine diseases, and to compare it with the indicators of healthy women. *Methods:* 50 patients with gynecological endocrine diseases admitted to our hospital from January 2022 to December 2023 were selected as the disease group, and 50 healthy women who underwent physical examinations in our hospital during the same period were selected as the healthy group. Chemiluminescence immunoassay was used to detect six sex hormones (follicle-stimulating hormone, luteinizing hormone, estradiol, progesterone, testosterone, and prolactin) in the two groups of research subjects, and the test results of the two groups were compared. *Results:* The levels of follicle-stimulating hormone, luteinizing hormone, testosterone and prolactin in the disease group were higher than those in the healthy group, while the levels of estradiol and progesterone were lower than those in the healthy group, and the differences were statistically significant ( $P < 0.05$ ). *Conclusion:* The detection of six sex hormones by chemiluminescent immunoassay is of great value in the diagnosis and treatment of gynecological endocrine diseases. By comparing with the indicators of healthy women, it can provide a reliable basis for the diagnosis and treatment of diseases.

**Keywords:** Chemiluminescence immunoassay; Six items of sex hormones; Gynecological endocrine diseases; Healthy women; Diagnostic and therapeutic value

**Online publication:** December 26, 2025

## 1. Introduction

Gynecological endocrine diseases are very common among women, including polycystic ovary syndrome, premature ovarian failure, and dysfunctional uterine bleeding. They can damage women's health and affect fertility<sup>[1]</sup>. Sex hormones have a great role in regulating female growth, development and reproductive functions, and abnormal levels are closely related to gynecological endocrine diseases. Chemiluminescence immunoassay has high sensitivity and specificity, and is widely used in hormone detection. Nowadays, women's life pressure is increasing, environmental factors have become complex, and the incidence of gynecological endocrine diseases is increasing every year, causing troubles for many women's lives. Early and accurate diagnosis and timely treatment are key to improving the prognosis of patients with

such diseases, and finding a reliable detection method is an important prerequisite for achieving this goal. Some previous detection methods were either insufficiently sensitive or cumbersome to operate, making it difficult to meet clinical needs. The emergence of chemiluminescence immunoassay provides the possibility to solve these problems, and it can accurately detect subtle changes in sex hormones. Based on these circumstances, this study used chemiluminescence immunoassay to detect six sex hormones in patients with gynecological endocrine diseases and healthy women. 50 patients with gynecological endocrine diseases admitted to our hospital from January 2022 to December 2023 were selected as the disease group. At the same time, 50 healthy women who underwent physical examinations in our hospital during the same period were selected as the healthy group. The results were compared and analyzed to clarify the value of this method in the diagnosis and treatment of gynecological endocrine diseases and provide some clinical reference.

## 2. Materials and methods

### 2.1. General information

Fifty patients with gynecological endocrine diseases admitted to our hospital from January 2022 to December 2023 were selected as the disease group, and 50 healthy women who underwent physical examinations in our hospital during the same period were selected as the healthy group. The age of the disease group was 22–55 years old, with an average age of  $(35.26 \pm 6.38)$  years old; the age of the healthy group was 21–56 years old, with an average age of  $(34.89 \pm 5.97)$  years old. Comparing the general data of the two groups, the difference was not statistically significant ( $P > 0.05$ ) and was comparable. Inclusion criteria: (1) The disease group met the diagnostic criteria for gynecological endocrine diseases; (2) The healthy group had no gynecological diseases and endocrine-related diseases; (3) All research subjects gave informed consent. Exclusion criteria: (1) People with severe liver and kidney dysfunction; (2) People who have recently used drugs that affect sex hormone levels; (3) Women who are pregnant or lactating.

### 2.2. Method

Both groups of research subjects drew 3 ml of venous blood in the early morning on an empty stomach. After centrifuging the serum, chemiluminescence immunoassay was used to detect six sex hormones, including follicle-stimulating hormone, luteinizing hormone, estradiol, progesterone, testosterone, and prolactin. The detection instrument is the Abbott i2000 chemiluminescent immunoanalyzer, and the reagents match the original reagents. The operation should be strictly carried out in accordance with the instructions of the instrument and reagents.

### 2.3. Observation indicators

The levels of six sex hormones (follicle-stimulating hormone, luteinizing hormone, estradiol, progesterone, testosterone, and prolactin) of the two groups of research subjects were compared.

### 2.4. Statistical methods

Data were analyzed using SPSS24.0. t-test for measurement data;  $\chi^2$  test for count data.  $P < 0.05$  represents a significant difference.

## 3. Results

### 3.1. Comparison of follicle-stimulating hormone and luteinizing hormone levels between the two groups

The levels of follicle-stimulating hormone and luteinizing hormone in the disease group were higher than those in the healthy group ( $P < 0.05$ ) (Table 1).



**Table 1.** Comparison of follicle-stimulating hormone and luteinizing hormone levels between the two groups (mean  $\pm$  SD, mIU/mL)

Group	Follicle-stimulating hormone	Luteinizing hormone
Healthy group (50)	6.23 $\pm$ 1.56	5.89 $\pm$ 1.42
Disease group (50)	12.56 $\pm$ 3.21	10.32 $\pm$ 2.87
<i>t</i>	12.541	9.783
<i>P</i>	0.000	0.000

### 3.2. Comparison of estradiol and progesterone levels between the two groups

The levels of estradiol and progesterone in the disease group were lower than those in the healthy group ( $P < 0.05$ ) (Table 2).

**Table 2.** Comparison of estradiol and progesterone levels between the two groups (mean  $\pm$  SD, estradiol: pg/mL; progesterone: ng/mL)

Group	Estradiol (pg/mL)	Progesterone (ng/mL)
Healthy group (50)	156.32 $\pm$ 32.45	8.23 $\pm$ 2.15
Disease group (50)	89.65 $\pm$ 25.32	3.56 $\pm$ 1.23
<i>t</i>	11.454	13.332
<i>P</i>	0.000	0.000

### 3.3. Comparison of testosterone and prolactin levels between the two groups

The testosterone and prolactin levels in the disease group were higher than those in the healthy group ( $P < 0.05$ ) (Table 3).

**Table 3.** Comparison of testosterone and prolactin levels between the two groups (mean  $\pm$  SD)

Group	Testosterone (ng/dL)	Prolactin (ng/mL)
Healthy group (50)	45.23 $\pm$ 8.65	15.67 $\pm$ 4.23
Disease group (50)	78.56 $\pm$ 12.34	32.45 $\pm$ 7.89
<i>t</i>	15.639	13.254
<i>P</i>	0.000	0.000

## 3. Discussions

The occurrence and development of gynecological endocrine diseases are closely related to sex hormone level disorders, so accurate detection of sex hormone levels is very important for disease diagnosis, treatment and prognosis assessment. As an advanced detection technology, chemiluminescence immunoassay combines the high sensitivity of chemiluminescence and the high specificity of immunoassay, and can quickly and accurately detect trace amounts of sex hormones in the body, thereby providing strong technical support for the diagnosis and treatment of gynecological endocrine diseases.

Judging from the results of this study, the follicle-stimulating hormone level in the disease group was significantly higher than that in the healthy group. The main function of follicle-stimulating hormone is to promote the development and maturation of follicles. In diseases such as ovarian hypofunction, because the ovary is less sensitive to follicle-stimulating hormone, the body will secrete more follicle-stimulating hormone to promote follicle development, resulting

in an increase in its level. For example, in patients with premature ovarian failure, the number and quality of follicles in the ovaries are reduced, which will cause the level of follicle-stimulating hormone to rise significantly. This is also one of the important indicators for the clinical diagnosis of premature ovarian failure. Detecting follicle-stimulating hormone through chemiluminescence immunoassay can promptly detect abnormal changes in its levels, providing a reliable basis for the diagnosis of ovarian function-related diseases. For some patients with ovarian hypofunction who have no obvious early symptoms, this detection method can detect the problem earlier, allowing the patient to receive treatment in time and delay the progression of the disease. The level of luteinizing hormone in the disease group was also higher than that in the healthy group. Luteinizing hormone plays a key role in ovulation and can promote the formation of the corpus luteum and the secretion of progesterone. In patients with polycystic ovary syndrome, elevated luteinizing hormone levels are common, which is related to dysregulation of the hypothalamic-pituitary-ovarian axis. Excessive luteinizing hormone levels will affect the normal development of follicles and ovulation, leading to irregular menstruation and infertility in patients. Accurate detection of luteinizing hormone levels with the help of chemiluminescence immunoassay can help diagnose and evaluate diseases such as polycystic ovary syndrome. It can also provide a reference for the formulation of subsequent treatment plans, such as regulating luteinizing hormone levels with drugs to restore normal ovulation function in patients. In clinical practice, many patients with polycystic ovary syndrome are troubled by abnormal ovulation. With accurate luteinizing hormone test results, doctors can use medications more targeted to improve treatment effects.

Estradiol is the main estrogen and plays an important role in the development and maintenance of female reproductive organs. In this study, the estradiol level in the disease group was lower than that in the healthy group, which is common in diseases such as ovarian hypofunction and menopausal syndrome. Reduced estradiol levels can lead to thinning of the endometrium, menstrual disorders, and, in severe cases, affect fertility. Using chemiluminescence immunoassay to detect estradiol levels can clearly reflect the estrogen status in the body, which is of great significance for judging ovarian function and assessing the health status of menopausal women. During treatment, the dose of estrogen supplementation therapy can also be adjusted by monitoring estradiol levels to achieve the best effect. For menopausal women, appropriate estrogen supplementation is very important, not only to relieve uncomfortable symptoms but also to avoid overdosing, and accurate estradiol detection is an important basis for adjusting the dosage.

Progesterone is mainly secreted by the corpus luteum, and its level is closely related to the function of the corpus luteum. The progesterone level in the disease group was lower than that in the healthy group, suggesting that the luteal function may be insufficient. Insufficient luteal function will affect the implantation of the fertilized egg and maintenance of pregnancy, and can easily lead to miscarriage, shortened menstrual cycle, etc.<sup>[2]</sup> Detecting progesterone levels by chemiluminescence immunoassay can promptly detect abnormal luteal function and provide assistance in the diagnosis and treatment of infertility, habitual abortion, and other diseases. In clinical treatment, doctors can timely supplement progesterone based on progesterone level testing results to improve pregnancy success rates and reduce miscarriage. Many patients with habitual miscarriage have insufficient luteal corpus function. After timely supplementation of progesterone, the pregnancy success rate is significantly improved. Although testosterone is an androgen, it is also present in women's bodies to a certain extent. Excessive levels can have adverse effects on women's reproductive functions and appearance. Testosterone levels in the disease group in this study were higher than those in the healthy group, which is common in patients with polycystic ovary syndrome. Excessive testosterone can inhibit ovulation, leading to irregular menstruation, hirsutism, acne, etc. Chemiluminescence immunoassay can accurately detect subtle changes in testosterone levels, which is important for the diagnosis and monitoring of polycystic ovary syndrome. During treatment, the therapeutic effect can be evaluated by monitoring testosterone levels, such as using anti-androgens to see if testosterone levels decrease, and then adjusting the treatment plan. For polycystic ovary syndrome patients with symptoms such as hirsutism and acne, reducing testosterone levels can effectively improve these external manifestations and improve the patient's quality of life. The main function of prolactin is to promote mammary gland development and milk secretion. Increased levels of prolactin will inhibit gonadal axis function, leading to menstrual disorders, amenorrhea, infertility, etc.<sup>[3]</sup> The prolactin level in the disease group was higher than that in the healthy group, which may be related to pituitary microadenoma, drug

effects, etc. The chemiluminescent immunoassay method has high sensitivity for detecting prolactin and can promptly detect abnormalities in its levels, providing a basis for the diagnosis of prolactinoma and other diseases. For gynecological endocrine diseases caused by excessive prolactin levels, the treatment effect can be evaluated by detecting prolactin levels. For example, after using drugs such as bromocriptine, it is necessary to see whether prolactin returns to normal to determine whether the treatment is effective. Some patients experience amenorrhea due to excessive prolactin. After drug treatment, as prolactin levels decrease, menstruation can gradually return to normal.

The chemiluminescent immunoassay method has many advantages in detecting six sex hormones. The detection speed is fast, and the results can be produced in a short time, which meets the needs of rapid clinical diagnosis. The test results have good reproducibility, and there is little difference in test results at different times and different batches, ensuring accuracy and reliability<sup>[4]</sup>. Compared with other detection methods, it does not require cumbersome operating steps, has a high degree of automation, reduces the impact of human factors on the detection results, and improves detection efficiency. These advantages make the chemiluminescent immunoassay method widely used in the diagnosis and treatment of gynecological endocrine diseases, and have become a common method for clinical detection of six sex hormones. In primary hospitals, this efficient and accurate testing method can also help doctors better diagnose diseases, allowing patients to get more accurate test results without going to large hospitals. Comparing the six levels of sex hormones in patients with gynecological endocrine diseases with healthy women can more clearly detect abnormal changes in sex hormone levels under disease conditions and provide clear reference standards for disease diagnosis<sup>[5,6]</sup>. In clinical practice, doctors can accurately diagnose the disease based on the patient's clinical symptoms and the results of six sex hormone tests. For example, in patients with irregular menstruation, if the levels of follicle-stimulating hormone and luteinizing hormone are elevated and the estradiol level is reduced, it may indicate ovarian hypofunction; if the levels of testosterone and prolactin are elevated, it may indicate polycystic ovary syndrome or pituitary microadenomas. This diagnostic method that combines symptoms and test results can reduce misdiagnosis and missed diagnosis. During the course of disease treatment, regular testing of six levels of sex hormones can evaluate the treatment effect and adjust the treatment plan in a timely manner. For example, in patients with polycystic ovary syndrome, after drug treatment, if the testosterone level decreases and the ratio of luteinizing hormone and follicle-stimulating hormone returns to normal, it means that the treatment is effective; if there is no significant change in the test results, it is necessary to consider adjusting the treatment drug or dose<sup>[7,8]</sup>.

At the same time, long-term monitoring of six levels of sex hormones can also predict disease prognosis. For example, the level of follicle-stimulating hormone in patients with premature ovarian failure continues to increase, indicating further decline in ovarian function and poor prognosis. Through dynamic monitoring, doctors can adjust treatment strategies in a timely manner to improve patient prognosis as much as possible. In addition, the six-item test of sex hormones can also be used for disease prevention and health management. Regular testing for healthy women can help them understand their endocrine status and detect potential health problems in a timely manner. For example, a slight increase in prolactin levels is found during physical examination. Although there are no obvious clinical symptoms, diseases such as pituitary microadenoma can be ruled out through further examination, so as to achieve early detection and early intervention to prevent the occurrence of gynecological endocrine diseases. For women with a family history of gynecological endocrine diseases, regular testing is even more necessary, and preventive measures can be taken in advance. Although the detection cost of chemiluminescence immunoassay is slightly higher than that of some traditional methods, considering the accuracy and efficiency of its detection, it is worth it from the overall diagnosis and treatment effect. It can reduce misdiagnosis and mistreatment caused by inaccurate detection and reduce the overall medical cost of patients. With the continuous development of technology, the cost of chemiluminescent immunoassay may gradually decrease, allowing it to be used in a wider range of applications. In future clinical practice, chemiluminescence immunoassay can also be combined with other detection methods to form a more complete diagnosis and treatment system and provide better medical services for patients with gynecological endocrine diseases. For example, combined with ultrasound examination, it can provide a more comprehensive understanding of the patient's condition and improve the accuracy of diagnosis<sup>[9,10]</sup>.

## 4. Conclusion

In summary, the chemiluminescence immunoassay method to detect six sex hormones is of great value in the diagnosis and treatment of gynecological endocrine diseases. By comparing with the indicators of healthy women, it can provide a reliable basis for disease diagnosis and help doctors accurately judge the condition; it can be used to evaluate the effect during treatment and guide the adjustment of treatment plans; it can also provide a reference for disease prognosis assessment and prevention. Therefore, in clinical work, we should pay attention to the application of chemiluminescence immunoassay in the detection of six sex hormones, give full play to its advantages, and provide better services for the diagnosis and treatment of patients with gynecological endocrine diseases.

## About the author

Yuan Xiu (1980-), female, Han nationality, native of Yancheng, Jiangsu Province, undergraduate, supervisor of inspector, main research direction is inspection and testing technology.

## Disclosure statement

The author declares no conflict of interest.

## References

- [1] Hou Q, 2025, Research on Process Optimization of Simultaneous Detection of Sex Hormones by Chemiluminescence Method. *Laboratory Testing*, 3(13): 57–59.
- [2] Li X, Yan Y, Yu Q, 2024, Effects of Gengniangan Capsule Combined with Hormone Replacement Therapy on Sex Hormone Levels, Thyroid Hormones and Immune Function in Patients with Menopausal Syndrome. *Chinese Journal of Gerontology*, 44(06): 1388–1391.
- [3] Zhang H, 2024, Clinical Value of CLIA Method for Detecting Six Sex Hormones in the Diagnosis of Female Reproductive Endocrine Diseases. *Systems Medicine*, 9(01): 153–156.
- [4] Sun L, Liang X, Liang C, et al., 2023, Correlation between Sex Hormone Levels and Immune Regulation Imbalance in PCOS Infertile Patients and Its Predictive Value for Ovulation Outcome after Ovulation Induction Treatment. *Chinese Sexual Science*, 32(12): 68–72.
- [5] Chen F, 2023, Expression and Correlation Analysis of miR-21/SIRT1 in Premature Ovarian Insufficiency. *Chinese Maternal and Child Health Care*, 38(17): 3269–3272.
- [6] Xiong D, 2023, Diagnostic Analysis of Gynecological Diseases Using Chemiluminescence Instrument to Detect Six Items of Sex Hormones. *China Medical Device Information*, 29(06): 87–89.
- [7] Deng Y, Huang M, Yu F, Jian C, 2022, Correlation between Sex Hormone Levels and Interleukin-6 in Patients with Postmenopausal Primary Sjögren's Syndrome. *Chinese Maternal and Child Health Care*, 37(21): 3906–3909.
- [8] Fan X, Zhu Z, Zhu H, et al., 2022, Correlation Analysis of Serum NO and ET Levels with Sex Hormone Levels and Sperm Quality in Patients with Varicocele. *Chinese Experimental Diagnostics*, 26(09): 1324–1327.
- [9] Huang W, 2022, Application Value of Chemiluminescent Immunoassay of Serum Hormones in Male Sexual Dysfunction. *Systems Medicine*, 7(13): 87–90.
- [10] Ge J, Yang N, Zhang X, et al., 2022, Comparative Analysis of Chemiluminescence Method and Liquid Chromatography Tandem Mass Spectrometry for the Determination of Sex Hormones in Women with Polycystic Ovary Syndrome. *Zhongnan Pharmacy*, 20(03): 561–564.

### Publisher's note

*Whioce Publishing remains neutral with regard to jurisdictional claims in published maps and institutional affiliations.*



# Analysis of the Application Effect of Preoperative Prehabilitation Based on the ERAS Concept in the Rapid Postoperative Recovery of Elderly Patients with Lung Cancer

Xiaoping Huang, Qiaoming Gao

Taizhou Hospital of Traditional Chinese Medicine, Taizhou 225300, Jiangsu, China

**Copyright:** © 2025 Author(s). This is an open-access article distributed under the terms of the Creative Commons Attribution License (CC BY 4.0), permitting distribution and reproduction in any medium, provided the original work is cited.

**Abstract:** *Objective:* To explore the application effect of preoperative prehabilitation based on the ERAS concept in the rapid postoperative recovery of elderly patients with lung cancer. *Methods:* The elderly lung cancer patients who received surgical treatment in our hospital from 2023.7 to 2024.7 were included. The total sample size included was 64 cases. They were divided into groups using the ball-touching method and carried out different clinical nursing methods. There were 32 cases in both the control group and the observation group. The corresponding nursing plan was routine care and preoperative prehabilitation based on the ERAS concept. *Results:* There was no significant difference in pulmonary function indicators between the groups at admission. The preoperative pulmonary function indicators of the observation group were higher than those of the control group,  $P < 0.05$ . The pulmonary function indicators of the patients decreased 7 days after surgery, but the FEV1, FVC, and PEF levels of the observation group were higher than those of the control group,  $P < 0.05$ . The incidence rate of pulmonary-related complications in the observation group (6.25%) was lower than that in the control group (25.00%),  $P < 0.05$ . The first time to get out of bed after surgery, recovery of bowel sounds, spontaneous urination time and total hospitalization time in the observation group were shorter than those in the control group,  $P < 0.05$ . *Conclusion:* Carrying out preoperative pre-rehabilitation based on the ERAS concept in the perioperative care of elderly lung cancer patients is of significant value in improving patients' preoperative pulmonary function and reducing the impact of surgery on postoperative pulmonary function. It can also effectively prevent the occurrence of postoperative pulmonary-related complications and promote the postoperative rehabilitation process.

**Keywords:** Elderly lung cancer; Perioperative period; ERAS concept; Preoperative prehabilitation; Pulmonary function; Complications

**Online publication:** December 26, 2025

## 1. Introduction

Lung cancer is one of the most common malignant tumors in the world. Its morbidity and mortality are particularly prominent among the elderly. With the advancement of medical technology, surgery has become the main method of treating early-stage lung cancer. However, elderly patients often face higher perioperative risks due to declining physiological functions and multiple comorbidities<sup>[1]</sup>. Postoperative pulmonary complications and delayed functional

recovery not only affect the treatment effect, but may also prolong hospitalization and increase medical burden<sup>[2]</sup>. The concept of accelerated recovery surgery provides a new idea to improve this situation. Preoperative pre-rehabilitation strengthens patients' physiological reserves through systematic intervention and becomes a key link in optimizing perioperative management<sup>[3]</sup>. This study focuses on elderly patients with lung cancer and explores the role of preoperative pre-rehabilitation based on the ERAS concept in promoting rapid postoperative recovery. It aims to provide feasible intervention programs for clinical use and fill the gap in research on the correlation between preoperative functional optimization and postoperative recovery in elderly patients.

## 2. Materials and methods

### 2.1. General information

The 64 elderly patients with lung cancer were all included between 2023.7 and 2024.7. The samples were divided into two groups (32 cases/group) using the ball-touching method. The group name was the control group [20 males and 12 females; Age threshold: 60–76 years old, mean (67.70±3.57) years old], observation group [19 males and 13 females; age threshold: 60–78 years old, mean (68.25±4.33) years old]. The baseline data of the two groups were balanced,  $P > 0.05$ .

Inclusion criteria: patients are  $\geq 60$  years old, diagnosed with primary lung cancer by pathology or imaging<sup>[4]</sup>, meet the surgical indications; tumor stage is stage I to IIIA; do not have severe cardiopulmonary failure; can cooperate to complete pre-rehabilitation training and postoperative follow-up; patients and their families sign informed consent, voluntarily participate in the study and complete the pre-rehabilitation plan.

Exclusion criteria: presence of distant metastasis; severe cardiovascular and cerebrovascular diseases; hepatic and renal insufficiency; active infection or immune system disease; presence of bone and joint disease or neurological disease that prevents the completion of pre-rehabilitation training; previous history of chest surgery, long-term dependence on hormone therapy, and participation in other clinical trials within 3 months.

### 2.2. Method

The control group received routine perioperative care, including preoperative health education, guidance on fasting and drinking, postoperative vital sign monitoring, incision care, pain management and basic respiratory function training. Patients were encouraged to move early according to traditional procedures after surgery.

The observation group implemented preoperative pre-rehabilitation based on the ERAS concept.

- (1) Preoperative respiratory function training: (a) Respiratory muscle endurance training: Patients were instructed to perform abdominal breathing combined with pursed lip breathing training every day. When inhaling, the abdomen bulged, and when exhaling, the lips were pursed and slowly exhaled. Repeat 10 times as one group, 3 groups per day. (b) Resistance breathing training: Use a breathing trainer and set the appropriate resistance level. The patient remains seated and performs deep and slow inhalation training for 5 seconds each time, twice a day, 10 minutes each time. (c) Aerobic exercise intervention: Based on the cardiopulmonary function assessment results, develop an individualized brisk walking or cycling training program, with the target heart rate maintained at 60–70% of the reserve heart rate, for 20 minutes a day.
- (2) Nutrition and metabolic regulation: Supplement whey protein powder daily from 3 days before surgery, with a target protein intake of 1.5 g/kg/d, taken three times with meals, combined with vitamin D and branched-chain amino acids; 400 mL of a 12.5% carbohydrate drink was taken orally 10 hours before surgery, and 200 mL was replenished 2 hours before surgery to maintain intraoperative glycogen reserves; probiotic preparations containing bifidobacteria were taken daily starting 1 week before surgery to regulate the balance of intestinal flora.
- (3) Psychological and pain intervention: A psychiatrist will conduct anxiety counseling 1 week before surgery, through mindfulness meditation and progressive muscle relaxation training, once a day for 30 minutes each time; use a visual analog scale to explain postoperative pain expectations in advance, and train patients to use non-drug

analgesic techniques such as acupressure and cold compresses. Gabapentin combined with acetaminophen will be administered orally 24 hours before surgery to reduce the risk of central sensitization.

- (4) Early postoperative activities: Start ankle pump exercise on the bed 6 hours after the operation, once every 2 hours; assist with bedside sitting training 12 hours after the operation; complete 5 minutes of standing and walking under supervision 24 hours after the operation. After surgery, the preoperative breathing training program was continued every day, combined with a vibrating expectoration device to assist in airway clearance, twice a day. Start drinking a small amount of water 4 hours after surgery, transition to enteral nutrition preparations 6 hours after surgery, and resume a high-protein diet within 24 hours.

### 2.3. Observation indicators

- (1) The patients' pulmonary function indicators, including forced expiratory volume in 1 s (FEV1), forced vital capacity (FVC) and maximum expiratory flow (PEF), were measured on admission, 1 day before surgery, and 7 days after surgery.
- (2) The incidence rates of pulmonary-related complications such as pulmonary infection, respiratory failure, atelectasis, and pulmonary embolism were calculated in the two groups.
- (3) The first time out of bed, recovery of bowel sounds, spontaneous urination time and total hospital stay were recorded in both groups.

### 2.4. Statistical methods

The calculation software used for the relevant data is SPSS 25.0, the pulmonary function indicators and postoperative recovery are measurement data, and the complication rate is count data; the former is described by mean  $\pm$  standard deviation (SD) and t-value test; the latter is described by frequency and constituent ratio,  $\chi^2$  test.  $P < 0.05$  is statistically significant.

## 3. Results

### 3.1. Compare the pulmonary function indicators of the two groups of patients on admission and 7 days after surgery

There was no significant difference in pulmonary function indicators between the groups at admission. The preoperative pulmonary function indicators of the observation group were higher than those of the control group,  $P < 0.05$ . The pulmonary function indicators of the patients decreased 7 days after surgery, but the FEV1, FVC, and PEF levels of the observation group were higher than those of the control group,  $P < 0.05$ . See **Table 1** for details

**Table 1.** Comparison of lung function indicators between the two groups (mean  $\pm$  SD)

Group	n	FEV1(L)			FVC(L)			PEF(L/s)		
		On admission	1 day before surgery	7 days after surgery	On admission	1 day before surgery	7 days after surgery	On admission	1 day before surgery	7 days after surgery
Control group	32	2.03 $\pm$ 0.45	2.05 $\pm$ 0.52	1.55 $\pm$ 0.48	2.75 $\pm$ 0.60	2.78 $\pm$ 0.57	1.78 $\pm$ 0.42	4.65 $\pm$ 0.80	4.67 $\pm$ 0.82	3.85 $\pm$ 0.64
Observation group	32	2.05 $\pm$ 0.52	2.45 $\pm$ 0.50	1.86 $\pm$ 0.64	2.78 $\pm$ 0.57	3.21 $\pm$ 0.69	2.30 $\pm$ 0.58	4.67 $\pm$ 0.82	5.40 $\pm$ 0.94	4.50 $\pm$ 0.67
<i>t</i>	--	0.165	3.134	2.121	0.205	2.719	4.108	0.099	3.310	3.968
<i>P</i>	--	0.870	0.003	0.038	0.838	0.009	0.000	0.922	0.002	0.000

### 3.2. Compare the occurrence of pulmonary-related complications between the two groups

The incidence rate of pulmonary-related complications in the observation group (6.25%) was lower than that in the control group (25.00%),  $P < 0.05$ . See **Table 2** for details.

**Table 2.** Comparison of complications between the two groups ( $n$ , %)

Group	n	Lung infection	Respiratory failure	Atelectasis	Pulmonary embolism	Overall incidence
Control group	32	2 (6.25%)	1 (3.13%)	3 (9.38%)	2 (6.25%)	8 (25.00%)
Observation group	32	1 (3.13%)	0 (0.00%)	1 (3.13%)	0 (0.00%)	2 (6.25%)
$t$	--	--	--	--	--	4.267
$P$	--	--	--	--	--	0.039

### 3.3. Compare the postoperative recovery of the two groups

The first time to get out of bed after surgery, recovery of bowel sounds, spontaneous urination time and total hospitalization time in the observation group were shorter than those in the control group,  $P < 0.05$ . See **Table 3** for details.

**Table 3.** Comparison of postoperative recovery conditions (mean  $\pm$  SD)

Group	n	Getting out of bed for the first time (h)	Return of bowel sounds (h)	Spontaneous urination (h)	Length of stay (d)
Control group	32	38.72 $\pm$ 10.35	30.85 $\pm$ 8.92	16.63 $\pm$ 4.47	10.45 $\pm$ 2.95
Observation group	32	28.45 $\pm$ 7.67	24.13 $\pm$ 6.54	12.25 $\pm$ 3.12	7.67 $\pm$ 2.53
$t$	--	4.510	3.437	4.545	4.047
$P$	--	0.000	0.001	0.000	0.000

## 4. Discussion

Elderly patients with lung cancer commonly have problems such as reduced lung function reserves and weakened immune defenses due to age-related decline in physiological functions. Surgical trauma will not only trigger an inflammatory response but also lead to respiratory muscle dysfunction and reduced ventilation efficiency<sup>[5]</sup>. Factors such as postoperative pain inhibiting deep breathing, anesthetic drug residue affecting ciliary movement, and long-term bed rest leading to pulmonary secretion accumulation significantly increase the risk of complications such as pulmonary infection and atelectasis. Patients have special needs for perioperative care, which requires targeted intervention in maintaining respiratory mechanics stability, optimizing gas exchange efficiency, and promoting airway cleaning to minimize the negative impact of surgery on respiratory function and ensure a smooth perioperative period<sup>[6]</sup>. The traditional perioperative nursing model has obvious limitations. It mainly focuses on the passive treatment of postoperative symptoms, lacks systematic preoperative functional reserve construction, respiratory training is single and insufficient in intensity, nutritional support lacks individualized plans, pain management and psychological intervention are relatively weak, resulting in patients' inadequate preoperative preparation and a slow and difficult postoperative recovery process<sup>[7]</sup>.

The implementation of preoperative prehabilitation can make full use of the critical window of the surgical waiting period, improve the patient's physiological functional reserve through multi-dimensional intervention, enhance the tolerance to surgical trauma, and create favorable conditions for rapid postoperative recovery. This is an important breakthrough that cannot be achieved by the traditional nursing model<sup>[8]</sup>. Preoperative prehabilitation based on the ERAS concept is a multidisciplinary collaborative intervention system based on evidence-based medicine. The core is to



reduce surgical stress reactions through systematic preoperative functional optimization<sup>[9]</sup>. Preoperative prehabilitation based on the ERAS concept integrates multiple key dimensions such as respiratory function training, precise nutritional support, psychological stress adjustment, and pain pre-adaptation. It improves lung compliance through respiratory muscle endurance training, maintains positive nitrogen balance through protein supplementation, and reduces stress reactions through psychological intervention, forming a comprehensive physiological protection mechanism<sup>[10]</sup>. Compared with traditional nursing, its outstanding advantage lies in the forward-looking, systematic, and individualized intervention, which can provide precise support for the special needs of elderly patients.

The results showed that there was no significant difference in pulmonary function indicators between the groups at admission. The preoperative pulmonary function indicators of the observation group were higher than those of the control group,  $P < 0.05$ . The pulmonary function indicators of the patients decreased 7 days after surgery, but the FEV1, FVC, and PEF levels of the observation group were higher than those of the control group,  $P < 0.05$ . The incidence rate of pulmonary-related complications in the observation group (6.25%) was lower than that in the control group (25.00%),  $P < 0.05$ . The first time to get out of bed after surgery, recovery of bowel sounds, spontaneous urination time and total hospitalization time in the observation group were shorter than those in the control group,  $P < 0.05$ . Reasons for analysis: Resistance breathing training effectively enhances the contraction endurance of the diaphragm and intercostal muscles, allowing patients to better overcome respiratory depression caused by postoperative pain; abdominal breathing training improves chest-abdominal coordination and maintains adequate ventilation; aerobic exercise improves cardiopulmonary endurance reserves. In terms of nutritional intervention, protein supplementation promotes the synthesis of alveolar surfactants, and carbohydrate loading reduces intraoperative catabolism, which all contribute to lung tissue repair; psychological intervention reduces the negative impact of catecholamines on respiratory function by reducing stress response; early activity combined with vibration expectoration effectively prevents the accumulation of secretions and reduces the risk of infection.

## 5. Conclusion

In summary, preoperative prehabilitation based on the ERAS concept in the perioperative care of elderly lung cancer patients is of significant value in improving patients' preoperative pulmonary function and reducing the impact of surgery on postoperative pulmonary function. It can also effectively prevent the occurrence of postoperative pulmonary-related complications and promote their postoperative rehabilitation process.

## About the author

Huang Xiaoping (1972.04-), female, Han nationality, Jiangsu, undergraduate, deputy chief nurse, Taizhou Hospital of Traditional Chinese Medicine, research direction: common thoracic surgery operations for esophageal cancer, lung cancer.

## Disclosure statement

The authors declare no conflict of interest.

## References

- [1] Zheng X, Luo X, Zhuo L, et al., 2025, A Review of the Scope of Preoperative Exercise Prehabilitation for Lung Cancer Patients. *Modern Clinical Nursing*, 24(3): 69–75.
- [2] Liu C, Huo X, Liu X, et al., 2024, Application of Prehabilitation Based on Comprehensive Geriatric Assessment in

- Preoperative Frail Elderly Lung Cancer Patients. *Practical Gerontology*, 38(11): 1153–1157.
- [3] Zhang F, Jiao J, Liu L, 2024, Summary of the Best Evidence for Preoperative Pre-rehabilitation Management of Lung Cancer Patients. *Chinese Nursing Education*, 21(7): 881–887.
  - [4] National Health Commission of the People's Republic of China, 2022, Guidelines for the Diagnosis and Treatment of Primary Lung Cancer (2022 Edition). *Exploration of Rational Drug Use in China*, 19(9): 1–28.
  - [5] He S, Huang N, Zhang G, et al., 2024, Summary of the Best Evidence for Preoperative Pre-rehabilitation Management of Lung Cancer. *Journal of Accelerated Recovery Surgery*, 7(2): 57–66.
  - [6] Zhang R, Wu M, Xia L, et al., 2024, Summary of the Best Evidence for Preoperative Prehabilitation in Elderly Patients with Early-stage Lung Cancer. *Journal of Nursing Education*, 39(7): 697–703.
  - [7] Shen L, 2024, Effect of Advanced Prehabilitation on Preoperative Pulmonary Function and Postoperative Pulmonary Complications in Elderly Patients Undergoing Thoracoscopic Lung Cancer Surgery. *Jilin Medicine*, 45(1): 228–230.
  - [8] Zhang W, Liang C, Shi Y, et al., 2023, Review of the Scope of Research on the Application of Prehabilitation in Preoperative Patients with Lung Cancer. *Journal of Nursing Management*, 23(10): 803–808.
  - [9] Xia P, Yin L, Yuan L, et al., 2023, Research on the Application of Preoperative Pre-rehabilitation Nursing Program in Patients Undergoing Thoracoscopic Surgery for Lung Cancer. *Chongqing Medicine*, 52(2): 245–249.
  - [10] Ren P, Sha Y, Kong Q, 2020, Research on the Application of Prehabilitation Concept in Preoperative Pulmonary Rehabilitation for Lung Cancer Patients. *Journal of Nursing Education*, 35(14): 1256–1260 + 1265.

**Publisher's note**

*Whioce Publishing remains neutral with regard to jurisdictional claims in published maps and institutional affiliations.*

# Evaluation of the Application Value of Routine Blood Tests in the Diagnosis of Iron Deficiency Anemia

Xilin Kuai\*

Guanyun County People's Hospital, Lianyungang 222200, Jiangsu, China

*\*Author to whom correspondence should be addressed.*

**Copyright:** © 2025 Author(s). This is an open-access article distributed under the terms of the Creative Commons Attribution License (CC BY 4.0), permitting distribution and reproduction in any medium, provided the original work is cited.

**Abstract:** *Objective:* To explore the application significance of routine blood testing in the diagnosis of iron deficiency anemia (IDA), analyze the diagnostic effects of different single indicators and combinations of indicators, and provide optimization strategies for early and accurate clinical diagnosis. *Methods:* 86 patients with suspected iron deficiency anemia admitted to our hospital from August 2024 to August 2025 were selected. Routine blood tests were performed on all patients. Serum ferritin detection combined with bone marrow iron staining was used as the benchmark standard to compare and analyze each individual indicator and the sensitivity, specificity and accuracy of 5 indicator combinations (MCV + MCH, MCV + MCH + MCHC, MCV + MCH + RDW, RBC + Hb + MCV, Hb + MCV + MCH + MCHC). *Results:* There were 62 IDA patients and 24 non-IDA patients diagnosed according to the baseline standards. Among single indicators, MCV and MCH have the best diagnostic effect; among indicator combinations, the Hb + MCV + MCH + MCHC quadruple combination has the highest diagnostic efficiency (sensitivity 95.16%, specificity 91.67%, accuracy 94.19%), followed by the MCV + MCH + MCHC triple combination. Both groups are significantly better than other combinations and single indicators ( $P < 0.05$ ). *Conclusion:* Among routine blood tests, the quadruple combination of Hb + MCV + MCH + MCHC is the most effective in diagnosing IDA, and the triple combination of MCV + MCH + MCHC is more cost-effective. It can be combined with actual clinical selection to provide reliable support for early screening and auxiliary diagnosis of IDA.

**Keywords:** Iron deficiency anemia; Routine blood testing; Mean corpuscular volume; Mean corpuscular hemoglobin content; Diagnostic value

**Online publication:** December 26, 2025

## 1. Introduction

Iron Deficiency Anemia (IDA) is a nutritional deficiency anemia with the highest clinical incidence. The core cause is insufficient iron intake, blocked absorption, or excessive iron loss in the body, resulting in insufficient hemoglobin synthesis and inducing various clinical symptoms<sup>[1]</sup>. The early symptoms of IDA are mostly atypical, often manifesting as fatigue, dizziness, etc., which are easily ignored. Delayed treatment may cause reduced immunity and affect the function of multiple organs, which is particularly harmful to the health of children and the elderly<sup>[2]</sup>. Therefore, early and accurate diagnosis of IDA is very important for timely intervention and improved prognosis. Currently, serum ferritin (SF) testing combined with bone marrow iron staining is the benchmark standard for diagnosing IDA. However, bone

marrow iron staining is an invasive examination, complicated to operate and not well accepted by patients. Serum ferritin testing is relatively expensive, which is not conducive to primary hospitals and large-scale screening<sup>[3]</sup>. As a routine clinical examination item, routine blood testing is easy to operate, fast, efficient, low-cost, and non-invasive. Its detection indicators can reflect the status of the body's hematopoietic function and are widely used in anemia screening. This study analyzes the diagnostic effect of core indicators of routine blood tests on IDA, clarifies its application significance, and provides a reference for clinical optimization of IDA diagnostic programs.

## 2. Materials and methods

### 2.1. General information

86 patients with suspected iron deficiency anemia admitted to our hospital from August 2024 to August 2025 were selected as the research subjects, including 35 males and 51 females, aged 18–76 ( $45.62 \pm 12.38$ ) years old. Inclusion criteria: (1) Existing anemia-related symptoms such as fatigue, dizziness, pale complexion, palpitations after activity; (2) Not receiving iron supplementation therapy or blood transfusion treatment; (3) Voluntarily participating in this study and signing an informed consent form. Exclusion criteria: (1) Combined with megaloblastic anemia, aplastic anemia, hemolytic anemia and other types of anemia; (2) Combined with severe liver and kidney insufficiency, malignant tumors, chronic infectious diseases; (3) Recent history of surgery, trauma or massive bleeding; (4) Pregnant and lactating women (separate analysis, not included in the overall statistics).

### 2.2. Method

All research subjects collected 5 mL of venous blood in the early morning on an empty stomach and divided it into two tubes, one tube was used for routine blood testing and the other tube was used for serum ferritin testing.

- (1) Routine blood testing: Use a fully automatic blood cell analyzer (model: Sysmex 2800) for testing, and operate in strict accordance with the instrument operating instructions. The testing indicators include red blood cells (RBC), hemoglobin (Hb), mean corpuscular volume (MCV), mean corpuscular hemoglobin content (MCH), mean corpuscular hemoglobin concentration (MCHC), and red blood cell distribution width (RDW). Reference value range: RBC ( $3.80\text{--}5.10 \times 10^{12}/\text{L}$  (female),  $(4.30\text{--}5.80) \times 10^{12}/\text{L}$  (male); Hb  $110\text{--}150\text{g/L}$  (female),  $120\text{--}160\text{g/L}$  (male); MCV  $80\text{--}100\text{fL}$ ; MCH  $27\text{--}34\text{pg}$ ; MCHC  $320\text{--}360\text{g/L}$ ; RDW  $11.5\%\text{--}14.5\%$ .
- (2) Gold standard test: Chemiluminescence immunoassay is used to detect serum ferritin (SF). The instrument is a fully automatic chemiluminescence immunoassay analyzer (Model: Antu 6200). The reference value range: SF  $< 12 \mu\text{g/L}$  (female),  $< 15 \mu\text{g/L}$  (male) is iron deficiency; combined with bone marrow iron staining examination, bone marrow iron staining shows negative extracellular iron and reduced intracellular iron, which is the basis for the diagnosis of IDA<sup>[4]</sup>. Two laboratory doctors with rich clinical experience will jointly read the films to ensure the accuracy of the diagnostic results.

### 2.3. Observation indicators

Using serum ferritin detection combined with bone marrow iron staining results as the gold standard, the study subjects were divided into the IDA group (confirmed patients) and the non-IDA group (excluded patients). The diagnostic sensitivity, specificity, and accuracy of every single indicator of blood routine (RBC, Hb, MCV, MCH, MCHC) and different indicator combinations (MCV + MCH, MCV + MCH + MCHC, RBC + Hb + MCV) were calculated, respectively. Diagnostic criteria: If the test result of a single indicator is lower than the lower limit of the corresponding reference value, it is positive; if at least 2 indicators in the indicator combination are lower than the lower limit of the reference value, it is positive.

## 2.4. Statistical methods

Data were analyzed using SPSS24.0 software. Count data are expressed in [*n* (%)]. Sensitivity = true positive/(true positive + false negative) × 100%; specificity = true negative/(true negative + false positive) × 100%; accuracy = (true positive + true negative) / (total number of samples) × 100%.

## 3. Results

### 3.1. Gold standard diagnostic results

Among the 86 suspected IDA patients, 62 were diagnosed as IDA patients (IDA group) by serum ferritin detection combined with bone marrow iron staining, including 21 males and 41 females, aged 18–74 ( $44.85 \pm 11.96$ ) years old; there were 24 non-IDA patients (non-IDA group), including 14 males and 10 females, aged 20–76 ( $47.23 \pm 13.12$ ) years old.

### 3.2. Comparison of diagnostic performance of individual blood routine indicators

Among the individual indicators of blood routine, MCV has the highest diagnostic sensitivity (87.10%) and accuracy (84.88%), MCH has the highest diagnostic specificity (83.33%), and RBC has the lowest diagnostic sensitivity (74.19%) and accuracy (73.26%). See **Table 1** for details.

**Table 1.** Comparison of diagnostic performance of individual indicators of blood routine [*n* (%)]

Indicator	Sensitivity	Specificity	Accuracy
RBC	74.19 (46/62)	70.83 (17/24)	73.26 (63/86)
Hb	80.65 (50/62)	79.17 (19/24)	80.23 (69/86)
MCV	87.10 (54/62)	80.00 (19/24)	84.88 (73/86)
MCH	83.87 (52/62)	83.33 (20/24)	83.72 (72/86)
MCHC	79.03 (49/62)	75.00 (18/24)	77.91 (67/86)

### 3.3. Comparison of diagnostic performance of different combinations of blood routine indicators

Among different indicator combinations, the Hb + MCV + MCH + MCHC quadruple combination has the best diagnostic performance, followed by the MCV + MCH + MCHC triple combination. Both are more efficient than the MCV + MCH double combination, MCV + MCH + RDW triple combination and RBC + Hb + MCV triple combination, and the diagnostic efficacy of each combination is significantly higher than the single indicator ( $P < 0.05$ ). Among them, the triple combination of MCV + MCH + MCHC is more effective than the double combination of MCV + MCH. See **Table 2** for details.

**Table 2.** Comparison of diagnostic performance of different combinations of blood routine indicators [*n* (%)]

Indicator combination	Sensitivity	Specificity	Accuracy
MCV + MCH (two combinations)	90.32 (56/62)	83.33 (20/24)	88.37 (76/86)
MCV + MCH + MCHC (triple)	93.55 (58/62)	87.50 (21/24)	91.86 (79/86)
MCV + MCH + RDW (triple)	91.94 (57/62)	83.33 (20/24)	89.53 (77/86)
RBC + Hb + MCV (triple)	87.10 (54/62)	81.25 (19/24)	84.88 (73/86)
Hb + MCV + MCH + MCHC (quadruple)	95.16 (59/62)	91.67 (22/24)	94.19 (81/86)



## 4. Discussions

Iron-deficiency anemia is a microcytic, hypochromic anemia caused by depletion of the body's iron reserves and lack of hemoglobin synthesis. Its pathogenesis is closely related to iron metabolism disorders<sup>[4]</sup>. Confirming the condition as early as possible and supplementing iron in a timely manner can effectively reduce the patient's discomfort and prevent the condition from worsening. Therefore, the use of efficient and simple diagnostic methods plays a very critical clinical role. Bone marrow iron staining is the core standard for diagnosing iron deficiency anemia. Although the detection accuracy is good, it is an invasive operation, and the operation steps are complicated and time-consuming, making patients less willing to cooperate. It is difficult to use it as a routine screening method. Serum ferritin detection can reflect the body's iron reserve status, but its detection results are easily interfered by factors such as inflammatory tumors and the detection cost is relatively high, which is not conducive to the implementation of primary medical institutions<sup>[5]</sup>.

Routine blood testing is the most basic clinical blood test item, which can quickly obtain multiple indicators such as the red blood cell system and platelet system. Among them, red blood cell-related indicators can directly reflect the body's hematopoietic function and anemia type. The results of this study show that among the single indicators of blood routine, MCV and MCH have the most ideal diagnostic effects, with sensitivities of 87.10% and 83.87%, and specificities of 80.00% and 83.33%, respectively. This is because patients with iron deficiency anemia suffer from insufficient hemoglobin synthesis due to insufficient iron. During the production of red blood cells, due to a shortage of raw materials, the volume becomes smaller and the hemoglobin content decreases, showing microcytic and hypochromic changes. MCV can reflect the average volume of red blood cells. MCH can reflect the average hemoglobin content in a single red blood cell and can directly reflect this morphological change. Therefore, it is highly targeted for the diagnosis of iron deficiency anemia<sup>[6]</sup>. In contrast, although RBC and Hb are commonly used indicators for diagnosing anemia, due to individual differences, blood loss and other factors, there may be no obvious abnormalities in the early stages of iron deficiency anemia, making the diagnostic sensitivity low and it is easy to miss the diagnosis when used alone.

This study further analyzed the diagnostic effects of different indicator combinations. The results showed that the diagnostic efficiency did not increase linearly with the increase in the number of indicators, but was closely related to the pertinence of the indicators to the core characteristics of iron deficiency anemia. Among them, the Hb + MCV + MCH + MCHC quadruple combination had the best diagnostic efficiency, with sensitivity, specificity, and accuracy, respectively. The results reached 95.16%, 91.67%, and 94.19%, which were significantly better than other combinations; followed by the MCV + MCH + MCHC triple combination, its efficacy was significantly higher than the MCV + MCH double combination. This result is in line with the diagnostic logic of multi-indicator combination and complementation, and also verifies the added value of MCHC in the diagnosis of iron deficiency anemia. The core hematological characteristic of iron deficiency anemia is microcytic hypochromia. MCV reflects the volume of red blood cells, which is microcytic manifestations. MCH reflects the hemoglobin content of single red blood cells, which is hypochromic manifestations. MCHC further quantifies the hemoglobin concentration in red blood cells. The combination of the three can comprehensively capture the morphological abnormalities of iron deficiency anemia from multiple aspects of volume content. Compared with the double combination that only reflects volume content, it can more accurately distinguish iron deficiency anemia from other non-microcytic hypochromic anemias, thus reducing the risk of misdiagnosis and missed diagnosis<sup>[7]</sup>.

The difference in efficacy of different triple combinations also confirms the importance of indicator targeting: the efficacy of the MCV + MCH + RDW triple combination is slightly higher than the MCV + MCH double combination, but significantly lower than the MCV + MCH + MCHC combination. The reason is that although RDW can reflect the heterogeneity of red blood cells, it can increase due to uneven red blood cell production in the advanced stage of iron deficiency anemia. However, the change in red blood cell heterogeneity in patients with early iron deficiency anemia is not obvious, and the increase in RDW is not unique to iron deficiency anemia. , may also occur in megaloblastic anemia and hemolytic anemia, resulting in limited specificity improvement in the diagnosis of iron deficiency anemia; the RBC + Hb + MCV combination has the lowest efficacy, and the core reason is that this combination lacks MCH and MCHC The

assessment of hypochromic characteristics can only determine the presence of microcytic and anemia, that is, reduced Hb and RBC, and cannot accurately fit the core phenotype of microcytic hypochromicity in iron deficiency anemia, and is easily confused with other microcytic anemias such as thalassemia<sup>[8]</sup>.

However, this study has certain flaws. The number of samples is relatively small and it is a single-center study. The results may be biased. It does not take into account the differences in blood routine indicators among patients with iron deficiency anemia of different age groups and different causes such as nutritional deficiencies and chronic blood loss. In the future, the number of samples can be expanded to conduct multi-center studies to further refine the analysis. In addition, actual indicator combinations need to be selected in clinical applications: Although the Hb + MCV + MCH + MCHC quadruple combination has the best diagnostic performance, there is no need to excessively pursue the combination of all indicators. For primary hospitals or large-scale screening, the MCV + MCH + MCHC triple combination can meet clinical needs and is both accurate and economical; for diagnosing difficult cases, the quadruple combination can be used to improve the diagnosis rate. At the same time, it should be noted that routine blood testing is only an auxiliary diagnostic method. For patients with positive combinations of indicators but atypical clinical symptoms, core standard examinations such as serum ferritin and bone marrow iron staining need to be combined for further diagnosis to avoid misdiagnosis.

## 5. Conclusion

In summary, among routine blood tests, the quadruple combination of Hb + MCV + MCH + MCHC has the best diagnostic performance for iron deficiency anemia, and the triple combination of MCV + MCH + MCHC is more cost-effective. Routine blood testing has the advantages of simple operation, rapid efficiency, low cost, and non-invasiveness. Among them, the targeted indicator combination can accurately capture the core characteristics of small cell hypochromia of iron deficiency anemia. It can be used as the first choice method for early screening and auxiliary diagnosis of clinical iron deficiency anemia, especially suitable for primary hospitals and large-scale population screening. Combined with serum ferritin detection or bone marrow iron staining, it can further improve the diagnostic accuracy and provide reliable basis for clinical treatment, which has very important clinical promotion value.

## Disclosure statement

The author declares no conflict of interest.

## References

- [1] Zhou X, Zhai S, 2023, Analysis of the Application Value of Routine Blood Testing in the Differential Diagnosis of Thalassemia and Iron Deficiency Anemia. *Clinical Research*, 31(1): 126–129.
- [2] Wang J, 2021, Analysis of the Value of Routine Blood Testing in Distinguishing Iron Deficiency Anemia and Thalassemia. *Contemporary Medicine*, 27(3): 154–155.
- [3] Xie C, 2019, The Application Value of Routine Blood Tests in the Diagnosis of Thalassemia. *Chinese Contemporary Medicine*, 26(26): 97–100.
- [4] Xu W, 2019, Diagnostic Value of Routine Blood Testing for Iron Deficiency Anemia in Infants and Young Children. *World Latest Medical Information Abstracts*, 19(67): 212 + 215.
- [5] Zhang J, 2019, The Application Value of Routine Blood Testing in the Diagnosis of Iron Deficiency Anemia. *World Latest Medical Information Abstracts*, 19(54): 148 + 150.
- [6] Liu K, 2019, Analysis of the Application Value of Routine Blood Tests in the Diagnosis and Identification of Common Anemia. *Journal of Clinical Rational Drug Use*, 12(8): 130–131.

- [7] Lin L, Lin P, 2019, Observation on the Application Effect of Routine Blood Tests in the Diagnosis of Thalassemia and Iron Deficiency Anemia. Chinese and Foreign Medical Research, 17(2): 62–64.
- [8] Zhang C, Huang L, 2018, Change Characteristics of Routine Blood Tests in Patients with Thalassemia and Iron Deficiency Anemia. Journal of Clinical Rational Drug Use, 11(22): 131–133.

**Publisher's note**

*Whioce Publishing remains neutral with regard to jurisdictional claims in published maps and institutional affiliations.*

# Research on Vaccine Distribution and Reserve Based on Service Level during Major Infectious Disease Epidemics

Hong Zhang\*

Changzhou Wujin District Center for Disease Control and Prevention, Changzhou 213100, Jiangsu, China

*\*Author to whom correspondence should be addressed.*

**Copyright:** © 2025 Author(s). This is an open-access article distributed under the terms of the Creative Commons Attribution License (CC BY 4.0), permitting distribution and reproduction in any medium, provided the original work is cited.

**Abstract:** *Purpose:* To explore the effect of vaccine distribution and reserve based on service level under major infectious disease epidemics. *Methods:* The study included 200 subjects, who were divided into 2 groups according to computer randomization method, with 100 subjects in the control group and the experimental group. The experimental group implements a vaccine allocation strategy based on service level, and the control group adopts conventional allocation. The implementation effect of the allocation strategy of the two groups is evaluated. *Results:* The experimental group had a higher complete vaccination rate (92.00% vs. 85.00%), and the comparison of vaccination coverage between the two groups was  $P > 0.05$ . The experimental group had a higher vaccine utilization rate (96.33% vs. 85.67%), and the comparison was  $P < 0.05$ . The average vaccination time in the experimental group was shorter, and the vaccination timeliness score was higher, with a comparison  $P < 0.05$ . The incidence of adverse reactions in the 2 groups (8.00% vs. 6.00%), comparison  $P > 0.05$ . The satisfaction score of the experimental group was higher, comparison  $P < 0.05$ . *Conclusion:* For major infectious disease epidemics, implementing a vaccine distribution strategy based on service levels in prevention and control can effectively improve the efficiency of vaccination and vaccine utilization, ensure the timeliness and safety of vaccination, and thereby improve public satisfaction.

**Keywords:** Vaccine distribution; Reserve strategy; Service level; Infectious disease epidemic; Public health

**Online publication:** December 26, 2025

## 1. Introduction

Infectious disease epidemics have become a persistent problem that seriously affects global public health security. The epidemic spreads quickly and affects a wide range, which has brought severe tests to the epidemic prevention work of various countries. Vaccination is the most direct and effective intervention in epidemic prevention and control. However, in actual work, it has been found that the actual prevention and control effect of the vaccine not only depends on the immune efficacy of the vaccine itself, but is also closely related to the rationality of the distribution strategy and reserve plan<sup>[1]</sup>. At present, the focus of vaccine prevention and control is mainly focused on breakthroughs in vaccine research and development technology and production processes. There is less research on how to scientifically distribute vaccines. As a result, when facing an emergency epidemic, vaccine supply is often difficult to meet all needs immediately. Therefore, it is of great significance to establish a scientific distribution mechanism to ensure that limited resources can maximize their effectiveness<sup>[2]</sup>. The service level-based distribution model provides an objective basis for vaccine allocation by

quantitatively assessing the epidemic risks and resource needs in different regions, thereby improving the overall effectiveness of epidemic prevention and control<sup>[3]</sup>. In this regard, this study analyzes the implementation effect of the service level-based vaccine distribution strategy to effectively respond to public health emergencies, which is summarized as follows:

## 2. Materials and methods

### 2.1. General information

The study included 200 subjects, who were divided into 2 groups according to the computer randomization method, with 100 subjects each in the control group and the experimental group. The experimental group included 56 males and 44 females, aged 22–65 years old, with an average age of  $43.28 \pm 12.35$  years old; the control group included 52 males and 48 females, aged 21–67 years old, with an average age of  $44.16 \pm 13.02$  years old. Comparison of baseline data between the 2 groups  $P > 0.05$ .

Inclusion criteria: (1) Age 18–70 years old; (2) Meet the vaccination indications; (3) Voluntarily participate in the study.

Exclusion criteria: (1) Immune system diseases; (2) Plans to leave the region during the study; (3) History of severe vaccine adverse reactions.

### 2.2. Method

The control group adopts the traditional vaccine distribution method, and allocates uniformly based on the number of applications submitted by each vaccination point, ensuring that the number of vaccines obtained by each vaccination unit is basically consistent with the number of applications. During the distribution process, the vaccine supply to all vaccination sites is handled according to the same standards. Each vaccination site independently determines the vaccination progress based on its own work capacity and the situation of the vaccination recipients. The vaccination order is flexibly controlled by the vaccination site staff based on the actual visit situation, and the principle of first-come, first-served is usually adopted.

The trial group adopts a vaccine allocation strategy based on service levels.

- (1) The assessment needs to fully consider key factors such as the number of confirmed cases in the region, population density, and medical resource carrying capacity. The assessment process is completed by professionals from the Centers for Disease Control and Prevention, and is dynamically updated once a week to ensure that the risk level classification can reflect the latest development trend of the epidemic promptly. The risk level is divided into three levels: high, medium, and low, and each level corresponds to a different resource allocation plan, providing a scientific basis for subsequent accurate allocation.
- (2) For areas with different risk levels, fully consider the priorities of epidemic prevention and control, formulate differentiated service level standards, and clarify the time requirements, resource allocation proportions and priorities for the entire process from vaccine distribution to completion of vaccination. High-risk areas receive the highest priority to ensure that limited resources are tilted towards areas most in need; medium-risk areas adopt the principle of moderate priority and are allocated on the premise of ensuring the needs of high-risk areas; low-risk areas serve as the final protection targets to ensure that basic epidemic prevention needs are met.
- (3) High-risk areas implement the strictest service standards. Starting from the arrival of the vaccine at the distribution center, vaccination of the target population must be completed within 24 hours, including special vehicle delivery, priority scheduling, and the establishment of temporary vaccination points. At the same time, sufficient medical personnel will be deployed, vaccination service hours will be extended, and 24-hour uninterrupted vaccination will be carried out when necessary. At the same time, vaccine reserves in high-risk areas should be maintained at 150% of regular demand to ensure that vaccination needs can still be met in emergencies.
- (4) The service standards in medium-risk areas are relatively loose, but clear time limits are also set. The entire process from vaccine distribution to completion of vaccination is controlled within 48 hours. Vaccine distribution adopts a



regular shuttle bus model, which departs at a fixed time every day. The number of vaccination points is reasonably set according to the population size, and the opening hours are extended to 12 hours; the vaccine reserve is maintained at 120% of regular demand, which not only ensures sufficient supply but also avoids waste of resources. When the epidemic escalates to high risk, it can immediately switch to high-risk regional service standards.

- (5) Basic service standards are implemented in low-risk areas, and the time limit for completing vaccination is relaxed to 72 hours. Vaccine distribution is included in the regular logistics system, with fixed delivery twice a week. Vaccination points mainly rely on existing medical institutions, and no additional temporary vaccination points will be added. Service hours remain normal. time; the vaccine reserve is maintained at 100% of regular demand, and an inter-regional adjustment mechanism is established. Under the premise of ensuring the basic needs of the region, some vaccines can be deployed to support other high-risk areas. When the epidemic situation fluctuates, the service standard upgrade process can be initiated within 12 hours.
- (6) In actual implementation, specific responsible persons should be set up for each link to ensure that all measures are implemented in place, the implementation effects are regularly evaluated, and the risk level classification standards and service level requirements are dynamically adjusted based on the evaluation results to form a continuously optimized closed-loop management.

### 2.3. Observation indicators

- (1) Vaccination coverage rate: actual number of people vaccinated/number of people to be vaccinated  $\times 100\%$
- (2) Timeliness of vaccination: the time from the arrival of the vaccine to the completion of vaccination; vaccination timeliness score:  $\leq 24$  h = 3 points, 25–48 h = 2 points, 49–72 h = 1 point,  $> 72$  h = 0 points.
- (3) Vaccine utilization rate: actual doses used/distributed doses  $\times 100\%$ .
- (4) Incidence rate of adverse reactions: number of cases of adverse reactions/total number of vaccinations  $\times 100\%$ .
- (5) Satisfaction rating: A 10-point scale is used and is subjectively evaluated by the subjects.

### 2.4. Statistical methods

The SPSS26.0 software was used to process the data involved in the study. Measurement data were expressed as “(mean  $\pm$  SD)” and tested by “t”; count data were expressed as “[n/(%)]” and tested by “ $\chi^2$ ”.  $P < 0.05$  indicated that the difference was significant.

## 3. Results

### 3.1. Comparison of vaccination coverage and vaccine utilization rates

The complete vaccination rate in the experimental group was higher (92.00% vs 85.00%), the comparison of vaccination coverage between the two groups was  $P > 0.05$ ; the vaccine utilization rate in the experimental group was higher (96.33% vs 85.67%), the comparison was  $P < 0.05$ . (Table 1).

**Table 1.** Comparison of vaccination coverage and vaccine utilization rates between the two groups [n (%)]

Group	Vaccination coverage (n=100)			Vaccine utilization		
	Fully vaccinated	Partial vaccination	Not vaccinated	Assign dose	Dosage	Utilization
Experimental group	92 (92.00)	6 (6.00)	2 (2.00)	1200	1156	96.33
Control group	85 (85.00)	10 (10.00)	5 (5.00)	1200	1028	85.67
$\chi^2$	2.563	83.354				
$P$	0.278	0.000				

### 3.2. Timeliness of vaccination

The average time of vaccination in the experimental group was shorter, and the vaccination timeliness score was higher, with a comparison  $P < 0.05$  (Table 2).

**Table 2.** Comparison of vaccination timeliness between two groups (mean  $\pm$  SD)

Group	n	Average time (h)	Timeliness score (points)
Experimental group	100	26.34 $\pm$ 8.72	2.38 $\pm$ 0.72
Control group	100	38.15 $\pm$ 12.46	1.65 $\pm$ 0.83
<i>t</i>	-	7.766	6.644
<i>P</i>	-	0.000	0.000

### 3.3. Incidence of adverse reactions

The incidence of adverse reactions in the 2 groups (8.00% vs 6.00%), comparison  $P > 0.05$  (Table 3).

**Table 3.** Comparison of the incidence of adverse reactions between the two groups [*n* (%)]

Group	n	Local reaction	Systemic reaction	Incidence rate (%)
Experimental group	100	5 (5.00)	3 (3.00)	8 (8.00)
Control group	100	4 (4.00)	2 (2.00)	6 (6.00)
$\chi^2$	—	—	—	0.307
<i>P</i>	—	—	—	0.579

### 3.4. Satisfaction score

The satisfaction score of the experimental group was higher, comparison  $P < 0.05$  (Table 4).

**Table 4.** Comparison of satisfaction scores between the two groups (mean  $\pm$  SD, points)

Group	n	Convenience of vaccination	Service attitude	Process efficiency	Overall satisfaction
Experimental group	100	8.72 $\pm$ 1.25	8.56 $\pm$ 1.32	8.91 $\pm$ 1.18	8.63 $\pm$ 1.27
Control group	100	7.35 $\pm$ 1.48	7.82 $\pm$ 1.54	6.97 $\pm$ 1.63	7.24 $\pm$ 1.52
<i>t</i>	-	7.072	3.648	9.641	7.018
<i>P</i>	-	0.000	0.000	0.000	0.000

## 4. Discussions

Vaccines are one of the most effective intervention methods for preventing and controlling infectious diseases. The scientific nature of their distribution and reserve strategies is directly related to the effectiveness of epidemic prevention and control. Currently, in response to sudden epidemics, although the conventional vaccine distribution method is reasonable to a certain extent, it has exposed many shortcomings<sup>[4]</sup>. Conventional allocation is based on the number of applications and adopts the principle of unified allocation. Although it is easy to operate, it ignores the differences in epidemic severity and resource demand in different regions, which can easily lead to insufficient vaccine supply in high-risk areas and idle resources in low-risk areas. This not only reduces the overall prevention and control efficiency, but also

fails to reflect the principle of fairness in public health resource allocation. In actual operation, routine allocation often lags behind the development of the epidemic due to the lack of a dynamic adjustment mechanism. Although the way in which vaccination sites independently determine the order of vaccination is flexible, it is difficult to ensure that high-risk groups receive priority vaccination rights<sup>[5]</sup>.

The core of the vaccine distribution strategy based on service level is to break the average distribution of the conventional distribution model. Through risk level assessment, comprehensively consider key indicators such as the number of confirmed cases, population density, and hospital carrying capacity, and establish a scientific, flexible, and operable hierarchical response mechanism to achieve accurate allocation of vaccine resources and ensure that limited vaccines can be tilted to areas most in need<sup>[6]</sup>.

The results of this study showed that the experimental group had a higher complete vaccination rate (92.00% vs. 85.00%), and the comparison of vaccination coverage between the two groups was  $P > 0.05$ . It shows that implementing a targeted allocation strategy can better meet the actual vaccination needs<sup>[6]</sup>. The vaccine utilization rate in the experimental group was higher (96.33% vs 85.67%), with a comparison  $P < 0.05$ . It fully demonstrates that implementing a hierarchical distribution strategy can significantly reduce resource waste and maximize the value of each dose of vaccine<sup>[7]</sup>.

The results of the study showed that the average vaccination time of the experimental group was shorter and the vaccination timeliness score was higher, with a comparison  $P < 0.05$ . It fully reflects that hierarchical service standards have a positive impact on process optimization. For high-risk areas, strict requirements to complete vaccination within 24 hours, combined with measures such as special vehicle delivery and temporary vaccination site settings, can effectively compress the time window from vaccine arrival to completion of vaccination. Although the time limit is relatively loose in medium and low-risk areas, clear time nodes and accountability systems can still ensure the orderly advancement of vaccination work. Through differentiated management, emergency needs in key areas are ensured, thereby improving overall efficiency<sup>[8]</sup>.

The results of the study showed: the incidence rate of adverse reactions in the 2 groups (8.00% vs 6.00%), comparison  $P > 0.05$ . The incidence rates of adverse reactions in the two groups were within a reasonable range and there was no significant difference, indicating that the implementation of the service level-oriented allocation strategy was not at the expense of safety, and that the use of hierarchical allocation would not increase vaccination pressure and thus affect operating specifications<sup>[9]</sup>.

The research results showed that the experimental group had a higher satisfaction score, comparison  $P < 0.05$ . It has been confirmed that the implementation of a distribution strategy based on service levels can effectively solve the resource misallocation problem in conventional distribution, effectively improve the timeliness and safety of vaccination, thereby meeting the expectations of the public and improving satisfaction with vaccination<sup>[8]</sup>.

## 5. Conclusion

In summary, for major infectious disease epidemics, implementing a vaccine distribution strategy based on service levels in prevention and control can effectively improve the efficiency of vaccination and vaccine utilization, ensure the timeliness and safety of vaccination, and thereby improve public satisfaction.

## About the author

Zhang Hong (1987.8), female, Han, Changzhou, Jiangsu, undergraduate, chief physician, Changzhou Wujin District Center for Disease Control and Prevention, research direction: vaccines and infectious disease management.

## Disclosure statement

The author declares no conflict of interest.

## References

- [1] Li F, Wei Y, 2024, Research on Countermeasures for the Spread of Infectious Diseases and Medical Resource Allocation Issues. *Industrial Engineering and Management*, 29(2): 114–129.
- [2] Ge H, Diao T, 2024, Key Technology Selection and Suggestions for Vaccine Research and Development in Response to Major Emerging Infectious Diseases. *Military Medicine*, 48(1): 12–15.
- [3] Yang K, Yuan R, Wu J, 2024, Research on New Technology System for Pathogen Identification of Respiratory Infectious Diseases and Its Application in Epidemic Prevention and Control. *China Science and Technology Achievements*, 25(4): 2.
- [4] Mo Y, Dong L, Deng S, 2025, Survey on the Knowledge, Beliefs and Practices of Head Teachers in Schools and Daycare Institutions in Jiading District, Shanghai. *Health Education and Health Promotion*, 20(2): 180–183.
- [5] Mao W, Li J, Jiang X, et al., 2023, Study on the Effectiveness and Cost-Effectiveness of Pneumonia Vaccination for the Elderly in Fengtai District, Beijing. *Medical Animal Control*, 39(4): 318–321.
- [6] Wang C, 2024, Epidemic Characteristics and Changing Trends of Hand, Foot and Mouth Disease Enterovirus under the Prevention and Control of the New Crown Epidemic. *World Chinese Journal of Digestion*, 32(4): 254–260.
- [7] Wang J, Xia X, Zhang H, 2024, Application of Infectious Disease Dynamics in the Prevention and Control of the New Crown Epidemic in Heilongjiang Province. *Journal of Engineering Mathematics*, 41(6): 1087–1097.
- [8] Yang L, Zhao Z, Hu M, et al., 2023, Application of Digital Technology Based on SEIR Model in Major Epidemic Emergency Plans. *China Health Management*, 40(11): 801–808.
- [9] Feng C, Jiang X, Zhou X, et al., 2024, Research on Vaccine Distribution and Reserve Based on Service Level under Major Infectious Disease Epidemics. *Journal of Management Engineering*, 38(2): 232–242.

### Publisher's note

*Whioce Publishing remains neutral with regard to jurisdictional claims in published maps and institutional affiliations.*

# Remodeling the Ischemic Stroke Immuno-Microenvironment via Microglial Phenotypic Switching

Xiaowen Wang<sup>1</sup>, Bingcang Huang<sup>2\*</sup>

<sup>1</sup>School of Gongli Hospital Medical Technology, University of Shanghai for Science and Technology, Shanghai 200093, China

<sup>2</sup>Department of Radiology Gongli Hospital of Shanghai Pudong New Area Shanghai 200135, China

\*Corresponding author: Bingcang Huang, hbc01275@glhospital.com

**Copyright:** © 2025 Author(s). This is an open-access article distributed under the terms of the Creative Commons Attribution License (CC BY 4.0), permitting distribution and reproduction in any medium, provided the original work is cited.

**Abstract:** Ischemic stroke triggers a complex cascade of sterile inflammation that critically influences neurological outcomes. While reperfusion therapies remain the standard of care, their efficacy is often undermined by secondary brain injury driven by the pro-inflammatory polarization of microglia. As the central orchestrators of the central nervous system (CNS) immuno-microenvironment, microglia exhibit dynamic plasticity, shifting between the neurotoxic M1 phenotype and the neuroprotective M2 phenotype. The pathological transition from an M2-dominant state to a sustained M1 state perpetuates neuronal death and blood-brain barrier disruption. This review comprehensively elucidates the spatiotemporal dynamics of microglial polarization and the molecular mechanisms governing this switch, with a particular focus on key signaling pathways. Furthermore, we summarize emerging therapeutic strategies, including pharmacological modulation, stem cell-derived exosomes, and stimuli-responsive nanomedicine, aimed at precisely remodeling the immuno-microenvironment. We conclude that promoting the M1-to-M2 phenotypic switch represents a promising therapeutic avenue to mitigate reperfusion injury and enhance long-term functional recovery.

**Keywords:** Ischemic stroke; Microglia; Neuroinflammation; Phenotypic switching; Immuno-microenvironment; Immunometabolism

**Online publication:** December 26, 2025

## 1. Introduction

Ischemic stroke remains a devastating global health crisis, standing as a leading cause of mortality and long-term disability worldwide. Currently, the restoration of cerebral blood flow through recombinant tissue plasminogen activator (rt-PA) thrombolysis or mechanical thrombectomy represents the gold standard for clinical treatment <sup>[1,2]</sup>. However, the efficacy of these recanalization therapies is severely constrained by narrow therapeutic time windows and the potential risk of hemorrhagic transformation. Crucially, successful recanalization does not guarantee tissue survival; on the contrary, the rapid restoration of blood supply often paradoxically exacerbates tissue damage and dysfunction, a phenomenon known as cerebral ischemia-reperfusion injury (IRI) <sup>[3]</sup>. This suggests that targeting vascular recanalization alone is insufficient, and there is an urgent need for neuroprotective adjuncts that can mitigate the secondary injury cascade following the initial ischemic insult.

Accumulating evidence underscores that stroke is not merely a hemodynamic event but a complex thrombo-inflammatory pathology. Following the onset of ischemia, the deprivation of glucose and oxygen leads to neuronal death



and the release of damage-associated molecular patterns (DAMPs), such as HMGB1 and ATP. These danger signals trigger a robust sterile immune response, transforming the ischemic brain into a highly dynamic “immuno-microenvironment.” This microenvironment is characterized by the breakdown of the blood-brain barrier (BBB), the accumulation of inflammatory mediators, and the complex interplay between resident glial cells and infiltrating peripheral immune cells. Among these components, the regulation of neuroinflammation has emerged as a critical determinant of stroke outcome, dictating whether the brain tissue progresses towards necrosis or recovery <sup>[4,5]</sup>.

Microglia, the resident macrophages and primary immune sentinels of the central nervous system (CNS), act as the “central orchestrators” of this immuno-microenvironment. Under physiological conditions, microglia maintain CNS homeostasis by monitoring synaptic activity and clearing metabolic debris. However, they are highly plastic and sensitive to environmental perturbations. In the context of ischemic stroke, microglia are the first responders, rapidly activating and undergoing morphological and functional transformations. Their ubiquity and rapid response capability make them the most pivotal therapeutic target for modulating the post-stroke inflammatory landscape <sup>[6]</sup>.

The functional role of microglia in ischemic stroke is often described as a “double-edged sword,” contingent upon their polarization phenotypes. Historically, activated microglia have been categorized into two distinct states: the “classically activated” M1 phenotype and the “alternatively activated” M2 phenotype. The M1 phenotype is pro-inflammatory, releasing cytotoxic cytokines (*e.g.*, TNF- $\alpha$ , IL-1 $\beta$ ) and reactive oxygen species (ROS) that exacerbate blood-brain barrier disruption and neuronal apoptosis. Conversely, the M2 phenotype exerts neuroprotective effects by phagocytosing cellular debris and secreting anti-inflammatory cytokines (*e.g.*, IL-10) and neurotrophic factors (*e.g.*, BDNF). In the pathology of stroke, a transient M2-like response is often overwhelmed by a sustained and aggressive M1-like polarization, leading to chronic inflammation and poor functional recovery. Therefore, shifting the microglial phenotype from the destructive M1 state to the reparative M2 state, rather than broadly suppressing the immune system, represents a promising strategy to remodel the immuno-microenvironment <sup>[7]</sup>.

In this review, we comprehensively summarize the spatiotemporal dynamics of microglial polarization and the molecular mechanisms governing this phenotypic switching. We specifically focus on key signaling pathways, including the TLR4/NF- $\kappa$ B and JAK/STAT axes, which serve as molecular switches for polarization. Furthermore, we highlight emerging therapeutic interventions, ranging from pharmacological modulation and natural compounds to advanced nanomedicine and stem cell-derived exosome therapies. By elucidating the mechanisms of microglial phenotypic switching, this review aims to provide new insights into remodeling the immuno-microenvironment for the treatment of ischemic stroke (**Figure 1**).

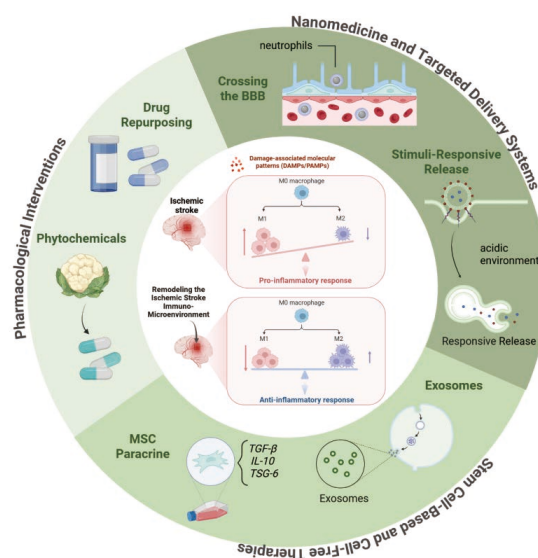


**Figure 1.** Schematic representation of therapeutic strategies targeting microglial phenotypic switching to remodel the ischemic stroke immuno-microenvironment.

## 2. Dynamic shifts of microglial phenotypes

### 2.1. The dichotomy of polarization

Historically, based on the macrophage classification system, activated microglia have been categorized into two opposing functional states: the “classically activated” M1 phenotype and the “alternatively activated” M2 phenotype. Although this binary classification is increasingly recognized as a simplification of a complex biological reality, it remains a valuable conceptual framework for understanding the duality of neuroinflammation.

#### 2.1.1. The M1 phenotype

Upon stimulation by DAMPs (*e.g.*, HMGB1, ATP) or pro-inflammatory mediators (*e.g.*, IFN- $\gamma$ ), resting microglia polarize towards the M1 state. These cells are characterized by the upregulation of surface markers such as CD16, CD32, CD86, and major histocompatibility complex II (MHC-II). Functionally, M1 microglia act as the “soldiers” of the immune system. They secrete high levels of pro-inflammatory cytokines (TNF- $\alpha$ , IL-1 $\beta$ , IL-6, IL-12) and cytotoxic mediators like nitric oxide (NO) generated by inducible nitric oxide synthase (iNOS) and ROS <sup>[8]</sup>. While this response is intended to combat pathogens, in the sterile environment of ischemic stroke, the excessive accumulation of M1-derived toxins exacerbates neuronal apoptosis, compromises BBB integrity, and expands the infarct volume <sup>[9,10]</sup>.

#### 2.1.2. The M2 phenotype

In contrast, the M2 phenotype represents a reparative state induced by cytokines such as IL-4, IL-13, and IL-10. M2 microglia are identified by the expression of CD206 (mannose receptor), Arg-1 (Arginase-1), and Ym1. The M2 population is functionally diverse and can be further subclassified into M2a (tissue repair), M2b (immunoregulation), and M2c (debris clearance). Collectively, M2 microglia secrete anti-inflammatory cytokines (IL-10, TGF- $\beta$ ) and potent neurotrophic factors and vascular endothelial growth factor (VEGF). These cells play a pivotal role in resolving inflammation, phagocytosing necrotic debris, and promoting angiogenesis and neurogenesis in the recovery phase <sup>[11,12]</sup>.

### 2.2. Spatiotemporal evolution

The polarization of microglia is not a fixed state but follows a distinct temporal trajectory during the progression of ischemic stroke. The imbalance in this temporal evolution, the failure to sustain the M2 phenotype, is a key driver of secondary brain injury.

#### 2.2.1. Acute phase (Hours to 3 Days)

In the hyper-acute phase immediately following ischemia, microglia are rapidly activated. Accumulating preclinical evidence suggests that resident microglia initially adopt an M2-dominant phenotype, limiting the spread of the lesion and scavenging early cellular debris. This early M2 response is likely a physiological attempt to restore homeostasis <sup>[13,14]</sup>.

#### 2.2.2. Subacute phase (3 Days to 7 Days)

As the ischemic cascade advances, the massive accumulation of necrotic debris and danger signals overwhelms the regulatory capacity of the microenvironment. This leads to a decisive phenotypic shift where the M2 population declines, and the M1 phenotype becomes predominant. This period coincides with the peak of the “cytokine storm,” where M1 microglia recruit circulating neutrophils and monocytes, further amplifying the inflammatory response <sup>[13–15]</sup>.

#### 2.2.3. Chronic phase (Weeks to Months)

In the chronic phase of stroke, while the acute inflammation subsides, M1-like microglia often remain chronically activated at the lesion border. This persistent, low-grade inflammation sustains oxidative stress and promotes the formation of a dense glial scar, which acts as a physical and chemical barrier to axonal regeneration. The inability of the brain to revert to or maintain an M2-resolving phenotype impedes long-term functional recovery <sup>[13,15]</sup>.

## 2.3. Spatial heterogeneity and transcriptomic complexity

Beyond temporal dynamics, microglial phenotypes exhibit significant spatial heterogeneity, particularly distinguishing the infarct core from the ischemic penumbra.

### 2.3.1. Core vs. penumbra

In the infarct core, where blood flow is severely restricted, microglia are rapidly depleted. In contrast, the penumbra, the metabolically compromised but salvageable tissue surrounding the core, is the primary site of microglial activation and self-renewal. Here, pro-inflammatory (CD16<sup>+</sup>) and anti-inflammatory (Arg1<sup>+</sup>) microglial phenotypes coexist, with their competing functions determining tissue fate through a “tug-of-war”. Notably, HDAC3 selectively drives proliferation of pro-inflammatory microglia without affecting anti-inflammatory subsets, suggesting that targeting this pathway specifically within the penumbra represents a promising therapeutic strategy<sup>[16,17]</sup>.

### 2.3.2. Beyond the binary

It is crucial to acknowledge that recent advances in single-cell RNA sequencing (scRNA-seq) have challenged the strict M1/M2 dichotomy. Transcriptomic analysis reveals that stroke-associated microglia do not simply fall into two distinct clusters but present a multidimensional spectrum of activation states. For instance, specific subsets such as “Disease-Associated Microglia” (DAM) have been identified, which express unique lipid-metabolism genes involved in debris clearance. While the M1/M2 classification remains useful for describing functional outcomes, researchers must recognize this complexity, suggesting that future therapies may need to target specific sub-populations rather than broadly modulating inflammation<sup>[18,19]</sup>.

## 3. Molecular mechanisms underlying polarization

The phenotypic switching of microglia is not a stochastic event but a tightly regulated process governed by an intricate network of intracellular signaling pathways, transcriptional regulators, and metabolic checkpoints.

### 3.1. Pro-inflammatory signaling axes

The rapid induction of the M1 phenotype following ischemia is primarily orchestrated by pattern recognition receptors (PRRs) and their downstream cascades. Among these, the TLR4/NF- $\kappa$ B axis and the NLRP3 inflammasome represent the most critical pathways.

#### 3.1.1. The TLR4/NF- $\kappa$ B canonical pathway

Toll-like receptor 4 (TLR4) serves as a pivotal gatekeeper in the sterile immune response. In the ischemic brain, necrotic neurons release high-mobility group box 1 (HMGB1), heat shock proteins (HSPs), which function as DAMPs<sup>[20]</sup>. Upon binding to these ligands, TLR4 undergoes homodimerization and recruits the cytosolic adaptor protein myeloid differentiation primary response 88 (MyD88)<sup>[21]</sup>.

This recruitment triggers a phosphorylation cascade involving IL-1 receptor-associated kinases (IRAK1 and IRAK4) and TNF receptor-associated factor 6 (TRAF6). TRAF6 subsequently activates the transforming growth factor- $\beta$ -activated kinase 1 (TAK1), which phosphorylates the I $\kappa$ B kinase (IKK) complex. The activated IKK complex targets the inhibitor of nuclear factor- $\kappa$ B (I $\kappa$ B $\alpha$ ) for phosphorylation and ubiquitination, leading to its proteasomal degradation. This liberation allows the NF- $\kappa$ B p65/p50 heterodimer to translocate from the cytoplasm to the nucleus. Once nuclear, NF- $\kappa$ B binds to specific consensus sequences on DNA, driving the transcription of pro-inflammatory genes<sup>[21]</sup>. This pathway not only initiates the cytokine storm but also upregulates the expression of NLRP3, setting the stage for inflammasome activation<sup>[22]</sup>.

### 3.1.2. The NLRP3 inflammasome

While NF- $\kappa$ B provides the “priming” signal by upregulating NLRP3 and pro-IL-1 $\beta$  expression, a secondary activation signal in the ischemic microenvironment triggers NLRP3 oligomerization<sup>[23]</sup>.

Upon activation, the NLRP3 sensor protein oligomerizes and recruits the adaptor protein ASC (apoptosis-associated speck-like protein containing a CARD) and pro-Caspase-1. This assembly leads to the autocatalytic cleavage of pro-Caspase-1 into active Caspase-1. Active Caspase-1 then processes the inactive precursors pro-IL-1 $\beta$  and pro-IL-18 into their mature, biologically active forms. Furthermore, Caspase-1 cleaves Gasdermin D (GSDMD), the N-terminal fragment of which forms pores in the plasma membrane, causing pyroptosis—a highly inflammatory form of programmed cell death that releases massive amounts of cytokines into the extracellular space, further propagating the M1 response<sup>[24]</sup>.

## 3.2. Anti-inflammatory signaling pathways

Counteracting the pro-inflammatory drive, several signaling pathways are responsible for inducing and maintaining the M2 phenotype. Enhancing these pathways is a key strategy for “immunomodulation.”

### 3.2.1. The JAK/STAT signaling pathway

The Janus kinase/signal transducer and activator of transcription (JAK/STAT) pathway plays a dual role in microglial polarization, with specific STAT isoforms dictating divergent outcomes. While STAT1 is generally associated with IFN- $\gamma$ -induced M1 polarization, STAT3 and STAT6 are critical drivers of the M2 phenotype<sup>[25]</sup>.

For instance, the binding of IL-4 or IL-13 to their respective receptors activates JAK1 and JAK3, which phosphorylate cytosolic STAT6. Phosphorylated STAT6 dimerizes and translocates to the nucleus, where it induces the transcription of M2 signature genes, such as Arg1 (Arginase-1), Mrc1 (CD206). Similarly, IL-10 exerts its anti-inflammatory effects primarily through the STAT3 signaling axis. The activation of STAT3 suppresses the expression of pro-inflammatory mediators and promotes the release of neurotrophic factors. The balance between STAT1 and STAT3/6 activation is often regarded as a molecular “switch” determining microglial fate<sup>[26]</sup>.

### 3.2.2. The Nrf2/HO-1 antioxidant axis

Oxidative stress is a potent trigger for inflammation. The nuclear factor erythroid 2-related factor 2 (Nrf2) is the master regulator of the cellular antioxidant defense. Under basal conditions, Nrf2 is sequestered in the cytoplasm by Kelch-like ECH-associated protein 1 (Keap1), which targets it for ubiquitination<sup>[27]</sup>.

In response to oxidative stress, Nrf2 dissociates from its cytoplasmic repressor Keap1, translocates to the nucleus, and binds to Antioxidant Response Elements (AREs) to promote the expression of antioxidant enzymes, notably heme oxygenase-1 (HO-1). HO-1 catalyzes heme degradation into biliverdin, iron, and carbon monoxide, thereby augmenting cellular antioxidant capacity<sup>[28]</sup>. Critically, Nrf2 activation concurrently suppresses the NLRP3 inflammasome and NF- $\kappa$ B signaling, leading to reduced expression of pro-inflammatory mediators including IL-1 $\beta$ , IL-6, and TNF- $\alpha$ . This dual antioxidant and anti-inflammatory effect is abrogated by pharmacological Nrf2 inhibition, confirming that Nrf2 acts as a master regulator coupling oxidative stress defense with inflammatory response modulation<sup>[27,28]</sup>.

## 4. Therapeutic strategies targeting phenotypic switching

Given the central role of microglial polarization in stroke pathology, shifting the microglial phenotype from the destructive M1 state to the reparative M2 state represents a pivotal therapeutic goal. Unlike broad-spectrum anti-inflammatory agents that may hinder the beneficial clearance of debris, “immunomodulatory” strategies aim to fine-tune the immune response, restoring the balance of the microenvironment.



## 4.1. Pharmacological interventions: repurposing and natural compounds

Pharmacological modulation remains the most accessible approach. This category includes the repurposing of FDA-approved drugs and the exploration of bioactive natural compounds (phytochemicals).

### 4.1.1. Drug repurposing

- (1) Metformin: Widely used for diabetes, metformin has demonstrated robust neuroprotective effects<sup>[29]</sup>. It promotes M2 polarization primarily by activating AMPK (AMP-activated protein kinase). Activated AMPK inhibits the NF- $\kappa$ B pathway and suppresses the NLRP3 inflammasome<sup>[30]</sup>. Furthermore, metformin improves mitochondrial function, supporting the metabolic shift required for the M2 phenotype<sup>[31]</sup>.
- (2) Fingolimod (FTY720): An immunomodulator approved for multiple sclerosis. While primarily known for sequestering lymphocytes, fingolimod also acts directly on microglial S1P receptors (S1PR)<sup>[32]</sup>, biasing them towards an anti-inflammatory state via the STAT3 pathway<sup>[33]</sup>.

### 4.1.2. Phytochemicals

- (1) Curcumin: Derived from turmeric, curcumin is a potent PPAR- $\gamma$  agonist. It inhibits TLR4 signaling and promotes M2 polarization. However, its clinical application is limited by poor bioavailability, necessitating novel formulation strategies<sup>[34,35]</sup>.
- (2) Resveratrol: A polyphenol found in grapes, resveratrol activates SIRT1 (Sirtuin 1). SIRT1 deacetylates the p65 subunit of NF- $\kappa$ B, inhibiting its transcriptional activity, thereby suppressing the M1 response and promoting antioxidant defenses via the Nrf2 axis<sup>[36,37]</sup>.

## 4.2. Stem cell-based and cell-free therapies

Stem cell therapy has evolved from the concept of “cell replacement” to “paracrine modulation.” Specifically, Mesenchymal Stem Cells (MSCs) are the most promising candidates due to their potent immunomodulatory properties.

### 4.2.1. MSC paracrine mechanisms

Transplanted MSCs secrete a “secretome” rich in soluble factors like TGF- $\beta$ , IL-10, and TSG-6. These factors interact with host microglia, suppressing M1 activation and fostering an M2-dominant microenvironment. Importantly, MSCs can “sense” the inflammatory environment and adjust their secretion profile accordingly<sup>[38,39]</sup>.

### 4.2.2. Exosomes

Direct stem cell transplantation faces challenges such as low survival rates, immune rejection, and tumorigenesis risks. Consequently, focus has shifted to Exosomes (small extracellular vesicles, 30-150 nm) derived from MSCs<sup>[40,41]</sup>.

Exosomes are stable, have low immunogenicity, and can cross the BBB more efficiently than whole cells. They function as carriers of biological information, primarily miRNAs. For example, MSC-derived exosomes enriched with miR-124 (a microglia-specific miRNA) or miR-223 have been shown to target molecules in the NF- $\kappa$ B pathway, effectively “silencing” pro-inflammatory genes and inducing M2 polarization. This “cell-free therapy” represents a safer and more controllable alternative for clinical translation<sup>[42]</sup>.

## 4.3. Nanomedicine and targeted delivery systems

A major hurdle in treating CNS disorders is the BBB, which prevents nearly 98% of small-molecule drugs from reaching the brain<sup>[43,44]</sup>. Furthermore, systemic administration of immunomodulators can cause off-target immunosuppression. Nanomedicine offers precise solutions to these challenges.



### 4.3.1. Crossing the BBB

Nanoparticles (NPs) such as liposomes, dendrimers, and polymeric micelles can be engineered to penetrate the BBB. Strategies include receptor-mediated transcytosis (*e.g.*, coating NPs with transferrin or lactoferrin) or “hitchhiking” on circulating immune cells (*e.g.*, neutrophils)<sup>[45–47]</sup> that naturally migrate to the ischemic brain.

### 4.3.2. Stimuli-Responsive release

The ischemic microenvironment has unique characteristics: acidosis (low pH) and high ROS levels. “Smart” ROS-responsive nanoparticles can be designed to degrade and release their drug cargo only when they encounter the high-ROS environment of the M1-polarized zone<sup>[48–50]</sup>. This spatiotemporal control maximizes therapeutic efficacy while minimizing systemic toxicity.

## 5. Conclusion

In summary, the phenotypic switching of microglia acts as a central fulcrum in the pathophysiology of ischemic stroke. The pathological transition from a reparative M2 phenotype to a detrimental M1 state is driven by a complex interplay between signaling pathways (*e.g.*, TLR4/NF- $\kappa$ B, JAK/STAT) and immunometabolic reprogramming. Therefore, therapeutic strategies capable of “remodeling” this microenvironment offer a superior approach compared to broad immunosuppression.

## Funding

This work is financially supported by the National Natural Science Foundation of China (Project No.: 82372029 & 22205133); Discipline Construction of Pudong New Area Health Commission (Project No.: PWZxk2022-03); Shanghai Pudong New District Health Committee Health Industry Special Project (Project No.: PW2024E-02); The Investigator-initiated Trial Program of Shanghai Pudong New Area Health Commission (the Cohort Study Program) (Project No.: 2025-PWDL-24)

## Disclosure statement

The author declares no conflict of interest

## References

- [1] Berge E, Whiteley W, Audebert H, et al., 2021, European Stroke Organisation (ESO) Guidelines on Intravenous Thrombolysis for Acute Ischaemic Stroke. *European Stroke Journal*, 6(1): I–LXII.
- [2] The GBD 2016 Lifetime Risk of Stroke Collaborators, 2018, Global, Regional, and Country-Specific Lifetime Risks of Stroke, 1990 and 2016. *New England Journal of Medicine*, 379(25): 2429–2437.
- [3] Herpich F, Rincon F, 2020, Management of Acute Ischemic Stroke. *Critical Care Medicine*, 48(11): 1654–1663.
- [4] Liu R, Song P, Gu X, et al., 2022, Comprehensive Landscape of Immune Infiltration and Aberrant Pathway Activation in Ischemic Stroke. *Frontiers in Immunology*, 12: 766724.
- [5] Shi K, Tian DC, Li ZG, et al., 2019, Global Brain Inflammation in Stroke. *The Lancet Neurology*, 18(11): 1058–1066.
- [6] Zhang W, Tian T, Gong SX, et al., 2021, Microglia-Associated Neuroinflammation Is a Potential Therapeutic Target for Ischemic Stroke. *Neural Regeneration Research*, 16(1): 6.
- [7] Qin C, Zhou LQ, Ma XT, et al., 2019, Dual Functions of Microglia in Ischemic Stroke. *Neuroscience Bulletin*, 35(5): 921–

933.

- [8] Chhor V, Le Charpentier T, Lebon S, et al., 2013, Characterization of Phenotype Markers and Neuronotoxic Potential of Polarised Primary Microglia in Vitro. *Brain, Behavior, and Immunity*, 32: 70–85.
- [9] Chen AQ, Fang Z, Chen XL, et al., 2019, Microglia-Derived TNF- $\alpha$  Mediates Endothelial Necroptosis Aggravating Blood Brain–Barrier Disruption after Ischemic Stroke. *Cell Death & Disease*, 10(7): 487–505.
- [10] Liu W, Qi Z, Li W, et al., 2022, M1 Microglia Induced Neuronal Injury on Ischemic Stroke via Mitochondrial Crosstalk between Microglia and Neurons. *Oxidative Medicine and Cellular Longevity*, 2022(1): 4335272.
- [11] Fan P, Wang S, Chu S, et al., 2023, Time-Dependent Dual Effect of Microglia in Ischemic Stroke. *Neurochemistry International*, 169: 105584.
- [12] Xia CY, Zhang S, Gao Y, et al., 2015, Selective Modulation of Microglia Polarization to M2 Phenotype for Stroke Treatment. *International Immunopharmacology*, 25(2): 377–382.
- [13] Shimizu T, Prinz M, 2025, Microglia across Evolution: From Conserved Origins to Functional Divergence. *Cellular & Molecular Immunology*, 22(12): 1533–1548.
- [14] Kanazawa M, Ninomiya I, Hatakeyama M, et al., 2017, Microglia and Monocytes/Macrophages Polarization Reveal Novel Therapeutic Mechanism against Stroke. *International Journal of Molecular Sciences*, 18(10): 2135.
- [15] Liddelow SA, Guttenplan KA, Clarke LE, et al., 2017, Neurotoxic Reactive Astrocytes Are Induced by Activated Microglia. *Nature*, 541(7638): 481–487.
- [16] Zhang Y, Li J, Zhao Y, et al., 2024, Arresting the Bad Seed: HDAC3 Regulates Proliferation of Different Microglia after Ischemic Stroke. *Science Advances*, 10(10): eade6900.
- [17] Jolivel V, Bicker F, Binamé F, et al., 2015, Perivascular Microglia Promote Blood Vessel Disintegration in the Ischemic Penumbra. *Acta Neuropathologica*, 129(2): 279–295.
- [18] Keren-Shaul H, Spinrad A, Weiner A, et al., 2017, A Unique Microglia Type Associated with Restricting Development of Alzheimer's Disease. *Cell*, 169(7): 1276–1290.e17.
- [19] Shao L, Chang Y, Liu J, et al., 2024, scRNA-Seq Reveals Age-Dependent Microglial Evolution as a Determinant of Immune Response Following Spinal Cord Injury. *Brain Research Bulletin*, 219: 111116.
- [20] Gelderblom M, Sobey CG, Kleinschmitz C, et al., 2015, Danger Signals in Stroke. *Ageing Research Reviews*, 24: 77–82.
- [21] Jiang L, Xu F, He W, et al., 2016, CD200Fc Reduces TLR4-Mediated Inflammatory Responses in LPS-Induced Rat Primary Microglial Cells via Inhibition of the NF- $\kappa$ B Pathway. *Inflammation Research*, 65(7): 521–532.
- [22] Khoshnavay F, Amirshahrokhi K, Namjoo Z, et al., 2024, Carvedilol Attenuates Inflammatory Reactions of Lipopolysaccharide-Stimulated BV2 Cells and Modulates M1/M2 Polarization of Microglia via Regulating NLRP3, Notch, and PPAR- $\gamma$  Signaling Pathways. *Naunyn-Schmiedeberg's Archives of Pharmacology*, 397(7): 4727–4736.
- [23] Shimada K, Crother TR, Karlin J, et al., 2012, Oxidized Mitochondrial DNA Activates the NLRP3 Inflammasome during Apoptosis. *Immunity*, 36(3): 401–414.
- [24] Swanson KV, Deng M, Ting JPY, 2019, The NLRP3 Inflammasome: Molecular Activation and Regulation to Therapeutics. *Nature Reviews Immunology*, 19(8): 477–489.
- [25] Ye Y, Rao Z, Xie X, et al., 2025, Naoqing Formula Alleviates Cerebral Ischemia/Reperfusion Injury Induced Inflammatory Injury by Regulating Csf3 Mediated JAK/STAT Pathway and Macrophage Polarization. *Phytomedicine*, 140: 156626.
- [26] Guan S, Lu T, Li L, et al., 2025, Targeting Hypercoagulability in Ischemic Stroke Modulates Fibrin-Driven Microglial Polarization via JAK-STAT Pathway. *Journal of Neuroinflammation*, 22(1): 258–279.
- [27] Xie X, Wang F, Ge W, et al., 2023, Scutellarin Attenuates Oxidative Stress and Neuroinflammation in Cerebral Ischemia/Reperfusion Injury through PI3K/Akt-Mediated Nrf2 Signaling Pathways. *European Journal of Pharmacology*, 957: 175979.
- [28] Sun YY, Zhu HJ, Zhao RY, et al., 2023, Remote Ischemic Conditioning Attenuates Oxidative Stress and Inflammation via the Nrf2/HO-1 Pathway in MCAO Mice. *Redox Biology*, 66: 102852.
- [29] Li W, Fan Y, Hussain SA, 2025, Neuroprotective Effects of Sinomenine and Metformin in Diabetic Stroke: Role of

- NLRP3/Caspase-1 and Mitophagy. *Experimental Physiology*: EP093135.
- [30] Reed S, Taka E, Darling-Reed S, et al., 2025, Neuroprotective Effects of Metformin through the Modulation of Neuroinflammation and Oxidative Stress. *Cells*, 14(14): 1064.
  - [31] Jin Q, Cheng J, Liu Y, et al., 2014, Improvement of Functional Recovery by Chronic Metformin Treatment Is Associated with Enhanced Alternative Activation of Microglia/Macrophages and Increased Angiogenesis and Neurogenesis Following Experimental Stroke. *Brain, Behavior, and Immunity*, 40: 131–142.
  - [32] Naseh M, Vatanparast J, Rafati A, et al., 2021, The Emerging Role of FTY720 as a Sphingosine 1-Phosphate Analog for the Treatment of Ischemic Stroke: The Cellular and Molecular Mechanisms. *Brain and Behavior*, 11(6): e02179.
  - [33] Qin C, Fan WH, Liu Q, et al., 2017, Fingolimod Protects against Ischemic White Matter Damage by Modulating Microglia toward M2 Polarization via STAT3 Pathway. *Stroke*, 48(12): 3336–3346.
  - [34] Abdollahi E, Johnston TP, Ghaneifar Z, et al., 2023, Immunomodulatory Therapeutic Effects of Curcumin on M1/M2 Macrophage Polarization in Inflammatory Diseases. *Current Molecular Pharmacology*, 16(1): 2–14.
  - [35] Cao X, Pu Y, 2025, Curcumin Regulates Microglia Polarization to Alleviate Ischemic Stroke by Targeting microRNA-205-5p/Kruppel-like Factor 2 (KLF2)/Activating Transcription Factor 2 (ATF2) Axis. *Chemical Biology & Drug Design*, 105(1): e70050.
  - [36] Bai Y, Sui R, Zhang L, et al., 2024, Resveratrol Improves Cognitive Function in Post-Stroke Depression Rats by Repressing Inflammatory Reactions and Oxidative Stress via the Nrf2/HO-1 Pathway. *Neuroscience*, 541: 50–63.
  - [37] Owjifard M, Rahimian Z, Karimi F, et al., 2024, A Comprehensive Review on the Neuroprotective Potential of Resveratrol in Ischemic Stroke. *Heliyon*, 10(14): e34121.
  - [38] Cunningham CJ, Redondo-Castro E, Allan SM, 2018, The Therapeutic Potential of the Mesenchymal Stem Cell Secretome in Ischaemic Stroke. *Journal of Cerebral Blood Flow & Metabolism*, 38(8): 1276–1292.
  - [39] Lee JY, Kim E, Choi SM, et al., 2016, Microvesicles from Brain-Extract-Treated Mesenchymal Stem Cells Improve Neurological Functions in a Rat Model of Ischemic Stroke. *Scientific Reports*, 6(1): 33038.
  - [40] Nouri Z, Barfar A, Perseh S, et al., 2024, Exosomes as Therapeutic and Drug Delivery Vehicle for Neurodegenerative Diseases. *Journal of Nanobiotechnology*, 22(1): 463–491.
  - [41] Dabrowska S, Andrzejewska A, Lukomska B, et al., 2019, Neuroinflammation as a Target for Treatment of Stroke Using Mesenchymal Stem Cells and Extracellular Vesicles. *Journal of Neuroinflammation*, 16(1): 178–195.
  - [42] Fu X, Li J, Yang S, et al., 2025, Blood-Brain Barrier Repair: Potential and Challenges of Stem Cells and Exosomes in Stroke Treatment. *Frontiers in Cellular Neuroscience*, 19: 1536028.
  - [43] Bao Q, Hu P, Xu Y, et al., 2018, Simultaneous Blood–Brain Barrier Crossing and Protection for Stroke Treatment Based on Edaravone-Loaded Ceria Nanoparticles. *ACS Nano*, 12(7): 6794–6805.
  - [44] Qiu Y, Zhang C, Chen A, et al., 2021, Immune Cells in the BBB Disruption after Acute Ischemic Stroke: Targets for Immune Therapy? *Frontiers in Immunology*, 12: 678744.
  - [45] Song J, Yang G, Song Y, et al., 2024, Neutrophil Hitchhiking Biomimetic Nanozymes Prime Neuroprotective Effects of Ischemic Stroke in a Tailored “Burning the Bridges” Manner. *Advanced Functional Materials*, 34(32): 2315275.
  - [46] Hu K, Ye J, Fan P, et al., 2025, Targeting and Reprogramming Microglial Phagocytosis of Neutrophils by Ginsenoside Rg1 Nanovesicles Promotes Stroke Recovery. *Bioactive Materials*, 47: 181–197.
  - [47] Zhao Y, Li Q, Niu J, et al., 2024, Neutrophil Membrane-Camouflaged Polyprodrug Nanomedicine for Inflammation Suppression in Ischemic Stroke Therapy. *Advanced Materials*: 2311803.
  - [48] Sun S, Lv W, Li S, et al., 2023, Smart Liposomal Nanocarrier Enhanced the Treatment of Ischemic Stroke through Neutrophil Extracellular Traps and Cyclic Guanosine Monophosphate-Adenosine Monophosphate Synthase-Stimulator of Interferon Genes (cGAS-STING) Pathway Inhibition of Ischemic Penumbra. *ACS Nano*, 17(18): 17845–17857.
  - [49] Jin L, Zhu Z, Hong L, et al., 2023, ROS-Responsive 18 $\beta$ -Glycyrrhetic Acid-Conjugated Polymeric Nanoparticles Mediate Neuroprotection in Ischemic Stroke through HMGB1 Inhibition and Microglia Polarization Regulation. *Bioactive Materials*, 19: 38–49.

- [50] Dong Z, Tang L, Zhang Y, et al., 2023, A Homing Peptide Modified Neutrophil Membrane Biomimetic Nanoparticles in Response to ROS/Inflammatory Microenvironment for Precise Targeting Treatment of Ischemic Stroke. *Advanced Functional Materials*: 2309167.

**Publisher's note**

*Whioce Publishing remains neutral with regard to jurisdictional claims in published maps and institutional affiliations.*

# Application of Integrated Animal and Cell Experiment Teaching Model in Demonstrating Ferroptosis in Cerebral Ischemia-Reperfusion Injury

Guangjie Sun<sup>1</sup>, Bingcang Huang<sup>2\*</sup>

<sup>1</sup>School of Gongli Hospital Medical Technology, University of Shanghai for Science and Technology, Shanghai 200093, China

<sup>2</sup> Department of Radiology, Gongli Hospital of Shanghai Pudong New Area, Shanghai 200135, China

\*Corresponding author: Bingcang Huang, [gl\\_huangbc@sumhs.edu.cn](mailto:gl_huangbc@sumhs.edu.cn)

**Copyright:** © 2025 Author(s). This is an open-access article distributed under the terms of the Creative Commons Attribution License (CC BY 4.0), permitting distribution and reproduction in any medium, provided the original work is cited.

**Abstract:** Traditional molecular medicine experimental teaching often suffers from a disconnection between theory and practice, as well as fragmented experimental content, making it difficult for students to integrate multi-level knowledge to address complex scientific problems. To address this, we redesigned our Molecular Medicine Experimental Techniques course around the pathophysiology of cerebral ischemia-reperfusion injury (CIRI), with a focus on the mechanism of ferroptosis. Our integrated pedagogical model links an in vivo transient middle cerebral artery occlusion (tMCAO) mouse model with an in vitro oxygen-glucose deprivation/reoxygenation (OGD/R) model in HT22 neuronal cells. Within this framework, students first observe in vivo phenotypes in the tMCAO model, including increased brain iron content, downregulated GPX4 expression, and accumulation of the lipid peroxidation marker 4-HNE. They then use the OGD/R cell model to validate key ferroptosis features at the molecular and ultrastructural levels, such as enhanced lipid peroxidation, glutathione depletion, and mitochondrial damage. This “phenotype-to-mechanism” approach allows students to intuitively understand the role of ferroptosis in CIRI while systematically mastering the full research cycle, from establishing disease models and applying multi-technique assays to integrating and interpreting data. By translating a cutting-edge scientific topic into a coherent experimental teaching module, this reform effectively bridges the gap between theoretical knowledge and hands-on research practice. It fosters students’ integrative scientific thinking and enhances their ability to tackle complex biomedical questions, offering a transferable paradigm for advancing high-level experimental training in molecular medicine.

**Keywords:** Cerebral ischemia-reperfusion injury; Ferroptosis; Molecular medicine experimental techniques; Teaching reform

**Online publication:** December 26, 2025

## 1. Introduction

Acute stroke is one of the leading causes of death and disability worldwide. The core strategy for its early treatment is to rapidly restore blood flow to the ischemic penumbra. However, this revascularization process can also induce CIRI, a common pathological process following thrombolysis or thrombectomy<sup>[1]</sup>. CIRI is a complex cascade response involving oxidative stress, inflammation, calcium overload, and multiple modes of cell death. This pathological mechanism not



only limits the benefits of reperfusion therapies but is also a key factor in poor neurological outcomes for patients<sup>[2]</sup>. Therefore, understanding the core molecular mechanisms underlying CIRI and exploring effective therapeutic targets have become critical research directions in the field of neuroscience. In recent years, ferroptosis, an iron-dependent cell death characterized by lipid peroxidation accumulation, has been identified as a crucial contributor to CIRI and has become a hotspot in neuroprotection research. Numerous studies have shown that the inhibition of GPX4 activity, the obstruction of lipid peroxidation clearance, and disruptions in iron metabolism collectively trigger ferroptosis, which exacerbates neuronal damage during CIRI. Understanding this mechanism not only provides new insights into the pathophysiology of CIRI but also opens up new opportunities for its treatment<sup>[3]</sup>.

The Molecular Medicine Experimental Techniques course aims to bridge the gap between molecular-level mechanism understanding and experimental skills, enabling students to complete the full research process from theoretical deduction to experimental validation. However, ferroptosis and its relationship with cerebral ischemia-reperfusion injury belong to rapidly developing frontier research areas that involve multiple signalling pathways, complex regulatory networks of cell death, and cross-level pathological changes. Due to the lack of intuitive, systematic, and easily operable experimental scenarios, students often struggle to establish clear causal chains between abstract concepts, molecular indicators, and actual pathological events. This leads to a significant “knowledge-action separation”. On the knowledge level, teaching mostly focuses on lectures and literature reading. Although students may remember key terms such as GPX4 and lipid peroxidation, they often lack an intuitive and dynamic understanding of how these molecules interact to form a complete “death signalling pathway” and how this pathway is activated and regulated in the complex *in vivo* microenvironment.

On the action level, the current experimental course structure faces systemic shortcomings. The course content typically consists of isolated verification experiments, such as performing Western blotting to detect a specific protein one week and cell culture the next. These techniques lack a cohesive logical thread, which results in students mastering fragmented experimental skills but struggling to integrate multiple techniques to solve a specific scientific problem. They do not know why they should choose a particular technique over another in a specific research context, nor do they know how to integrate multidimensional data, such as cell viability, molecular expression, and biochemical markers, into a comprehensive scientific picture. Traditional cell-based experiments tend to focus on specific markers, which can demonstrate changes at the molecular and cellular levels but fail to reflect the true tissue damage state in the *in vivo* environment. Animal experiments, while capable of presenting the overall physiological and pathological process, are time-consuming, complex, and subject to strict ethical requirements, making it difficult to conduct in-depth mechanistic exploration within limited class time. The separation between these two approaches prevents students from seeing the complete scientific logical chain from *in vivo* pathology to *in vitro* model validation, hindering their ability to form a systematic, integrated understanding of disease mechanisms.

Ultimately, this disconnection between theory and practice, between technology and scientific problems, has resulted in a passive learning habit. Students tend to follow pre-established experimental protocols mechanically, rather than actively designing experiments, analyzing data, and engaging in critical thinking. When faced with real scientific questions, such as “how to demonstrate the role of ferroptosis in CIRI”, they often find themselves at a loss. Therefore, in the reform of Molecular Medicine Experimental Techniques, the urgent need is to construct a teaching model that bridges multiple biological levels and integrates theoretical depth with experimental operability. Using ferroptosis and cerebral ischemia-reperfusion injury as a teaching vehicle, the integration of animal and cell models can enable students to observe pathological phenotype changes at the *in vivo* level, while also validating the underlying mechanisms at the cellular and molecular levels. This approach holds the potential to achieve seamless knowledge integration from macroscopic to microscopic levels, helping students build a more comprehensive framework for understanding disease mechanisms (**Figure 1**).

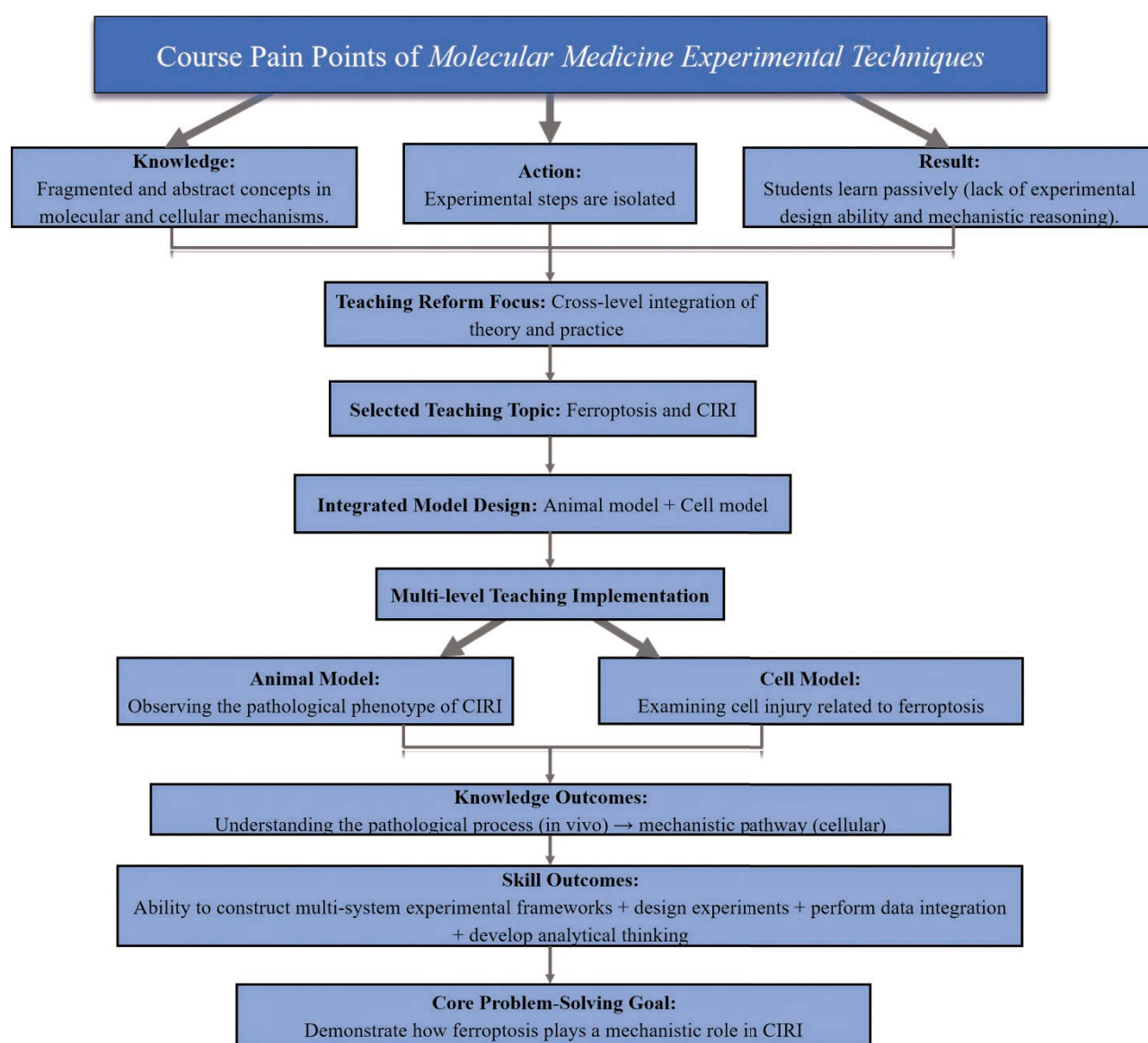


**Figure 1.** Teaching reform logic for the course “Molecular medicine experimental techniques”.

## 2. Related theoretical foundation

### 2.1. Cerebral ischemia-reperfusion injury

Cerebral ischemia-reperfusion injury is a complex pathological process that cannot be ignored during the treatment of acute ischemic stroke. When blood supply is interrupted due to vascular blockage, brain tissue rapidly experiences energy metabolism disorders, ionic homeostasis disruption, and neuronal dysfunction<sup>[4]</sup>. Although reperfusion is crucial for salvaging the ischemic penumbra, the process itself triggers a series of secondary damage responses that further harm brain tissue. During the ischemic phase, blood flow interruption causes a loss of oxygen and glucose supply to the brain, resulting in severe disturbances in cellular energy metabolism. Reduced ATP synthesis impairs the function of the sodium-potassium pump and calcium pump, causing a massive accumulation of sodium and calcium ions. The imbalance in ionic concentrations inside and outside the cell further leads to cell swelling, acidosis, and excessive release of excitotoxic substances such as glutamate, which exacerbates neuronal injury<sup>[5]</sup>. Meanwhile, the hypoxic and low-energy environment

during ischemia leads to the accumulation of metabolic intermediates, generating a large amount of free radicals, particularly hydrogen peroxide ( $\text{H}_2\text{O}_2$ ) and superoxide anions ( $\text{O}^{2-}$ ), intensifying oxidative stress and activating multiple cell damage pathways, including lipid peroxidation, protein oxidation, and DNA damage. However, after blood reperfusion, a surge of oxygen floods the damaged tissues, causing a dramatic burst of oxidative stress. During the reperfusion phase, high concentrations of reactive oxygen species (ROS), including highly reactive molecules like hydroxyl radicals, are rapidly generated. These oxidative molecules not only further damage cell membranes, mitochondria, and nucleic acids but also cause mitochondrial dysfunction by opening mitochondrial permeability transition pores (mPTP), releasing a large amount of pro-apoptotic factors such as cytochrome C, which intensifies cell death<sup>[6]</sup> (**Figure 2**).

In the process of CIRI, the activation of inflammatory responses also plays a significant role. Following reperfusion, the blood-brain barrier is compromised, allowing peripheral immune cells, such as neutrophils and monocytes, to enter brain tissue and release large amounts of pro-inflammatory cytokines, such as tumor necrosis factor- $\alpha$  (TNF- $\alpha$ ) and interleukins (IL-1 $\beta$ , IL-6). These cytokines not only further exacerbate local inflammation but also accelerate neuronal damage by activating glial cells and astrocytes through inflammatory pathways. The excessive release of inflammatory factors can also promote excitotoxicity in neurons, leading to further neuronal death<sup>[7]</sup>. Moreover, various forms of cell death are involved in CIRI, including classical apoptosis, necrosis, pyroptosis, and ferroptosis, which has garnered increasing attention in recent years.

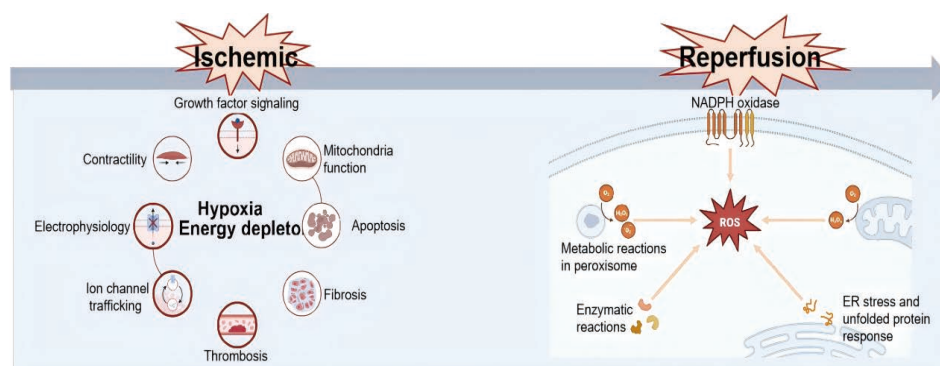


**Figure 2.** Schematic representation of the cellular mechanisms in ischemia and reperfusion.

## 2.2. Molecular mechanism of ferroptosis and its role in cerebral ischemia-reperfusion injury

Ferroptosis is a form of regulated cell death characterized by the accumulation of iron-catalyzed lipid peroxides. Unlike traditional apoptotic or necrotic pathways, ferroptosis arises from a combination of disrupted iron homeostasis, damaged membrane lipid structures, and insufficient antioxidant defences. In neurological disorders, particularly CIRI, ferroptosis has been established as one of the key mechanisms leading to neuronal dysfunction and tissue damage. The occurrence of ferroptosis involves multiple molecular regulatory axes, primarily including the following aspects (**Figure 3**):

### 2.2.1. Disruption of iron homeostasis leading to iron ion accumulation

During cerebral ischemia-reperfusion injury, intracellular iron homeostasis is severely disrupted. The upregulation of transferrin receptor 1 promotes iron uptake, while autophagic pathways of ferritin are activated, releasing stored iron into the cell. This results in a significant increase in the concentration of free ferrous iron ( $\text{Fe}^{2+}$ ) within the cell. Excess  $\text{Fe}^{2+}$  reacts with hydrogen peroxide through the Fenton reaction, producing highly reactive hydroxyl radicals. These radicals initiate protein carbonylation, DNA damage, and lipid peroxidation, directly disrupting the structural and functional integrity of the cell<sup>[8]</sup>.

### 2.2.2. Membrane lipid components are prone to oxidation, enhancing lipid peroxidation

Neuronal membranes are rich in polyunsaturated fatty acids, which are chemically vulnerable to oxidative stress. After

ischemia-reperfusion, the level of oxidative stress rises sharply, leading to the oxidation of polyunsaturated fatty acids in membrane lipids and the generation of a large amount of lipid peroxides. Enzymes such as ACSL4 and LPCAT3 promote the incorporation of specific fatty acids into membrane phospholipids, making them the primary substrates for oxidation. Additionally, the activation of lipoxygenases and other oxidases further drives the cascading process of lipid peroxidation. The accumulating lipid peroxides weaken the stability of membrane structures, ultimately causing membrane rupture, which is a critical step in ferroptosis execution<sup>[9]</sup>.

### 2.2.3. Impaired antioxidant defenses and reduced GPX4 activity

Cells rely on multiple antioxidant mechanisms to limit lipid peroxidation, with GPX4 being the most crucial defense factor. GPX4 reduces phospholipid peroxides to relatively stable alcohols, thereby protecting the cell membrane from oxidative damage. Its activity depends on GSH, the production of which is reliant on cysteine uptake. Under ischemia-reperfusion conditions, oxidative stress and metabolic limitations lead to GSH depletion, while insufficient cysteine supply further reduces GPX4 activity. The collapse of the antioxidant system prevents the timely clearance of lipid peroxides, pushing the cell into an irreversible ferroptosis state. Studies have shown that ferroptosis is closely related to cell death in CIRI models, where iron ions enhance oxidative stress and lipid peroxidation, promoting neuronal death and causing irreversible brain tissue damage<sup>[10]</sup>.

During the progression of CIRI, ferroptosis is not merely a form of cell death but a central process that amplifies neuronal damage. The reduction in energy production during the ischemic phase leads to a diminished ability to maintain cellular homeostasis. The oxygen influx during reperfusion drastically increases oxidative pressure, accelerating iron-dependent lipid peroxidation. The membrane damage caused by this process is irreversible, ultimately resulting in extensive neuronal death. This highlights that ferroptosis is not only a critical mechanism in CIRI but also a potential target for future therapeutic strategies.

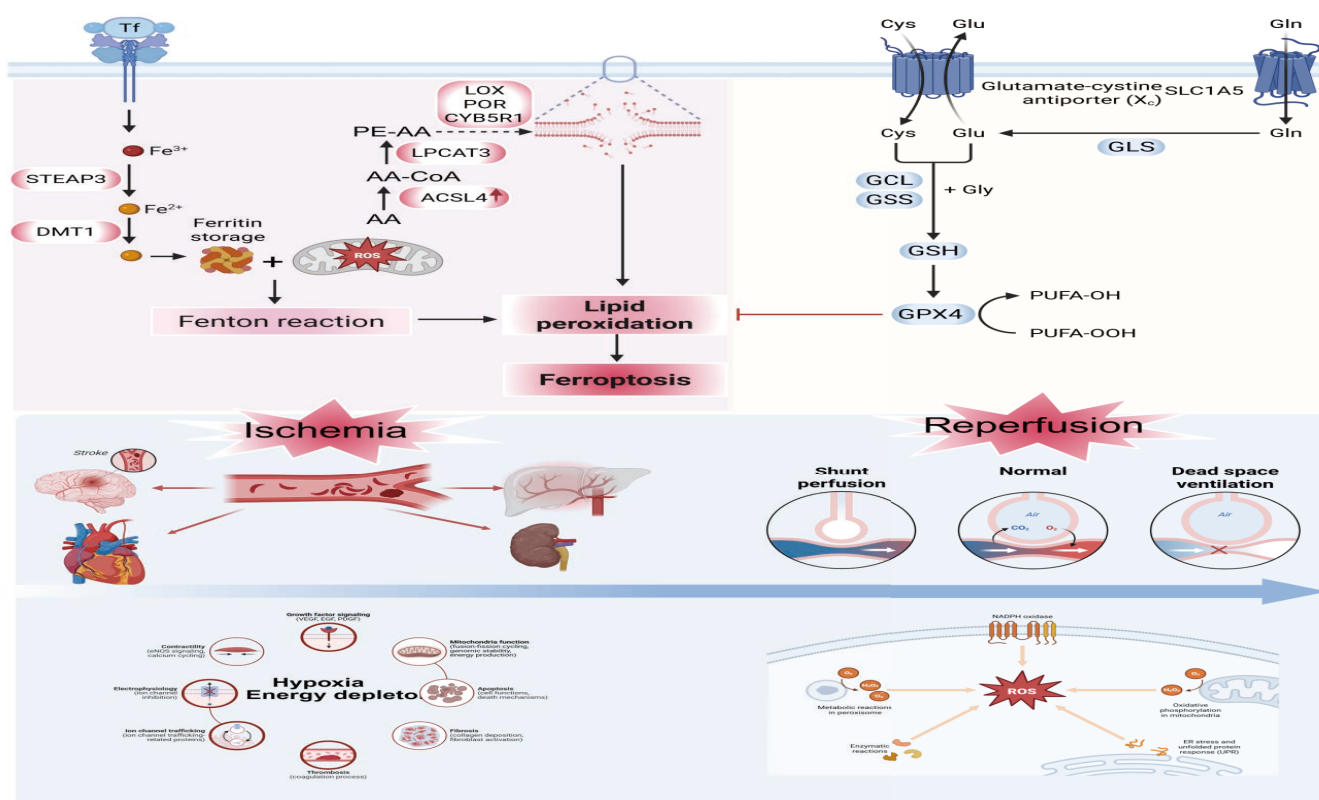


Figure 3. Molecular pathways of ferroptosis.



### 3. Analysis of animal and cell experiments based on the “molecular medicine experimental techniques” course

#### 3.1. Animal experiment

In the Molecular Medicine Experimental Techniques course, to observe the dynamic changes of ferroptosis during CIRI, we established a transient middle cerebral artery occlusion/reperfusion (tMCAO/R) model using 6-8-week-old C57BL/6 mice. After anesthetizing the mice with 4% pentobarbital sodium via intraperitoneal injection, we carefully isolated the left common carotid artery, external carotid artery, and internal carotid artery under a microscope. The middle cerebral artery was then occluded for 1.5 hours using an intraluminal suture technique. After removing the suture to restore blood flow and reperfusion for 24 hours, brain tissue was collected to evaluate ferroptosis-related markers and to systematically assess the molecular and cellular changes induced by ischemia-reperfusion<sup>[11]</sup>.

First, we measured the free iron levels in the brain tissue using an iron content assay kit. The results showed a significant increase in iron content in the tMCAO group compared to the control group (**Figure 4a**), suggesting that ischemia-reperfusion severely disrupts iron homeostasis, a key prerequisite for ferroptosis. To further assess the molecular features of ferroptosis, we examined the expression levels of the critical ferroptosis-related protein GPX4 and the lipid peroxidation product 4-HNE. Immunofluorescence results indicated a significant reduction of GPX4 signal in the brain tissue of the tMCAO group (**Figure 4b**), indicating impaired neuronal ability to clear lipid peroxides. At the same time, the fluorescence signal for 4-HNE was significantly enhanced (**Figure 4c**), indicating the accumulation of lipid peroxides, which is highly consistent with the typical process of ferroptosis. To explore the relationship between ferroptosis and inflammation, we further measured the levels of common inflammatory cytokines associated with ischemia-reperfusion injury. ELISA results showed that the expression of TNF- $\alpha$ , IL-1 $\beta$ , and IL-6 in the tMCAO group was significantly higher than in the control group (**Figure 4d-f**). These results suggest that ferroptosis is significantly activated during cerebral ischemia-reperfusion and is accompanied by a strong inflammatory response. This inflammatory amplification effect may play a crucial role in exacerbating tissue damage and advancing the pathological process.

In summary, the tMCAO/R model demonstrated a series of typical ferroptosis phenotypes, including elevated iron content, downregulation of GPX4, enhanced lipid peroxidation, and increased inflammatory cytokine levels. These findings suggest that ferroptosis may be an important pathological mechanism in cerebral ischemia-reperfusion injury.

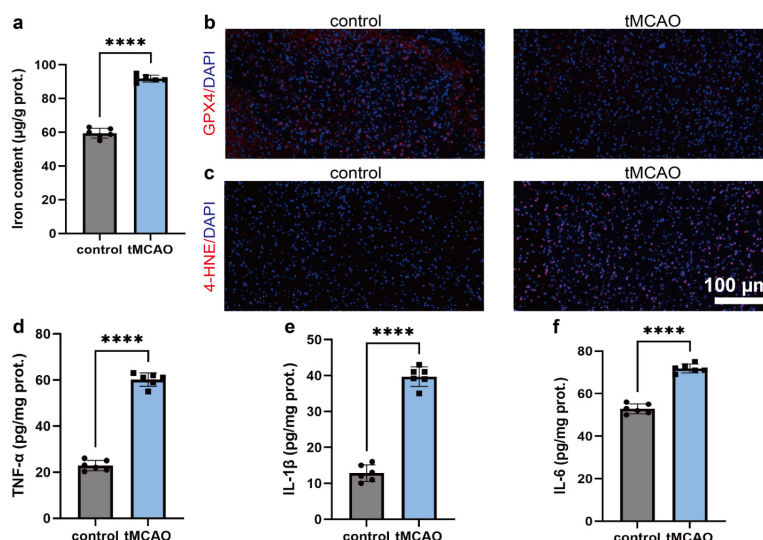


**Figure 4.** Assessment of ferroptosis- and inflammation-related indicators in the tMCAO/R mouse model.

(a) Quantification of total iron levels in brain tissue from control and tMCAO mice using an iron content assay. (b) Immunofluorescence staining of GPX4 in coronal brain sections, with nuclei labeled by DAPI. (c) Immunofluorescence staining of the lipid peroxidation marker 4-HNE, counterstained with DAPI. d-f) Measurement of TNF- $\alpha$  (d), IL-1 $\beta$  (e), and IL-6 (f) concentrations in brain homogenates by ELISA. All assays were performed 24 h after reperfusion following 1.5 h tMCAO. Data are presented as mean  $\pm$  SEM. \*\*\*\*P < 0.0001.



### 3.2. Cell experiment

To further validate the role of ferroptosis in ischemia-reperfusion injury, we treated HT22 cells, a mouse hippocampal neuronal cell line, using an oxygen-glucose deprivation (OGD)/reperfusion (R) model *in vitro*. HT22 cells were chosen due to their neuronal characteristics and suitability for studying oxidative stress and neurodegenerative processes. First, HT22 cells were seeded in culture dishes and allowed to adhere for 24 hours. The cells were then switched to glucose-free MEM medium and placed in an anaerobic chamber (Mitsubishi, Japan) for 4 hours of OGD treatment. After the treatment, normal culture medium was added, and the cells were transferred to a 5 % CO<sub>2</sub> incubator for an additional 24 hours to simulate ischemia-reperfusion conditions.

To assess the level of lipid peroxidation in the cells, we used the BODIPY 581/591 C11 fluorescent probe. After OGD/R treatment, the oxidized (green) signal in the cells was significantly enhanced, indicating a substantial accumulation of lipid peroxides within the cells (**Figure 5a**). This change is consistent with the occurrence of ferroptosis. We then measured the levels of GSH and malondialdehyde (MDA) in the cells to further evaluate changes in the oxidative-reductive state. The GSH level in the neurons after OGD/R treatment was significantly lower than that in the control group (**Figure 5b**), suggesting impaired antioxidant capacity. Meanwhile, the MDA level in the OGD/R group was significantly higher (**Figure 5c**), further confirming the intensification of lipid peroxidation and the activation of the ferroptosis process. Finally, we used transmission electron microscopy (TEM) to observe the ultrastructure of the neurons. In the control group, the mitochondria of the neurons appeared intact, with clear inner membrane structures. However, in the neurons treated with OGD/R, the mitochondria showed signs of shrinkage, membrane densification, and loss of inner membrane structure (**Figure 5d**), which are highly consistent with mitochondrial damage associated with ferroptosis.

In summary, the characteristics of ferroptosis were confirmed both in the mouse model and in cultured HT22 neurons. The increased iron content, reduced GPX4 expression, enhanced 4-HNE levels, and elevated inflammatory factors in the mouse brain tissue all indicate that ferroptosis was significantly activated during ischemia-reperfusion. In HT22 neurons treated with OGD/R, lipid peroxidation, GSH depletion, elevated MDA levels, and changes in mitochondrial morphology further support the occurrence of ferroptosis. These results suggest that ferroptosis may play a key role in cerebral ischemia-reperfusion injury, exacerbating brain tissue damage through oxidative stress and inflammatory responses.

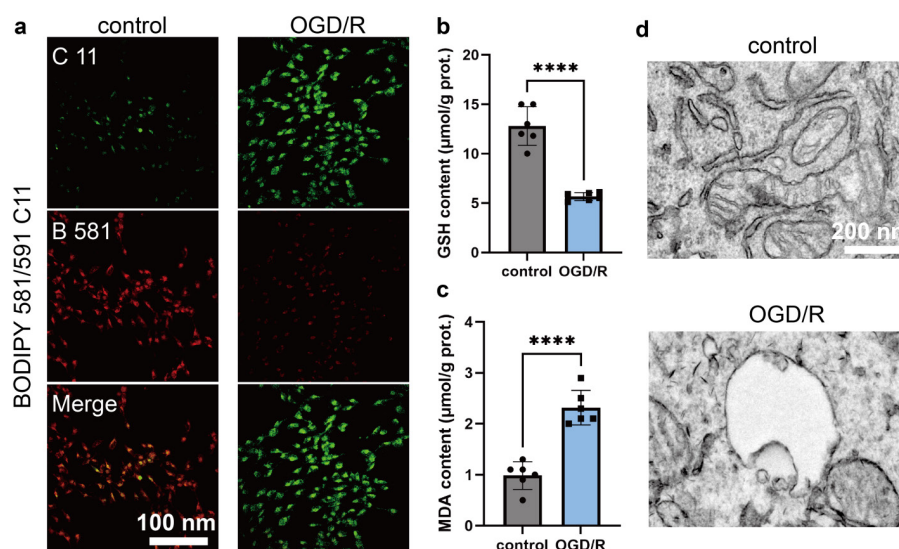


**Figure 5.** Ferroptosis and mitochondrial damage in HT22 cells subjected to OGD/R treatment.

(a) Lipid peroxidation assessed by BODIPY 581/591 C11 probe. (b) GSH content measurement. (c) MDA content measurement. (d) Transmission electron microscopy images showing mitochondrial morphology in control and OGD/R-treated HT22 cells. Data are presented as mean  $\pm$  SEM. \*\*\*\* $P < 0.0001$ .

## 4. Conclusions

Ferroptosis, a novel form of cell death, plays a crucial role in cerebral ischemia-reperfusion injury. By regulating iron metabolism, antioxidant responses, and lipid peroxidation, ferroptosis can be effectively mitigated, thereby protecting brain tissue and reducing the damage caused by ischemia-reperfusion. Through the experimental content in the Molecular Medicine Experimental Techniques course, students can gain a deeper understanding of the molecular mechanisms of ferroptosis and provide experimental evidence for related therapeutic strategies. As research advances, targeted treatment of ferroptosis is expected to become an important strategy in the treatment of cerebral ischemia-reperfusion injury and may lead to new breakthroughs in the treatment of neurodegenerative diseases.

This study focuses on the key pathological mechanisms of cerebral ischemia-reperfusion injury, particularly the ferroptosis process, which has garnered significant attention in recent years. We have developed a comprehensive teaching model that deeply integrates animal and cell experiments. By combining the mouse middle cerebral artery occlusion model with the HT22 cell oxygen-glucose deprivation/reperfusion model, students are able to simultaneously observe changes in ferroptosis-related molecular markers at both the *in vivo* and cellular levels. This approach provides an intuitive understanding of the role of ferroptosis in cerebral ischemia-reperfusion injury. Practical results demonstrate that this teaching model not only addresses the gap between theory and experiment in traditional education but also enhances students' systematic understanding of complex pathological mechanisms. It strengthens their experimental design, data analysis, and scientific thinking abilities.

Additionally, ferroptosis, as a key regulatory target in cerebral ischemia-reperfusion injury, involves disruptions in iron homeostasis, accumulation of lipid peroxides, and imbalances in antioxidant systems. These mechanisms are closely linked to neuronal structural damage and functional loss. By incorporating these cutting-edge mechanisms into experimental teaching, the model not only expands students' understanding of molecular medicine's frontier but also provides a feasible path for future innovative experimental courses.

In conclusion, the integration of animal and cell models in experimental teaching enhances the depth and breadth of the course and presents a new, replicable, and scalable paradigm for molecular medicine experimental education reform. Future teaching efforts can further incorporate multi-omics technologies, advanced imaging techniques, and explore additional novel cell death mechanisms to continuously optimize the experimental teaching system, thereby improving students' ability to understand disease mechanisms and foster scientific innovation.

## 5. Acknowledgements

All animal experiments were performed with the approval of the Ethics Committee of Shanghai University (Project No.: ECSHU-2021-029). This work is financially supported by the National Natural Science Foundation of China (Project No.: 82372029, 22205133), Discipline Construction of Pudong New Area Health Commission (Project No.: PWZxk2022-03), Shanghai Pudong New District Health Committee Health Industry Special Project (Project No.: PW2024E-02) and The Investigator-initiated Trial Program of Shanghai Pudong New Area Health Commission (the Cohort Study Program) (Project No.: 2025-PWDL-24).

## Disclosure statement

The author declares no conflict of interest.

## References

- [1] Feigin VL, Brainin M, Norrving B, et al., 2025, World Stroke Organization: Global Stroke Fact Sheet 2025. *Int J Stroke*,

20(2): 132-144.

- [2] Wu L, Xiong X, Wu X, et al., 2020, Targeting Oxidative Stress and Inflammation to Prevent Ischemia-Reperfusion Injury. *Front Mol Neurosci*, 13: 28.
- [3] Li J, Cao F, Yin HL, et al., 2020, Ferroptosis: past, present and future. *Cell Death & Disease*, 11(2): 88.
- [4] Yang M, Liu B, Chen B, et al., 2025, Cerebral ischemia-reperfusion injury: mechanisms and promising therapies. *Front Pharmacol*, 16: 1613464.
- [5] Zhang M, Liu Q, Meng H, et al., 2024, Ischemia-reperfusion injury: molecular mechanisms and therapeutic targets. *Signal Transduction and Targeted Therapy*, 9(1): 12.
- [6] Lee P, Chandel NS, Simon MC, 2020, Cellular adaptation to hypoxia through hypoxia inducible factors and beyond. *Nature Reviews Molecular Cell Biology*, 21(5): 268-283.
- [7] Li Z, Li M, Fang Z, et al., 2025, Immunological Mechanisms and Therapeutic Strategies in Cerebral Ischemia-Reperfusion Injury: From Inflammatory Response to Neurorepair. *Int J Mol Sci*, 26(17).
- [8] Ru Q, Li Y, Chen L, et al., 2024, Iron homeostasis and ferroptosis in human diseases: mechanisms and therapeutic prospects. *Signal Transduction and Targeted Therapy*, 9(1): 271.
- [9] Mortensen MS, Ruiz J, Watts JL, 2023, Polyunsaturated Fatty Acids Drive Lipid Peroxidation during Ferroptosis. *Cells*, 12(5): 804.
- [10] Forcina GC, Dixon SJ, 2019, GPX4 at the Crossroads of Lipid Homeostasis and Ferroptosis. *Proteomics*, 19(18): e1800311.
- [11] Chaparro-Cabanillas N, Arbaizar-Roviroso M, Salas-Perdomo A, et al., 2023, Transient Middle Cerebral Artery Occlusion Model of Stroke. *J Vis Exp*, 11(198).

#### **Publisher's note**

Whioce Publishing remains neutral with regard to jurisdictional claims in published maps and institutional affiliations.

# Plant-derived Extracellular Vesicles in the Central Nervous System: Emerging Mechanisms and Therapeutic Opportunities

Zelun Zheng<sup>1</sup>, Fanfan Cao<sup>2\*</sup>

<sup>1</sup>School of Gongli Hospital Medical Technology, University of Shanghai for Science and Technology, Shanghai 200093, China.

<sup>2</sup>Shanghai Health Commission Key Lab of Artificial Intelligence (AI)-Based Management of Inflammation and Chronic Diseases, Department of Central Laboratory, Pudong Gongli Hospital, Shanghai University of Medicine & Health Sciences, Shanghai 200135, China

*\*Author to whom correspondence should be addressed.*

**Copyright:** © 2025 Author(s). This is an open-access article distributed under the terms of the Creative Commons Attribution License (CC BY 4. 0), permitting distribution and reproduction in any medium, provided the original work is cited.

**Abstract:** Exosomes are nanoscale extracellular vesicles secreted by cells that transport proteins, nucleic acids and lipids, thereby mediating intercellular communication and regulating a wide range of physiological and pathological processes. In recent years, plant-derived extracellular vesicles have emerged as promising therapeutic agents, particularly for neurological disorders. This Review summarizes current knowledge of the biogenesis of plant exosomes, highlights their similarities and differences with animal-derived exosomes, and discusses the mechanisms governing their intercellular transfer. We further outline the molecular mechanisms underlying major neurological diseases and examine the signaling pathways through which plant-derived extracellular vesicles may exert neuroprotective and therapeutic effects. Together, these insights underscore the potential of plant-derived exosomes as a novel and versatile platform for the treatment of neurological disorders.

**Keywords:** plant-derived extracellular vesicles; neurological disorders; Alzheimer's disease Parkinson's disease; molecular mechanisms

**Online publication:** December 26, 2025

## 1. Introduction

Exosomes are nanoscale extracellular vesicles (typically ~40–150 nm in diameter) that have been identified across diverse biological systems, including animals, plants and bacteria<sup>[1]</sup>. Once regarded as cellular debris, exosomes are now recognized as integral mediators of intercellular communication, capable of transferring proteins, nucleic acids and lipids to modulate recipient-cell phenotypes<sup>[2]</sup>. Eukaryotic cell-derived exosomes have attracted substantial interest as delivery vehicles for neurological disorders, owing to their biocompatibility and amenability to engineering<sup>[3]</sup>. Plant-derived exosome-like nanovesicles (ELNs) have recently emerged as an appealing complement to animal-derived vesicles. Compared with their mammalian counterparts, ELNs are generally associated with low immunogenicity, favourable biocompatibility and an abundant repertoire of bioactive cargos, including antioxidants and nucleic acids. Notably, ELNs can be administered via non-invasive routes such as oral or intranasal delivery, and their production benefits from readily



accessible sources, lower cost and scalability. In addition, the relatively robust lipid architecture of plant ELNs may confer enhanced physicochemical stability, which could be advantageous for systemic delivery and for traversing biological barriers such as the blood–brain barrier (BBB)<sup>[4]</sup>.

Neurological disorders are broadly classified into diseases of the central nervous system (CNS) and those of the peripheral nervous system (PNS). Here, we focus on recent advances in CNS disorders, including Alzheimer’s disease, ischaemic stroke and Parkinson’s disease. The onset and progression of these conditions typically reflect the interplay of environmental exposures, genetic susceptibility and immune dysregulation. Their pathophysiology converges on several core processes, including neurodegeneration, aberrant glial activation and disrupted neurotransmission. Despite substantial clinical heterogeneity, many CNS disorders share conserved molecular hallmarks, most notably neuroinflammation, oxidative stress, mitochondrial dysfunction and synaptic impairment<sup>[5]</sup>. Current therapeutic strategies span multiple modalities, including nanogel-based delivery systems, liposomal formulations and gene regulation approaches targeting long non-coding RNAs (lncRNAs). However, nanogels remain limited by concerns over biocompatibility and potential neurotoxicity, as well as suboptimal penetration and delivery efficiency within brain tissue, which complicates access to deep parenchymal regions<sup>[6]</sup>. Liposomes, although widely used, can exhibit insufficient targeting specificity, constrained drug loading and release kinetics, and reduced bioavailability, thereby diminishing therapeutic benefit. Moreover, translation of lncRNA-based interventions is still hindered by a central challenge—achieving safe, specific and durable *in vivo* delivery—often necessitating sequence optimization and chemical modification to improve stability while minimizing immunogenicity<sup>[7]</sup>. Against this backdrop, plant-derived exosome-like nanovesicles (ELNs) have attracted growing interest as delivery vehicles because of their favourable delivery performance and reported potential to traverse the blood–brain barrier, positioning them as a promising platform for CNS therapeutics.

Plant-derived extracellular vesicles have been increasingly investigated as therapeutic mediators across a range of disease contexts. Accumulating evidence suggests that they can promote neuroprotection by modulating inflammatory signalling, engaging autophagy-associated pathways and attenuating oxidative stress. Consistent with these activities, plant-derived vesicles have been reported to exert pleiotropic biological effects, including anti-inflammatory, antioxidant, antitumour and neuroprotective functions. In the context of neuroinflammation, these vesicles appear capable of dampening pro-inflammatory mediators. For example, Yan et al. showed in a model of enteritis/intestinal inflammation that ginger-derived exosome-like vesicles reduced the production or expression of TNF, IL-6 and IL-1 $\beta$ , thereby mitigating inflammatory responses<sup>[8]</sup>.

This Review summarizes recent advances in plant-derived extracellular vesicles, with an emphasis on their distinctive features and practical advantages, cellular uptake routes, and the molecular mechanisms underlying neurological disease initiation and progression. We discuss candidate pathways through which plant-derived vesicles may modulate neural and neuroimmune circuits, highlighting opportunities for therapeutic intervention. Finally, we outline key challenges and outstanding limitations that must be addressed to facilitate clinical translation of plant-derived extracellular vesicle-based strategies for complex neurological disorders.

## 2. Exosome production and comparison

### 2.1. Production of Extracellular Vesicles

Plant-derived extracellular vesicles have attracted growing attention and share several structural and compositional features with mammalian extracellular vesicles. Although the mechanisms governing their biogenesis and release remain incompletely resolved, current evidence supports at least three major routes: secretion via multivesicular body (MVB) fusion with the plasma membrane, unconventional secretion mediated by extracellular vesicle–positive organelles (EXPOs), and plasma membrane budding to generate microvesicles<sup>[9]</sup>.

In the MVB pathway, endocytosis-derived early endosomes mature into MVBs, within which the limiting membrane invaginates to form intraluminal vesicles (ILVs). During ILV formation, selected cargos—including RNAs, lipids and



proteins—are incorporated into the vesicles. Fusion of MVBs with the plasma membrane then releases ILVs into the extracellular space as exosome or exosome-like vesicles, enabling intercellular communication and signal transmission. Support for this route has been obtained in model plants such as *Arabidopsis thaliana*<sup>[10]</sup>.

By contrast, the EXPO pathway represents a plant-specific, non-canonical secretory route that is independent of the classical ER–Golgi–endosome trafficking axis. EXPOs typically display a characteristic double-membrane architecture and show limited colocalization with canonical organelle markers, including those of the Golgi apparatus, the trans-Golgi network/early endosomes, or MVBs/late endosomes. EXPOs can fuse directly with the plasma membrane, releasing their contents into the apoplast<sup>[11]</sup>. Emerging studies further implicate EXPO-associated processes in plant adaptation to abiotic stress, potentially contributing to cellular homeostasis and stress signalling under salinity, drought, oxidative stress and metal toxicity<sup>[12]</sup>.

In addition to these routes, plant immune responses have been linked to direct fusion between the vacuole and the plasma membrane, enabling rapid extracellular discharge of hydrolases and defence-related proteins. This mechanism may facilitate the prompt establishment of local defence barriers and enhance disease resistance<sup>[13]</sup>.

## 2.2. Comparison of exosomes

Compared with mammalian extracellular vesicles, plant-derived vesicles are often reported to display greater physicochemical stability, low apparent toxicity and a relatively narrow size distribution, alongside practical advantages such as abundant source materials, reduced cost and scalability of production. Collectively, these attributes support their development as nanodelivery platforms in nanomedicine. At the molecular level, plant-derived exosome-like vesicles also differ substantially from mammalian exosomes. Their membranes are enriched in phospholipids and glycolipids as well as phytosterols, and the absence of cholesterol is expected to confer distinct bilayer organization and biophysical properties. In addition, cell wall-associated polysaccharides (including cellulose, hemicellulose and pectin) may provide an added protective interface under complex or harsh conditions, further enhancing stability and environmental resilience. Plant vesicles can also carry and enrich plant-specific bioactive metabolites—such as polyphenols, carotenoids, terpenoids and alkaloids—which may contribute to antioxidant capacity and the maintenance of cellular homeostasis<sup>[2]</sup>.

Antioxidants have considerable potential for mitigating oxidative stress and may help to counteract ageing and reduce the risk of cancer and neurodegenerative disease. However, their clinical translation is frequently limited by poor in vivo stability, low bioavailability and inadequate tissue targeting. Encapsulation of antioxidant bioactives within natural nanocarriers, such as extracellular vesicles, could enhance cargo protection and delivery efficiency, offering a potentially more effective therapeutic strategy—particularly for disorders of the central nervous system<sup>[3]</sup>. For example, exosome-like nanocarriers derived from saffron-enriched, engineered tomatoes (Tomafran) have been reported to confer neuroprotection in models of neuronal injury, and permeability assessments at the blood–brain barrier suggested that vesicle encapsulation may improve the utilization and efficacy of the active compounds<sup>[14]</sup>.

## 2.3. Uptake mechanisms of plant exosomes

Plant-derived exosome-like vesicles can be internalized by recipient cells through multiple routes. In the context of neurological applications, interactions between vesicle surface components and target-cell membranes—and the ensuing uptake pathways—are likely to be major determinants of in vivo delivery efficiency and translational feasibility<sup>[15]</sup>. Broadly, cellular entry of plant vesicles can be grouped into three modes: endocytosis-dependent uptake; internalization mediated by membrane-surface interactions; and uptake or fusion behaviours shaped by the nanovesicle membrane composition, including lipid and glycan features.

Endocytosis describes the internalization of extracellular material through plasma-membrane invagination and vesicle formation. Major endocytic routes include phagocytosis, caveolin-mediated endocytosis and clathrin-mediated endocytosis. Phagocytosis is largely restricted to professional phagocytes and supports the clearance of relatively large particles. Caveolin-mediated uptake is commonly associated with lipid-raft microdomains and may promote cytosolic

delivery while limiting lysosomal trafficking, thereby reducing degradative loss of cargo. By contrast, clathrin-mediated endocytosis involves the assembly of clathrin-coated pits and vesicles and typically cooperates with specific receptors to enable comparatively selective internalization.

Beyond canonical endocytic routes, molecular interactions at the interface between the plasma membrane and plant-derived extracellular vesicles are also likely to shape uptake efficiency and cellular tropism. Plant vesicle membranes can display bioactive small molecules and surface proteins that engage cognate receptors on recipient cells, thereby promoting receptor-mediated internalization. In addition, vesicle lipids and glycan-bearing constituents, including glycoproteins, may cooperate to strengthen adhesion and facilitate entry, potentially improving targeting precision and enhancing therapeutic efficacy<sup>[16]</sup>.

### 3. Molecular mechanisms in the nervous system

#### 3.1. Alzheimer's disease

Alzheimer's disease (AD) is a progressive neurodegenerative disorder characterized clinically by cognitive decline and pathologically by extracellular amyloid- $\beta$  (A $\beta$ ) deposition, intracellular neurofibrillary tangles, glial activation and neuronal loss. A $\beta$  pathology arises from proteolytic processing of amyloid precursor protein (APP) by  $\beta$ - and  $\gamma$ -secretases, generating A $\beta$  peptides—particularly the aggregation-prone A $\beta$ 42—that assemble into soluble oligomers and ultimately deposit as plaques<sup>[17]</sup>.

Notably, substantial evidence indicates that soluble A $\beta$  oligomers are more synaptotoxic than mature plaques, inducing synaptic dysfunction, perturbing calcium homeostasis and elevating oxidative stress, while also amplifying inflammatory signalling and promoting tau pathology. Tau pathology is driven by aberrant tau hyperphosphorylation and detachment from microtubules, which compromises microtubule stability and axonal transport; importantly, neurofibrillary tangle burden correlates closely with neuronal injury and clinical severity. In parallel, pathogenic A $\beta$  and tau species activate microglia and astrocytes. Although these glial cells can contribute to A $\beta$  uptake and clearance, chronic activation favours the release of pro-inflammatory cytokines and reactive oxygen/nitrogen species and, through complement-associated mechanisms, can facilitate aberrant synaptic pruning that accelerates synapse loss<sup>[18]</sup>. Together, A $\beta$ -mediated synaptic toxicity, tau-driven cytoskeletal disruption and sustained glia-dependent neuroinflammation converge to reduce synaptic integrity and promote neuronal degeneration, thereby driving disease progression.

#### 3.2. Ischemic stroke

Ischaemic stroke (ischaemic cerebrovascular accident) results from occlusion of a cerebral vessel, leading to a focal reduction in blood flow and subsequent hypoxia–ischaemia that precipitates neuronal injury and infarction. The underlying pathophysiology is often conceptualized as a stereotyped ischaemic cascade encompassing energetic failure, excitotoxicity, calcium dysregulation with mitochondrial injury, oxidative stress, neuroinflammation and disruption of the blood–brain barrier (BBB). Energetic failure constitutes an early initiating event. Abrupt interruption of oxygen and glucose delivery compromises mitochondrial oxidative phosphorylation, rapidly depleting ATP and disabling energy-dependent ion pumps. The ensuing membrane depolarization and loss of ionic homeostasis promote glutamate accumulation in the extracellular space through increased release and impaired reuptake, driving excitotoxic signalling via sustained activation of NMDA and AMPA receptors and a large influx of Ca<sup>2+</sup>. Calcium overload then propagates mitochondrial dysfunction by increasing mitochondrial membrane permeability and further suppressing ATP generation, while also promoting cytochrome c release and caspase-dependent apoptotic programmes. During ischaemia–reperfusion, mitochondrial impairment together with activation of oxidative enzymes, including NADPH oxidases, results in excessive production of reactive oxygen and nitrogen species (ROS/RNS). These species damage lipids, proteins and nucleic acids, trigger lipid peroxidation and accelerate cell death<sup>[19]</sup>. In parallel, neuroinflammation is rapidly engaged: microglia are activated early, followed by recruitment and infiltration of peripheral immune cells. Through pathways such as NF- $\kappa$ B

signalling and inflammasome activation, these cells drive the production of inflammatory mediators including TNF, IL-1 $\beta$  and IL-6, thereby amplifying tissue injury. BBB breakdown represents another central component of the cascade and is closely coupled to oxidative and inflammatory stress, involving endothelial injury, degradation of tight-junction proteins and increased protease activity (for example, MMP-2 and MMP-9), ultimately increasing permeability and promoting vasogenic oedema<sup>[20]</sup>.

### 3.3. Parkinson's disease

Parkinson's disease (PD) is a progressive neurodegenerative disorder defined pathologically by the degeneration of dopaminergic neurons in the substantia nigra pars compacta (SNpc) and clinically by consequent dysfunction of nigrostriatal circuitry. The resulting loss of SNpc neurons leads to a marked reduction in striatal dopamine, which underlies key motor manifestations of the disease<sup>[21]</sup>. PD pathogenesis is multifactorial and involves convergent processes, including  $\alpha$ -synuclein misfolding and aggregation, mitochondrial and bioenergetic impairment, oxidative stress, neuroinflammation and defective proteostasis. A central molecular hallmark is the accumulation of misfolded  $\alpha$ -synuclein into Lewy bodies and Lewy neurites. These assemblies can disrupt synaptic function, vesicular trafficking and neurotransmitter release, thereby exacerbating network-level dysfunction.

Mitochondrial dysfunction is also prominent, with reduced complex I activity reported in PD, contributing to impaired ATP production and increased generation of reactive oxygen species (ROS). In parallel, disruption of mitochondrial quality control pathways—most notably those governed by PINK1 and Parkin—can compromise mitophagy, allowing damaged mitochondria to accumulate and further amplifying bioenergetic failure and oxidative injury<sup>[22]</sup>. Oxidative stress is reinforced by the intrinsic chemistry of dopamine metabolism and is further shaped by iron dyshomeostasis and weakened antioxidant capacity within the substantia nigra, collectively accelerating neuronal vulnerability. Neuroinflammation represents an additional driver: chronic microglial activation, through signalling axes such as TLR–NF- $\kappa$ B and the NLRP3 inflammasome, promotes the production of cytokines including IL-1 $\beta$  and IL-6 and sustains injurious inflammatory cascades<sup>[23]</sup>. Finally, impairment of protein degradation pathways—including the ubiquitin–proteasome system and the autophagy–lysosome network—limits clearance of misfolded and aggregated proteins (including  $\alpha$ -synuclein), destabilizes proteostasis and further promotes pathological protein accumulation and neurodegeneration.

## 4. New advances in plant extracellular vesicles for treating neurological diseases

Neurological disorders such as Alzheimer's disease, ischaemic stroke and Parkinson's disease exhibit convergent molecular pathologies, including impaired mitochondrial function and energy metabolism, redox imbalance with oxidative stress, dysregulated calcium signalling and excitotoxicity, and sustained neuroinflammation driven by innate and adaptive immune pathways. Emerging evidence suggests that plant-derived extracellular vesicles can influence several of these processes and may therefore represent a promising strategy for modulating neuroinflammation and related neuropathology.

### 4.1. Mitochondrial function and energy metabolic pathways

Mitochondria are central hubs of cellular bioenergetics, generating ATP primarily through oxidative phosphorylation. Disruption of the electron transport chain—particularly at complex I—reduces ATP output and precipitates energetic failure, which compromises energy-dependent ion pumps and perturbs intracellular homeostasis. Mitochondrial dysfunction is also tightly coupled to oxidative stress and can promote cytochrome c release, thereby engaging caspase-dependent apoptotic programmes that culminate in neuronal injury and cell death<sup>[24]</sup>. Recent work suggests that plant-derived extracellular vesicles can modulate mitochondrial quality control.

For example, exosome-like vesicles isolated from kudzu root (*Pueraria lobata*) (Pu-Exos) have been reported to exhibit efficient transmembrane and barrier-crossing delivery properties and to activate PINK1–Parkin-dependent mitophagy, facilitating the clearance of damaged mitochondria. In parallel, Pu-Exos were associated with preservation



of respiratory chain complex I and V activities and improved ATP availability, ultimately protecting dopaminergic neurons and ameliorating Parkinson's disease-related phenotypes<sup>[25]</sup>. More broadly, extracellular vesicles have also been explored as nanocarriers to enhance delivery of mitochondrial-acting bioactives. In one study, milk-derived exosomes loaded with curcumin and resveratrol increased tissue accumulation and potentiated antiproliferative and mitochondria-dependent pro-apoptotic effects in breast cancer models. Alzheimer's disease (AD): If plant-derived extracellular vesicles (pEVs) can attenuate reactive oxygen species (ROS) and reverse metabolic reprogramming (for example, compensatory upregulation of glycolysis), they may restore cellular bioenergetic homeostasis and alleviate mitochondrial stress, thereby indirectly dampening the downstream amplification of A $\beta$ /Tau-driven neurotoxic cascades<sup>[26]</sup>. Ischaemic stroke: During the secondary-injury window following ischaemia–reperfusion, pEVs are more likely to confer neuroprotection by suppressing oxidative stress and lipid peroxidation (including ferroptosis-related processes) while engaging pro-survival signalling axes, thus limiting further mitochondrial destabilization, reducing neuronal loss and mitigating blood–brain barrier (BBB) disruption<sup>[27]</sup>. Parkinson's disease (PD): Relative to other indications, pEVs appear to align more closely with the mitochondrial–bioenergetic pathology central to PD. A plausible mechanism is the enhancement of mitophagy coupled with restoration of respiratory-chain capacity, which could more directly support the survival and functional maintenance of substantia nigra pars compacta (SNpc) dopaminergic neurons<sup>[25]</sup>.

## 4.2. Oxidative stress and antioxidant pathways

Oxidative stress arises from an imbalance between the production and clearance of reactive oxygen and nitrogen species (ROS/RNS), resulting in a sustained elevation of cellular oxidative burden. Excess ROS/RNS can drive lipid peroxidation, oxidative protein modifications and DNA damage, thereby compromising cellular integrity and function<sup>[28]</sup>. A major endogenous antioxidant defence axis is mediated by the Nrf2–ARE pathway: under stress, Nrf2 accumulates in the nucleus and binds antioxidant response elements (AREs), inducing a transcriptional programme that upregulates detoxification and antioxidant systems, including glutathione metabolism and superoxide dismutases, to reinforce radical scavenging and redox homeostasis.

Consistent with these mechanisms, vesicle-based interventions have been reported to attenuate oxidative injury. For example, ginseng-derived exosome-like vesicles reduced cisplatin-induced cardiomyocyte damage, at least in part by dampening MAPK-associated oxidative stress and apoptotic signalling<sup>[29]</sup>. More generally, extracellular vesicles have been proposed to deliver Nrf2 or to potentiate downstream antioxidant signalling, thereby enhancing ARE-dependent gene expression and restoring redox balance—effects that may support tissue repair and potentially ameliorate aspects of ageing and age-associated diseases. Alzheimer's disease (AD): Plant-derived extracellular vesicles (pEVs) may reduce the A $\beta$ /Tau-associated ROS burden and engage the Nrf2–ARE-driven endogenous antioxidant programme, thereby alleviating synaptic injury and neuronal toxicity and, at a functional level, slowing the trajectory of cognitive decline<sup>[30]</sup>. Ischaemic stroke (ischaemia–reperfusion): In the acute phase, pEVs could blunt the reperfusion-triggered oxidative burst and lipid peroxidation (including ferroptosis-related chain reactions) while preserving blood–brain barrier integrity, ultimately limiting secondary neuronal loss and cerebral oedema<sup>[26]</sup>. Parkinson's disease (PD): pEVs may counteract the sustained oxidative pressure arising from aberrant dopamine metabolism and mitochondrial dysfunction, and reinforce Nrf2-associated antioxidant defences, thereby safeguarding nigral dopaminergic neurons and improving motor phenotypes<sup>[31]</sup>.

## 4.3. Calcium ion signaling and excitotoxicity pathways

Ca<sup>2+</sup> is a central intracellular second messenger that orchestrates diverse physiological processes, including synaptic transmission, neuronal plasticity and cell-survival signalling. Under pathological conditions, excessive glutamate release and sustained activation of NMDA and AMPA receptors can drive a large Ca<sup>2+</sup> influx, precipitating excitotoxicity. The ensuing Ca<sup>2+</sup> overload activates multiple Ca<sup>2+</sup> dependent effectors—including proteases, phospholipases and nitric oxide synthases—thereby aggravating mitochondrial dysfunction and oxidative stress and ultimately promoting neuronal injury and cell death<sup>[32]</sup>. Beyond its role in excitotoxic signalling, Ca<sup>2+</sup> dynamics can also influence extracellular vesicle

biogenesis and cargo. For example, DETD-35 was reported to induce ROS-associated mitochondrial structural and functional damage while elevating cytosolic  $\text{Ca}^{2+}$  levels, leading to  $\text{Ca}^{2+}$  dependent exosome release from tumour cells. Notably, this process was accompanied by a reshaping of exosomal protein composition and biological activity, endowing the vesicles with the capacity to suppress proliferation of triple-negative breast cancer cells and to attenuate malignant behaviours such as migration and invasion<sup>[33]</sup>. Alzheimer's disease (AD): If plant-derived extracellular vesicles (pEVs) can curb  $\text{A}\beta$ -driven overactivation of glutamate receptors and limit  $\text{Ca}^{2+}$  influx, they may alleviate  $\text{Ca}^{2+}$  dyshomeostasis-induced synaptic dysfunction and mitochondrial injury, thereby weakening neurotoxic cascade amplification and slowing cognitive decline<sup>[34]</sup>. Ischaemic stroke (ischaemia–reperfusion): By reducing post-ischaemic glutamate accumulation and the ensuing NMDA/AMPA receptor-mediated  $\text{Ca}^{2+}$  overload, pEVs could suppress the escalation of excitotoxicity and cell-death programmes, ultimately constraining infarct expansion and promoting neurological recovery. Parkinson's disease (PD): If pEVs stabilize  $\text{Ca}^{2+}$  homeostasis in dopaminergic neurons and attenuate  $\text{Ca}^{2+}$ -dependent mitochondrial stress and oxidative burden, they may lower excitotoxic pressure and the degeneration risk of vulnerable neuronal populations, thereby improving motor phenotypes<sup>[35]</sup>.

#### 4.4. Neuroinflammation and immune signaling pathways

Neuroinflammation is largely orchestrated by microglia and astrocytes and is underpinned by signalling modules such as NF- $\kappa$ B and MAPK pathways and activation of the NLRP3 inflammasome, which together drive the induction and release of pro-inflammatory cytokines including TNF, IL-1 $\beta$  and IL-6<sup>[36]</sup>. Although acute inflammatory responses can support debris clearance and restoration of tissue homeostasis, sustained or excessive activation promotes neuronal injury and can engage reinforcing feedback with oxidative stress and cell-death programmes, thereby accelerating disease progression. Plant-derived nanovesicles have been reported to modulate neuroinflammatory signalling in vivo. For example, oral administration of oat-derived nanoparticles (oatN) attenuated alcohol-induced pro-inflammatory signalling by altering intracellular trafficking and subcellular localization of the dectin-1-associated complex in microglia, resulting in reduced neuroinflammation and improved cognitive performance<sup>[37]</sup>. In addition, exosome-like nanovesicles isolated from *Allium tuberosum* (A-ELNs) were shown to mitigate microglia-driven inflammation by activating the HO-1 antioxidant axis and suppressing iNOS/NO production and inflammatory mediator expression through miRNA-dependent regulation of anti-inflammatory gene programmes. Notably, A-ELNs were also proposed as efficient carriers for anti-inflammatory therapeutics. Alzheimer's disease (AD): If plant-derived extracellular vesicles (pEVs) can restrain chronic reactive activation of microglia and astrocytes and downregulate pro-inflammatory signalling axes such as NF- $\kappa$ B, MAPK and the NLRP3 inflammasome, they may reduce cytokine- and complement-driven aberrant synaptic pruning, thereby mitigating synapse loss and slowing cognitive decline. Ischaemic stroke (ischaemia–reperfusion): In the acute phase, pEVs may attenuate the amplified innate-immune response (for example, via inhibition of NF- $\kappa$ B/NLRP3 and reduced TNF- $\alpha$ /IL-1 $\beta$ ) and bias the immune milieu from a damage-amplifying state towards a reparative programme, thus limiting cerebral oedema and blood–brain barrier disruption, reducing secondary neuronal death and promoting functional recovery. Parkinson's disease (PD): By potentially intercepting  $\alpha$ -synuclein-linked microglial TLR–inflammasome pathways and lowering chronic neuroinflammation and its accompanying oxidative burden, pEVs could enhance the resilience of nigral dopaminergic neurons, decelerate neurodegeneration and improve motor phenotypes<sup>[38]</sup>.

## 5. Challenges and limitations

Despite rapidly expanding interest in plant-derived extracellular vesicles (PDEVs), also referred to as exosome-like nanoparticles (ELNs), several conceptual and practical barriers continue to impede mechanistic understanding and clinical translation. A central challenge is the absence of a unified definition and a definitive assignment of biogenic origin. In contrast to mammalian exosomes—which are canonically derived from multivesicular bodies—plant vesicle secretion is less well resolved, raising uncertainty as to whether isolated preparations represent bona fide exosomes or a heterogeneous



mixture of membrane-derived nanostructures. This ambiguity complicates comparisons across studies and can confound interpretation of reported biological activities. A second major limitation is the incomplete understanding of in vivo behaviour, including biodistribution, cellular tropism and long-term safety. Although PDEVs are frequently described as biocompatible and weakly immunogenic, rigorous and standardized toxicological and immunological assessments remain sparse, and an aligned regulatory framework for evaluation is still emerging. Addressing these gaps will be essential to move PDEVs from experimental systems toward robust and clinically deployable therapeutic platforms.

## 6. Conclusion

Plant-derived extracellular vesicles are emerging as a potentially versatile therapeutic modality for neurological disorders, bridging naturally derived nanostructures with drug-delivery strategies. Their reported biocompatibility, low apparent toxicity and capacity to traverse the blood–brain barrier support their exploration as platforms for CNS therapeutics. Moreover, chemical or biomolecular surface engineering of plant vesicles can be used to tune biodistribution, cellular tropism and cargo delivery, potentially enhancing targeting specificity and therapeutic efficacy and enabling new intervention strategies for neurological disease.

At present, plant-derived extracellular vesicles remain at an early stage of translational development. Robust preclinical and clinical evidence is still required to establish therapeutic efficacy, long-term biological effects, safety and potential immunological consequences in the context of neurological disorders. To date, most work has been confined to proof-of-concept and mechanistic studies, and systematic clinical evaluation has yet to be initiated.

In summary, plant-derived extracellular vesicles hold considerable promise as therapeutic platforms for neurological disorders. Nevertheless, rigorous validation—particularly through well-designed human studies—will be essential before these approaches can be translated into routine clinical application.

## Disclosure statement

The author declares no conflict of interest.

## References

- [1] Chen YF, et al., 2024, Exosomes: A Review of Biologic Function, Diagnostic and Targeted Therapy Applications, and Clinical Trials. *Journal of Biomedical Science*, 31(1): 67.
- [2] Langellotto MD, et al., 2025, Plant-Derived Extracellular Vesicles: A Synergetic Combination of a Drug Delivery System and a Source of Natural Bioactive Compounds. *Drug Delivery and Translational Research*, 15(3): 831-845.
- [3] Kalluri R, LeBleu VS, 2020, The Biology, Function, and Biomedical Applications of Exosomes. *Science*, 367(6478): eaau6977.
- [4] Isik S, et al., 2025, Plant-Derived Exosome-Like Nanovesicles: Mechanisms and Molecular Understanding in Neurological Disorders with Potential Therapeutic Applications. *Drug Delivery and Translational Research*: 1-27.
- [5] Mani S, et al., 2025, Pathogenic Synergy: Dysfunctional Mitochondria and Neuroinflammation in Neurodegenerative Diseases Associated with Aging. *Frontiers in Aging*, 6: 1615764.
- [6] Manimaran V, et al., 2023, Nanogels as Novel Drug Nanocarriers for CNS Drug Delivery. *Frontiers in Molecular Biosciences*, 10: 1232109.
- [7] Ammad M, et al., 2024, Advancements in Long Non-Coding RNA-Based Therapies for Cancer: Targeting, Delivery, and Clinical Implications. *Medical Oncology*, 41(11): 292.
- [8] Yan L, et al., 2025, Ginger Exosome-Like Nanoparticle-Derived miRNA Therapeutics: A Strategic Inhibitor of Intestinal

- Inflammation. *Journal of Advanced Research*, 69: 1-15.
- [9] Farley JT, Eldahshoury MK, de Marcos Lousa C, Unconventional Secretion of Plant Extracellular Vesicles and Their Benefits to Human Health: A Mini.
  - [10] Li X, et al., 2018, Biogenesis and Function of Multivesicular Bodies in Plant Immunity. *Frontiers in Plant Science*, 9: 979.
  - [11] Wang J, et al., 2010, EXPO, an Exocyst-Positive Organelle Distinct from Multivesicular Endosomes and Autophagosomes, Mediates Cytosol to Cell Wall Exocytosis in Arabidopsis and Tobacco Cells. *The Plant Cell*, 22(12): 4009-4030.
  - [12] Neves J, et al., 2022, Relevance of the Exocyst in Arabidopsis *exo70e2* Mutant for Cellular Homeostasis Under Stress. *International Journal of Molecular Sciences*, 24(1): 424.
  - [13] Hatsugai N, et al., 2009, A Novel Membrane Fusion-Mediated Plant Immunity Against Bacterial Pathogens. *Genes & Development*, 23(21): 2496-2506.
  - [14] Etxebeste-Mitxelorena M, et al., 2024, Neuroprotective Properties of Exosomes and Chitosan Nanoparticles of Tomafran, a Bioengineered Tomato Enriched in Crocins. *Natural Products and Bioprospecting*, 14(1): 9.
  - [15] Mulcahy LA, Pink RC, Carter DRF, 2014, Routes and Mechanisms of Extracellular Vesicle Uptake. *Journal of Extracellular Vesicles*, 3(1): 24641.
  - [16] Dad HA, et al., 2021, Plant Exosome-Like Nanovesicles: Emerging Therapeutics and Drug Delivery Nanoplatforms. *Molecular Therapy*, 29(1): 13-31.
  - [17] De Strooper B, Karran E, 2016, The Cellular Phase of Alzheimer's Disease. *Cell*, 164(4): 603-615.
  - [18] Hong S, et al., 2016, Complement and Microglia Mediate Early Synapse Loss in Alzheimer Mouse Models. *Science*, 352(6286): 712-716.
  - [19] Lo EH, Dalkara T, Moskowitz M A, 2003, Mechanisms, Challenges and Opportunities in Stroke. *Nature Reviews Neuroscience*, 4(5): 399-414.
  - [20] Xue S, et al., 2023, Stroke-Induced Damage on the Blood–Brain Barrier. *Frontiers in Neurology*, 14: 1248970.
  - [21] Poewe W, et al., 2017, Parkinson Disease. *Nature Reviews Disease Primers*, 3(1): 1-21.
  - [22] Gao XY, et al., 2022, Mitochondrial Dysfunction in Parkinson's Disease: From Mechanistic Insights to Therapy. *Frontiers in Aging Neuroscience*, 14: 885500.
  - [23] Li Y, et al., 2021, Targeting Microglial  $\alpha$ -Synuclein/TLRs/NF-kappaB/NLRP3 Inflammasome Axis in Parkinson's Disease. *Frontiers in Immunology*, 12: 719807.
  - [24] Zhao XY, et al., 2019, Mitochondrial Dysfunction in Neural Injury. *Frontiers in Neuroscience*, 13: 30.
  - [25] Xu Y, et al., 2024, Plant-Derived Exosomes as Cell Homogeneous Nanoplatforms for Brain Biomacromolecules Delivery Ameliorate Mitochondrial Dysfunction Against Parkinson's Disease. *Nano Today*, 58: 102438.
  - [26] Calzoni E, et al., 2025, Rhubarb-Derived Extracellular Vesicles Mitigate Oxidative Stress and Metabolic Dysfunction in an Alzheimer's Cellular Model. *Nutrients*, 17(23): 3771.
  - [27] Zhang SY, et al., 2025, Houttuynia cordata Thunb-Derived Extracellular Vesicle-Like Particles Alleviate Ischemic Brain Injury by miR159a Targeting ACSL4 to Suppress Ferroptosis. *Chinese Medicine*, 20(1): 141.
  - [28] Ngo V, Duennwald ML, 2022, Nrf2 and Oxidative Stress: A General Overview of Mechanisms and Implications in Human Disease. *Antioxidants*, 11(12): 2345.
  - [29] Yang S, et al., 2024, The Cardioprotective Effect of Ginseng Derived Exosomes via Inhibition of Oxidative Stress and Apoptosis. *ACS Applied Bio Materials*, 8(1): 814-824.
  - [30] Zhang Y, et al., 2024, Response Surface Methodology Optimization of Exosome-Like Nanovesicles Extraction from Lycium ruthenicum Murray and Their Inhibitory Effects on A $\beta$ -Induced Apoptosis and Oxidative Stress in HT22 Cells. *Foods*, 13(20): 3328.
  - [31] Kim DK, Rhee WJ, 2021, Antioxidative Effects of Carrot-Derived Nanovesicles in Cardiomyoblast and Neuroblastoma Cells. *Pharmaceutics*, 13(8): 1203.
  - [32] Bano D, Ankarcrona M, 2018, Beyond the Critical Point: An Overview of Excitotoxicity, Calcium Overload and the Downstream Consequences. *Neuroscience Letters*, 663: 79-85.

- [33] Shiao JY, et al., 2017, Phytoagent Deoxyelephantopin and Its Derivative Inhibit Triple Negative Breast Cancer Cell Activity through ROS-Mediated Exosomal Activity and Protein Functions. *Frontiers in Pharmacology*, 8: 398.
- [34] Yoon HJ, et al., 2024, Green Onion-Derived Exosome-Like Nanoparticles Prevent Ferroptotic Cell Death Triggered by Glutamate: Implication for GPX4 Expression. *Nutrients*, 16(19): 3257.
- [35] Lu W, et al., 2025, A Programmed Ca<sup>2+</sup> Nanomodulator by Dynamically Regulating Autophagy and Neuroinflammation for Parkinson's Disease Therapy. *Chemical Engineering Journal*: 166324.
- [36] Shafi A, et al., 2025, A Mechanistic Insight of Neuro-Inflammation Signaling Pathways and Implication in Neurodegenerative Disorders. *Inflammopharmacology*: 1-10.
- [37] Xu F, et al., 2022, Restoring Oat Nanoparticles Mediated Brain Memory Function of Mice Fed Alcohol by Sorting Inflammatory Dectin-1 Complex into Microglial Exosomes. *Small*, 18(6): 2105385.

**Publisher's note**

Whioce Publishing remains neutral with regard to jurisdictional claims in published maps and institutional affiliations.

# The Effect of Health Education Using Clinical Nursing Pathways in Patients with Schizophrenia and Diabetes

Jingwen Hu\*

Haian Third People's Hospital, Haian 226600, Jiangsu, China

*\*Author to whom correspondence should be addressed.*

**Copyright:** © 2025 Author(s). This is an open-access article distributed under the terms of the Creative Commons Attribution License (CC BY 4.0), permitting distribution and reproduction in any medium, provided the original work is cited.

**Abstract:** *Objective:* To analyze the nursing effect of health education intervention using clinical nursing pathways for patients with schizophrenia and diabetes, and to provide a basis for optimizing nursing intervention strategies for this type of patients. *Methods:* 200 cases of schizophrenia and diabetes in our hospital from January 2023 to December 2024 were selected as research samples, and were divided into equal groups using the random number table method, namely the control group ( $n = 100$ ) and the observation group ( $n = 100$ ). The control group received routine health education, and the observation group received health education based on clinical nursing pathways. The intervention period was 8 weeks in both cases. The nursing effects of the two groups were compared. *Results:* After the intervention, the total health knowledge mastery rate of the observation group (92.0%) was significantly higher than that of the control group (75.0%),  $P < 0.05$ . The FPG, 2hPG and PANSS scores of the observation group were significantly lower than those of the control group ( $P < 0.05$ ). The PSQI score of the observation group was lower than that of the control group ( $P < 0.05$ ). In terms of MCMQ scores, compared with the control group, the observation group had higher scores on the facing dimension and avoidance dimension, and lower scores on the yielding dimension ( $P < 0.05$ ). *Conclusion:* Health education for patients with schizophrenia and diabetes mellitus through the use of clinical nursing pathways can improve the patient's cognitive level of the disease, improve their blood sugar control, mental symptoms, sleep quality and active coping ability. It is a structured and efficient nursing intervention model with clinical application and promotion value. **Keywords:** Schizophrenia; Diabetes; Clinical nursing pathway; Health education; Nursing effect; Blood sugar control; Quality of life

**Online publication:** December 26, 2025

## 1. Introduction

Schizophrenia is a chronic mental disorder that can cause abnormal manifestations in patients' consciousness, behavior, and perception, and significantly impair the patient's social functions<sup>[1]</sup>. Diabetes Mellitus (DM) is a chronic metabolic disease with high incidence in the world. According to the 2023 report of the International Diabetes Federation (IDF), there are more than 570 million patients worldwide, and the prevalence rate in my country is as high as 12.4%<sup>[2]</sup>. Management of the condition is particularly complex when schizophrenia and diabetes co-occur. On the one hand, antipsychotic drugs often induce or aggravate metabolic disorders and aggravate the progression of diabetes<sup>[3]</sup>. On the other hand, abnormal blood sugar fluctuations can also affect the function of the central nervous system and may induce or worsen psychiatric symptoms. Studies have shown that patients with schizophrenia are 2-3 times more likely to develop diabetes than the

general population<sup>[4]</sup>. Such patients often suffer from impaired cognitive function, reduced self-management ability and poor treatment compliance due to the disease itself, which makes the dual control of blood sugar and mental symptoms face severe challenges and seriously affects their quality of life<sup>[5]</sup>.

Health education is the core part of comprehensive management of chronic diseases, aiming to enhance patients' self-management effectiveness through knowledge transfer and behavioral intervention. The traditional conventional health education model has limitations such as fragmented content, insufficient pertinence, and a single form, and is difficult to meet the complex and special health needs of patients with schizophrenia and diabetes<sup>[6]</sup>. Clinical Nursing Pathway (CNP) is a standardized and process-based nursing management model guided by evidence-based medicine, using a timeline as a framework, and integrating multi-dimensional content such as diagnosis, treatment, nursing, nutrition, rehabilitation, health education and discharge planning<sup>[7]</sup>. Its core lies in multidisciplinary collaboration to provide patients with continuous, coordinated and individualized care services. Existing studies have confirmed that CNP is effective in single disease management<sup>[8]</sup>, but there are relatively few studies on its effectiveness in systematically implementing health education in patients with schizophrenia and diabetes. This study aims to explore better nursing intervention programs by comparing the effects of conventional health education and CNP-based health education, and provide a reference for clinical practice. The report is as follows.

## 2. Materials and methods

### 2.1. Research objects

200 patients with schizophrenia and diabetes who were hospitalized in our hospital from January 2023 to December 2024 were selected. Use the random number table method to divide them into two groups, with 100 cases in each group. Control group: 58 males and 42 females; age ( $42.5 \pm 8.3$ ) years old; disease duration ( $8.2 \pm 3.1$ ) years old. Observation group: 60 males and 40 females; age ( $43.2 \pm 7.9$ ) years old; disease duration ( $8.5 \pm 2.8$ ) years old. There was no significant difference in parallel comparison of information data between 2 or more groups  $P > 0.05$ .

Inclusion criteria: (1) Meet the diagnostic criteria for schizophrenia in the International Classification of Diseases (ICD-10) and the diagnostic criteria for diabetes by the World Health Organization (WHO); (2) Aged 18 to 65 years old; (3) Clear consciousness and basic communication skills; (4) The patient or his legal guardian gave informed consent and signed an informed consent form.

Exclusion criteria: (1) Combined with severe heart, liver, and renal failure; (2) Suffering from other serious mental disorders (such as major depressive episode, manic episode of bipolar disorder) that interferes with the assessment; (3) Voluntarily withdrawn or lost to follow-up during the study.

### 2.2. Intervention methods

Control group: Implement routine health education. The responsible nurse organizes a group health lecture once a week, each time for about 30 minutes. The content covers the basic knowledge of schizophrenia and diabetes, clinical manifestations, treatment principles, drug use precautions, diet and exercise guidance, etc.; disease knowledge brochures are distributed; while the patient is hospitalized, oral health education is given from time to time according to the situation, emphasizing the importance of following medical treatment. The intervention lasted 8 weeks.

Observation group: Implement health education based on CNP. The specific plan is as follows:

- (1) Team formation: Establish a CNP team, including 1 deputy chief physician of the psychiatry department, 1 attending physician of the endocrinology department, 2 psychiatric nurses in charge, 2 diabetes specialist nurses, and 1 nutritionist. The team jointly developed a CNP form, clarified the division of responsibilities, and conducted regular case discussions and professional knowledge training to ensure professionalization and standardization of intervention.
- (2) Path formulation: Based on the patient's disease characteristics, treatment process and clinical experience,



formulate a staged CNP table. Day 1 of admission: Complete the admission assessment and environmental introduction; psychiatrists and endocrinologists will jointly explain the disease definition, etiology, pathophysiology, main hazards and treatment goals to patients and guardians; issue a customized health manual and self-management record card. Days 2 to 20 of hospitalization: Nutritional management: Individualized dietary guidance (calorie calculation, recipe formulation) will be provided by a responsible nurse or nutritionist every day, emphasizing the timing and quantitative principles of diabetic diet. Exercise guidance: Develop an exercise plan based on the patient's physical condition and supervise its execution. Medication management: Psychiatric and diabetes specialist nurses jointly provide medication education, explaining in detail the mechanism of action, usage and dosage, potential adverse reactions and coping strategies of various drugs. Knowledge enhancement: 2 special lectures are held every week. Psychological support: For patients with anxiety, depression and other emotional problems, psychological counselors or trained nurses provide individualized psychological counseling to promote the establishment of a positive treatment attitude. 3 days before discharge: Skills training: guide patients/family members to master the operation of blood glucose meters, self-monitoring methods and frequency of blood glucose; standardize insulin injection techniques, emphasizing aseptic operation. Discharge plan: clearly inform the discharge medication plan, follow-up time and location; formulate a personalized home rehabilitation plan; establish follow-up files, and provide consultation channels such as telephone and WeChat.

- (3) Path implementation and feedback: Implement health education strictly in accordance with the CNP table. After each education, the responsible nurse assesses the patient's understanding and mastery through questions, retellings, scenario simulations, etc., and dynamically adjusts the content and methods of subsequent education based on feedback. The intervention period is 8 weeks.

### 2.3. Observation indicators

- (1) Health knowledge mastery: assessed using a self-designed questionnaire, including basic knowledge of diseases, treatment points, self-management skills (diet, exercise, medication, monitoring), etc., with a full score of 100 points.  $\geq 85$  is classified as "mastered", 60–84 is classified as "basic mastered", and  $< 60$  is classified as "not mastered". Total mastery rate = (number of mastered cases + basic mastered cases)/total number of cases  $\times 100\%$ .
- (2) Blood glucose level: Blood samples were collected from patients before and after the pre-pregnancy test to detect fasting blood glucose (FPG) and 2-h postprandial blood glucose (2hPG).
- (3) Assessment of mental symptoms: Use the Positive and Negative Syndrome Scale (PANSS)<sup>[6]</sup> to assess mental symptoms. The higher the score, the more serious the patient's mental disorder.
- (4) Sleep quality assessment: Use the Pittsburgh Sleep Quality Index (PSQI)<sup>[7]</sup> score. The higher the total score, the worse the sleep quality.
- (5) Coping style assessment: The Medical Coping Style Questionnaire (MCMQ)<sup>[8]</sup> is used to assess, including three dimensions: facing (active coping), avoidance (avoiding problems), and yielding (negative acceptance). The score of each dimension reflects the patient's degree of coping tendencies.

### 2.4. Statistical methods

All the data in this article were analyzed with the help of SPSS 26.0, and the measurement data involved are expressed as follows: mean  $\pm$  standard deviation (SD), that is, the mean plus or minus the standard deviation, all are t tests, and the count data are expressed as follows: [n (%)], all are  $\chi^2$  tests, and  $P < 0.05$  is considered statistically significant.

## 3. Results

### 3.1. Comparison of health knowledge mastery between the two groups

After the intervention, the total health knowledge mastery rate of the observation group was higher than that of the control

group, and there was a difference ( $P < 0.05$ ). See **Table 1** for details.

**Table 1.** Comparison of health knowledge mastery between two groups of patients after intervention [n(%)]

Group	n	Master	Basic mastery	Not mastered	Total mastery (%)
Control group	100	38 (38.0)	37 (37.0)	25 (25.0)	75 (75.0)
Observation group	100	55 (55.0)	37 (37.0)	8 (8.0)	92 (92.0)
$\chi^2$	-	-	-	-	10.488
$P$	-	-	-	-	0.001

### 3.2. Comparison of blood glucose levels and PANSS scores between the two groups of patients

Before intervention, there was no statistically significant difference in FPG, 2hPG and PANSS scores between the two groups of patients ( $P > 0.05$ ). After intervention, the FPG, 2hPG and PANSS scores of the observation group were lower than those of the control group, and there were differences ( $P < 0.05$ ). Intra-group comparison showed that all indicators in the two groups were significantly improved after the intervention compared with before the intervention ( $P < 0.001$ ). **Table 2** for details.

**Table 2.** Comparison of blood glucose levels and PANSS scores between the two groups of patients before and after intervention (mean  $\pm$  SD)

Group	n	FPG (mmol/L)		2hPG (mmol/L)		PANSS (Score)	
		Before intervention	After intervention	Before intervention	After intervention	Before intervention	After intervention
Control group	100	8.5 $\pm$ 1.2	7.8 $\pm$ 1.0	13.2 $\pm$ 2.1	11.8 $\pm$ 1.8	78.5 $\pm$ 8.3	72.3 $\pm$ 7.5
Observation group	100	8.3 $\pm$ 1.1	6.5 $\pm$ 0.8	13.0 $\pm$ 2.0	9.5 $\pm$ 1.2	78.2 $\pm$ 8.1	65.2 $\pm$ 6.8
$t$	-	1.229	10.151	0.690	10.632	0.259	7.013
$P$	-	0.221	0.000	0.491	0.000	0.796	0.000

### 3.3. Comparison of PSQI and MCMQ scores between the two groups of patients

Before the intervention, there was no statistical significance in the scores of PSQI and MCMQ between the two groups of patients ( $P > 0.05$ ). After the intervention, the PSQI score of the observation group was lower than that of the control group; in terms of MCMQ score, the face and avoidance dimensions of the observation group increased, while the yielding dimension decreased significantly ( $P < 0.05$ ). **Table 3** for details.

**Table 3.** Comparison of PSQI and MCMQ scores between two groups of patients before and after intervention (mean  $\pm$  SD)

Group	n	PSQI (points)		MCMQ-face (points)		MCMQ-Avoidance (points)		MCMQ-Yield (Points)	
		Before intervention	After intervention	Before intervention	After intervention	Before intervention	After intervention	Before intervention	After intervention
Control group	100	8.2 $\pm$ 1.5	7.5 $\pm$ 1.3	18.5 $\pm$ 2.3	19.2 $\pm$ 2.1	14.2 $\pm$ 1.8	14.8 $\pm$ 1.6	10.5 $\pm$ 1.2	10.8 $\pm$ 1.0
Observation group	100	8.0 $\pm$ 1.4	<b>6.2 <math>\pm</math> 1.0</b>	18.3 $\pm$ 2.2	<b>22.5 <math>\pm</math> 2.5</b>	14.0 $\pm$ 1.7	<b>16.5 <math>\pm</math> 1.9</b>	10.3 $\pm$ 1.1	<b>8.5 <math>\pm</math> 0.8</b>
$t$	-	0.975	7.926	0.628	10.107	0.808	6.844	1.229	17.960
$P$	-	0.331	0.000	0.530	0.000	0.420	0.000	0.221	0.000

## 4. Discussions

Effective management of patients with schizophrenia and diabetes is the focus and difficulty of current clinical nursing research. This study focuses on the application effect of the structured health education model. The results show that health education based on CNP is significantly better than conventional health education in improving patients' health knowledge level, improving physiological indicators (blood sugar), mental symptoms, sleep quality and promoting positive coping.

The health knowledge mastery rate of patients in the observation group increased significantly (92.0% vs. 75.0%), verifying the advantages of the CNP model in knowledge transfer. CNP systematically plans educational content, clarifies time points, integrates multidisciplinary resources (physicians, nurses, nutritionists, psychologists), and uses diversified educational forms to overcome the shortcomings of fragmentation and lack of depth in conventional education and ensure the comprehensiveness, continuity and individual adaptability of knowledge transfer<sup>[9]</sup>, thereby effectively improving patients' cognitive level in the management of complex comorbidities. In terms of blood sugar control, the significant improvement in FPG and 2hPG in the observation group was because CNP deeply integrated the core elements of diabetes management (individualized diet prescription, regular exercise prescription, refined medication guidance, standardized blood sugar monitoring and insulin injection skills training) into each stage of the path, and was followed up and supervised by specialist nurses. This integrated and intensive lifestyle intervention and medication management can significantly improve patients' treatment compliance and self-management efficacy<sup>[10,11]</sup>. At the same time, the simultaneous improvement of mental symptoms (PANSS score) may be due to the stabilizing effect of optimization of blood sugar control on neurological function on the one hand, and is also closely related to the regular medication guidance, self-identification, and coping strategies of mental symptoms, and targeted psychological counseling emphasized in the CNP path. Together, these interventions promote overall stabilization of the patient's condition. The improvement in sleep quality (PSQI score) and more active coping styles of the patients in the observation group highlighted the value of CNP in paying attention to the psychosocial aspects of patients. Patients with schizophrenia and diabetes often bear a huge disease burden and psychological pressure, and are prone to anxiety and depression, which in turn affects sleep and coping styles. The specialized psychological counseling sessions, coping skills guidance, and positive guidance on disease recognition in the CNP path can help patients relieve negative emotions, establish a more effective stress coping mechanism, and improve their psychological flexibility and self-efficacy<sup>[12]</sup>, thereby improving sleep quality and overall adaptability.

## 5. Conclusion

In summary, the health education model based on the clinical nursing path, through its characteristics of standardization, structuring, multidisciplinary collaboration, and individual customization, can effectively improve the disease recognition and self-management ability of patients with schizophrenia and diabetes. It has shown significant advantages in improving blood sugar control, alleviating mental symptoms, optimizing sleep quality, and promoting active coping, and provides clinical nursing intervention programs that are highly operable and effective.

## Disclosure statement

The author declares no conflict of interest.

## References

- [1] Huang S, Xia H, Liu C, 2021, Nursing Research on Individualized Comprehensive Nursing Intervention for Patients with Schizophrenia and Diabetes. *Chinese Community Physicians*, 37(20): 151–153.

- [2] Lin L, Zhang Y, He M, 2023, Research on the Nursing Care of Patients with Schizophrenia and Diabetes Based on Individualized Intervention Under the Recovery Concept. *Chinese General Medicine*, 21(11): 1972–1976.
- [3] Gan J, 2021, Analysis of Nursing Intervention Effects and Related Indicators for Schizophrenia Combined with Diabetes. *Diabetes New World*, 24(3): 109–111 + 114.
- [4] Yu X, Yu X, Zou R, et al., 2024, Analysis of the Effectiveness of Health Education Using Clinical Nursing Pathways in Patients with Schizophrenia and Diabetes. *Diabetes World*, 21(10): 129–130.
- [5] World Health Organization, 2018, *International Statistical Classification of Diseases and Related Health Problems (ICD-10)*. People's Medical Publishing House, Beijing.
- [6] Zhang M, 2018, *Psychiatric Rating Scale Manual*. Hunan Science and Technology Press, Changsha.
- [7] Liu X, Tang M, Hu L, et al., 1996, Study on the Reliability and Validity of the Pittsburgh Sleep Quality Index. *Chinese Journal of Psychiatry*, 29(2): 103–107.
- [8] Shen X, Jiang Q, 2000, Test Report on 701 Cases of the Chinese Version of the Medical Coping Style Questionnaire. *Chinese Behavioral Medical Sciences*, 9(1): 18–20.
- [9] Li K, 2022, Application Effect of Refined Nursing in Patients with Schizophrenia and Mania with Diabetes. *Chinese Medical Guide*, 20(14): 165–167.
- [10] Fan X, 2020, Effect of Solution-Focused Nursing Intervention on the Rehabilitation of Patients with Schizophrenia and Diabetes. *Journal of Qiannan National Medical College*, 33(4): 271–273.
- [11] Wang L, 2022, Application of Clinical Interventional Nursing in Patients with Schizophrenia and Type 2 Diabetes and Its Impact on Quality of Life and Blood Sugar Indicators. *Diabetes New World*, 25(1): 135–138 + 155.
- [12] Guo S, 2023, Effect of Dual-Heart Intervention Model on Compliance and Self-Care Ability of Patients with Schizophrenia and Diabetes. *Heilongjiang Medical Sciences*, 46(4): 71–72 + 75.

**Publisher's note**

*Whioce Publishing remains neutral with regard to jurisdictional claims in published maps and institutional affiliations.*

# Exploration and Analysis of the Efficacy of Tubeless Percutaneous Nephroscopy in Treating Upper Urinary Tract Stones

Liang Zhu, Wenchao Zhao\*

Department of Urology, Taizhou People's Hospital Affiliated to Nanjing Medical University, Taizhou 225700, Jiangsu, China

*\*Author to whom correspondence should be addressed.*

**Copyright:** © 2025 Author(s). This is an open-access article distributed under the terms of the Creative Commons Attribution License (CC BY 4.0), permitting distribution and reproduction in any medium, provided the original work is cited.

**Abstract:** *Objective:* To explore the clinical efficacy of tubeless percutaneous nephrolithotomy (PCNL) in the treatment of upper urinary tract stones. *Methods:* 100 patients with upper urinary tract stones and concurrent PCNL surgery who were treated in Taizhou People's Hospital Affiliated to Nanjing Medical University from September 2023 to September 2025 were randomly divided into two groups using a random number table method according to whether a nephrostomy tube was left in place after surgery, with 50 cases in each group, namely the observation group (without pyelostomy tube) and the control group (with pyelostomy tube). The two groups of patients were compared in terms of clinical data, perioperative indicators, renal function test indicators and surgical complications. *Results:* There was no statistical difference in clinical baseline data between the two groups ( $P > 0.05$ ). However, in terms of length of hospitalization, VAS score, postoperative urinary catheter indwelling time, frequency of analgesic drug use, and postoperative recovery levels of Scr and BUN, the observation group showed significant improvement compared to the control group, with statistical significance ( $P < 0.05$ ). There was no statistical difference in the incidence of complications between the two groups ( $P > 0.05$ ). *Conclusion:* Both tubeless and standardized PCNL can effectively break lithotripsy, but tubeless technology has the advantages of lower postoperative pain, faster postoperative recovery, and shorter hospitalization time, and has practical clinical application value.

**Keywords:** Tubeless; Percutaneous nephrolithotomy; Upper urinary tract stones; Complications

**Online publication:** December 26, 2025

## 1. Introduction

At present, the incidence of urolithiasis is on the rise, especially among young adults<sup>[1]</sup>. In the urinary tract stone system, upper urinary tract stone attacks are more severe and often cause sudden, severe pain in the waist or flank, which can radiate to the groin or perineum. In severe cases, symptoms such as nausea and vomiting may also occur<sup>[2]</sup>. Upper urinary tract stones include kidney and ureteral stones. Kidney stones are more common, with an incidence rate of 6% to 14%, mostly in men<sup>[3]</sup>. At present, the main method for treating upper urinary tract stones is percutaneous nephrolithotomy (PCNL). PCNL has a series of advantages, such as small trauma, fast recovery, and a high stone clearance rate. However, after routine surgery, a pyelostomy tube will be left at the renal puncture port. Postoperative pain, bleeding, infection,



urinary extravasation, and other conditions that may affect the patient's postoperative recovery process may occur<sup>[4]</sup>. Relevant studies have shown that tubeless technology has many advantages, such as shortening the length of hospital stay and relieving postoperative pain<sup>[5]</sup>. This article aims to conduct a comparative analysis of the clinical effects of tubeless and tubed PCNL in patients with upper urinary tract stones, to provide a certain reference value for subsequent clinical research.

## 2. Materials and methods

### 2.1. General information

Statistics were conducted on inpatients with upper urinary tract stones in our hospital from 2023.09.01 to 2025.09.01, and 100 patients who underwent PCNL were selected and divided into two groups according to whether nephrostomy tubes were placed during the operation, namely the observation group (no nephrostomy tubes placed) and the control group (nephrostomy tubes placed). 50 cases in each group. In the observation group, there were 27 males and 23 females; the average age was  $50.78 \pm 13.26$  years old; the diameter of the stones was about  $1.81 \pm 0.58$ ; there were 33 cases of kidney stones and 17 cases of ureteral stones. In the control group, there were 31 males and 19 females; the average age was  $51.12 \pm 13.39$ ; the diameter of the stones was about  $1.66 \pm 0.53$ ; there were 28 cases of kidney stones and 22 cases of ureteral stones. After the calculation, statistical analysis was performed between the two groups, as shown in **Table 1**. *P* was all  $> 0.05$ . The difference was not statistically significant and was comparable. This study was approved by the hospital ethics committee, and all patients participated voluntarily.

**Table 1.** Comparison of baseline data between the two groups (n, mean  $\pm$  SD)

Group	Gender (male/female)	Age (years)	Stone diameter (cm)	Stone type (kidney/ureter)
Observation group (50)	27/23	50.78 $\pm$ 13.26	1.81 $\pm$ 0.58	33/17
Control group (50)	31/19	51.12 $\pm$ 13.39	1.66 $\pm$ 0.53	28/22
$\chi^2/t$	0.657	0.128	1.351	1.051
<i>P</i>	0.418	0.899	0.180	0.305

### 2.2. Inclusion criteria and exclusion criteria

Inclusion criteria: (1) Medical imaging showed upper urinary tract stones; (2) The surgical method was percutaneous nephroscopic surgery; (3) The stone diameter was less than 3.0cm; (4) The informed consent form had been signed by the patient and his family.

Exclusion criteria: (1) Severe organic dysfunction; (2) Congenital renal malformation, solitary kidney or ureteral stenosis; (3) Possible urinary tract infection; (4) Multiple stones ( $> 3$ ) with stone diameter  $> 3$  cm; (5) Refusal to sign the consent form.

### 2.3. Surgical methods

Patients in the tubeless group were placed in the lithotomy position after general anesthesia, and the lower abdomen and perineum were disinfected and draped with 0.5% iodophor. A Leesonoscope was inserted through the urethra to observe that the urethral mucosa was normal throughout, the bladder mucosa was smooth and free of new organisms, and the bilateral ureteral openings were clear. The guidewire was retrogradely inserted into the ureteral opening on the affected side. An F6 ureteral catheter was placed under the guidance of the guidewire and connected with normal saline to prepare artificial hydronephrosis. At the same time, a ureteral catheter was left in place. The patient was changed to the prone position, the draping was re-sterilized, B-ultrasound was used to locate the location of the renal pelvis on the affected side, and the 18G puncture needle was successfully inserted into the target renal calyx to elicit clarified urine. Then a super-hard guidewire

was inserted, and the sheath was expanded along the guidewire to 18F to establish a stone channel. The target stone was seen under Leeson's microscope, and the holmium laser was used for lithotripsy and flushing. Another B-ultrasound examination showed no remaining stones, and an F7 stent was placed through the puncture channel. The guidewire is left in place, and the sheath is withdrawn under direct vision. If there is no active bleeding from the puncture channel, the incision is sutured. Observe that the urine drained by the urinary catheter is light-bloody in color. In the tube group, a 16F pyelostomy tube was left in place after the sheath was withdrawn, and it was routinely removed 48 to 72 hours after surgery. The other conditions were the same as those in the tubeless group. Postoperative anti-infective treatment was routine.

## 2.4. Observation indicators

All patients will be re-examined 1 month after discharge. If the imaging shows that the stones disappear, the operation is considered successful, and the ureteral stent on the affected side can be removed.

- (1) Compare a series of indicators, including perioperative operation duration, intraoperative blood loss, length of hospitalization, postoperative VAS score, postoperative urinary catheter indwelling time, one-time stone clearance rate, frequency of analgesic medication, and hemoglobin drop value.  
(VAS refers to the visual analogue score of pain - visual analogue score, 0 to 10 points. The higher the score, the more obvious the pain.)
- (2) Compare the levels of renal function factors, namely blood creatinine (Scr) and blood urea nitrogen (BUN), between the two groups of patients before surgery and 1 month after surgery.
- (3) Compare the complications that occurred during hospitalization and postoperative review between the two groups of patients, including fever, hematuria, urinary extravasation, perinephric effusion, urinary tract infection, ureteral stricture, etc.

## 2.5. Statistical methods

This study used GraphPad Prism9.5 as the statistical software for analysis. The results were presented as mean  $\pm$  standard deviation (SD). The measurement data were tested by t test; the count data were tested by  $\chi^2$ .  $P < 0.05$  was considered statistically significant.

## 3. Result

### 3.1. Comparison of perioperative indicators

Comparing the two groups of patients, there was no significant statistical difference in operation time, intraoperative blood loss, one-time stone clearance rate, and hemoglobin drop value ( $P > 0.05$ ), but the differences in length of hospitalization, VAS score, postoperative urinary catheter retention time, and analgesic drug use frequency were statistically significant ( $P < 0.05$ ). The VAS score of the control group was significantly higher than that of the observation group, and the frequency of analgesic drugs was lower than that of the observation group (Table 2).

**Table 2.** Comparison of perioperative indicators between the two groups

Group	Operation time (min)	Intraoperative bleeding (mL)	Length of hospitalization (d)	VAS score (points)	Postoperative urinary catheter indwelling time (d)	One-time stone clearance rate [n(%)]	Frequency of analgesic drugs (times)
Observation Group (50)	97.54 $\pm$ 10.61	95.04 $\pm$ 11.66	6.04 $\pm$ 1.24	4.18 $\pm$ 0.90	2.92 $\pm$ 0.92	48 (96%)	15
Control group (50)	98.50 $\pm$ 8.92	94.8 $\pm$ 11.57	6.54 $\pm$ 1.13	5.18 $\pm$ 0.92	3.36 $\pm$ 0.88	47 (94%)	35
$\chi^2/t$	0.490	0.585	2.104	5.508	2.447	0.211	16
$P$	0.626	0.56	0.038	< 0.001	0.016	0.646	< 0.001

### 3.2. Comparison of renal function factor levels

There was no statistical difference in the Scr and BUN levels between the two groups of patients before surgery ( $P > 0.05$ ). However, one month after surgery, the Scr and BUN levels of the two groups of patients showed an upward trend, and there was a statistical difference between the two groups ( $P < 0.05$ ). The control group was higher than the observation group (Table 3).

**Table 3.** Comparison of renal function test index levels between the two groups

Group	Scr ( $\mu\text{mol/L}$ )		BUN ( $\text{mmol/L}$ )	
	Before surgery	After surgery	Before surgery	After surgery
Observation group (50)	$87.02 \pm 10.39$	$91.54 \pm 8.31$	$5.22 \pm 0.98$	$5.54 \pm 0.83$
Control group (50)	$86.92 \pm 9.38$	$96.60 \pm 9.77$	$5.24 \pm 0.89$	$6.03 \pm 0.79$
<i>t</i>	0.960	2.789	0.096	3.025
<i>P</i>	0.051	0.006	0.923	0.003

### 3.3. Comparison of complications

Statistical analysis of postoperative complications between the two groups showed that there was no statistical difference between the two groups ( $P > 0.05$ ) (Table 4).

**Table 4.** Statistics of complications in the two groups of patients

Group	Fever (n)	Hematuria (n)	Urinary extravasation (n)	Perinephric effusion/blood (n)	Urinary tract infection (n)	Ureteral stricture (n)	Incidence rate [n(%)]
Observation group (50)	2	1	0	0	1	1	10%
Control group (50)	2	2	1	1	3	0	18%
$\chi^2$							3.474
<i>P</i>							0.627

## 4. Discussion

PCNL is currently the preferred surgical method to replace open upper urinary tract stones and is the most widely used and most effective treatment option in most hospitals in China. In the past, a fistula tube was left in place after PCNL, which could compress and stop bleeding and promote drainage. However, problems such as delayed recovery, increased pain, and increased chance of postoperative complications were inevitable<sup>[4]</sup>. Therefore, tubeless PCNI, as a newer minimally invasive method of PCNI, has important clinical significance.

Wickham et al. first proposed the concept of partially tubeless PCNI in 1984, but then Winfield questioned and reported that failure to leave an indwelling fistula tube could lead to serious complications such as hematuria and urinary extravasation. Finally, Bellman and Moosanejad confirmed the feasibility of tubeless PCNI through a large number of clinical studies, and this technology was eventually promoted<sup>[6-9]</sup>. At present, a large number of studies can support the advantages of tubeless PCNI. Scholars such as Liu Jun compared 87 PCNI patients and found that there were statistical differences between the two groups in postoperative hospitalization time, postoperative first time out of bed, postoperative complications, and postoperative VAS scores<sup>[10]</sup>. Another scholar, Huang Huihu, conducted PCNI analysis on 96 patients and also found that the hospitalization time, VDS score, hospitalization expenses, and postoperative recovery time of the

control group were higher than those of the observation group, and the control group had a higher probability of fever and infection<sup>[11]</sup>. In this study, our research results are similar to those of previous studies. Among the included patients, there was no statistical difference between the two groups in the baseline data after eliminating interference ( $P > 0.05$ ). Among the perioperative indicators, length of stay, VAS score, postoperative urinary catheter time and analgesic drug use. There was a big difference in frequency ( $P < 0.05$ ), especially in the VAS and analgesic drug evaluation, the observation group was significantly lower than the control group ( $P < 0.001$ ), which shows that tubeless PCNI can indeed greatly reduce the pain of PCNI patients while improving the quality of life. There was no difference between the two groups in terms of operation time and intraoperative bleeding, ruling out interference from the surgeon's operating level. Although there was no difference in the one-time stone clearance rates between the two groups, the success rates were extremely high, 96% and 94%, respectively, indicating that urinary tract stones can be effectively removed with or without a fistula tube, and there is no obvious treatment advantage or disadvantage. Regarding common indicators for clinical evaluation of renal function, Scr and BUN showed relatively obvious changes. One month after surgery, the levels of Scr and BUN in both groups showed an upward trend, and the levels in the observation group were lower than those in the control group ( $P < 0.05$ ), indicating that PCNL may cause renal function damage to a certain extent, and not placing a fistula tube can accelerate the recovery of patients' renal function damage. Finally, the incidence rates of fever, hematuria, urinary extravasation, perirenal effusion, infection, and ureteral stricture (10%) in the observation group were lower than those in the control group. Although there was no statistical significance between the two groups, the results showed that tubelessization has the potential to reduce the probability of postoperative complications.

Although the many advantages of tubeless PCNL have been described, it does not mean that tubeless PCNL can be applied to all patients, nor does it mean that tubeless PCNL is necessarily better than conventional PCNL. Tubeless is only one of the options for PCNL, rather than a new innovative technology. The only difference between the two is the presence or absence of an indwelling pyelostomy tube<sup>[1]</sup>. If the patient is found to have a tear in the renal pelvic system, ureteral stenosis or distal obstruction, indications for second-stage surgery, severe infection, bleeding and other signs during the operation, tubeless PCNI will no longer be suitable<sup>[12]</sup>.

## 5. Conclusion

In summary, both conventional and tubeless PCNL are effective ways to remove upper urinary tract stones. When contraindications are eliminated, tubeless PCNL can be used as the first choice. It is safe and reliable, helps reduce pain, shortens the length of hospitalization, promotes renal function recovery, reduces postoperative complications, and improves the quality of life. It has clinical practical value.

## About the author

Corresponding author: Zhao Wenchao, April 1985, male, Han nationality, Heze City, Shandong Province, deputy chief physician, Taizhou People's Hospital Affiliated to Nanjing Medical University, research direction: urinary tract stones  
First author: Zhu Liang (1998-06), male, Han, Suqian, Jiangsu, master's degree, resident physician, Taizhou People's Hospital, research direction: urinary tract stones.

## Disclosure statement

The authors declare no conflict of interest.

## References

- [1] Chen B, Hu H, Zhang Y, et al., 2020, Research Progress on Tubeless Percutaneous Nephroscopy in the Treatment of Kidney Stones. *Lingnan Modern Clinical Surgery*, 20(5): 659–663.
- [2] Wang X, 2022, Effect of Flexible Ureteroscopic Holmium Laser Lithotripsy Combined with Standard Channel Percutaneous Nephrolithotomy in the Treatment of Patients with Upper Urinary Tract Stones. *Chinese Journal of Civil Health*, 34(22): 43–46.
- [3] Ichaoui H, Samet A, Ben H, et al., 2019, Percutaneous Nephrolithotomy (PCNL): Standard Technique Versus Tubeless – 125 Procedures. *Cureus*, 11(3): e4251.
- [4] Zhang Q, 2020, Comparative Analysis of Partially Tubeless and Indwelling Nephrostomy Tube Percutaneous Nephrolithotomy for the Treatment of Upper Urinary Tract Stones. *Chinese Medical Guide*, 18(12): 155–156.
- [5] Wang Q, Wang X, Feng C, et al., 2023, Research on the Clinical Application of Tubeless Minimally Invasive Percutaneous Nephrolithotomy in Kidney and Upper Ureteral Stones. *Chinese and Foreign Medical Research*, 21(20): 1–5.
- [6] Wickham J, Miller R, Kellett M, et al., 1984, Percutaneous Nephrolithotomy: One Stage or Two? *British Journal of Urology*, 56(6): 582–585.
- [7] Winfield H, Weyman P, Clayman R, 1986, Percutaneous Nephrostolithotomy: Complications of Premature Nephrostomy Tube Removal. *Journal of Urology*, 136(1): 77–79.
- [8] Bellman G, Davidoff R, Candela J, et al., 1997, Tubeless Percutaneous Renal Surgery. *Journal of Urology*, 157(5): 1578–1582.
- [9] Moosanejad N, Firouzian A, Hashemi S, et al., 2016, Comparison of Totally Tubeless Percutaneous Nephrolithotomy and Standard Percutaneous Nephrolithotomy for Kidney Stones: A Randomized Clinical Trial. *Brazilian Journal of Medical and Biological Research*, 49(4): e4878.
- [10] Liu J, He W, Lou Y, et al., 2024, Discussion on the Safety and Feasibility of Partially Tubeless Percutaneous Nephrolithotomy. *Chinese Journal of General Medicine*, 22(10): 1679–1683.
- [11] Huang H, Huang W, Guo X, et al., 2020, Treatment Experience of Percutaneous Nephrolithotomy without Nephrostomy Tube. *Chinese Journal of Endoscopy*, 26(8): 55–60.
- [12] Zilberman D, Lipkin M, De La Rosette J, et al., 2010, Tubeless Percutaneous Nephrolithotomy—The New Standard of Care? *Journal of Urology*, 184(4): 1261–1266.

### Publisher's note

*Whioce Publishing remains neutral with regard to jurisdictional claims in published maps and institutional affiliations.*



